1993

Azatranes and atranes of the group 13 elements

Jiri Pinkas
Iowa State University

Order Number 9414013

Azatranes and atranes of the group 13 elements

Pinkas, Jiri, Ph.D.

Iowa State University, 1993

U·M·I
300 N. Zeeb Rd.
Ann Arbor, MI 48106

Azatranes and atranes of the group 13 elements

by

Jiri Pinkas

A Dissertation Submitted to the

Graduate Faculty in Partial Fulfillment of the

Requirements for the Degree of

DOCTOR OF PHILOSOPHY

Department: Chemistry
Major: Inorganic Chemistry

Approved:

Signature was redacted for privacy.

In Charge of Major Work

Signature was redacted for privacy.

For the Major Department

Signature was redacted for privacy.

For the Graduate College

Iowa State University
Ames, Iowa

1993

DEDICATION

To my wife, mother, and sister for their love
and to the memory of my father

TABLE OF CONTENTS

GENERAL INTRODUCTION

This dissertation consists of six sections. The first section is a general introduction containing a statement of the project and an outline of the goals of the research described herein. Each of the subsequent four sections represents research as it was published or submitted for journal publication. Literature citations, tables, figures, and supplementary materials pertain only to the section in which they are included. The final section is a general summary of the results achieved. All contributions to the work presented herein are acknowledged at the end of each paper.

The chemistry of azatranes of group 14 and 15 elements and several transition metals has been explored in detail by our group and others. Azatranes feature a variety of interesting physical and chemical properties. A few of the important such properties are volatility, an unusual basicity in the case of $P(RNCH_2CH_2)_3N$, flexibility of the transannular bond with a possibility of tuning the interbridgehead distance by varying the steric and electronic properties of the axial and equatorial substituents, and a remarkable metathetical reactivity of $R\text{-}Sn(MeNCH_2CH_2)_3N$.

In contrast to azatranes of groups 14 and 15, no analogues of group 13 had been known in the literature before our experiments started. These molecules appeared to be a viable target for synthesis owing to their expected volatility and the fact that the central atom is surrounded exclusively by nitrogens. This makes them interesting potential precursors for the preparation of nitrides of the group 13 elements by organometallic chemical vapor deposition (OMCVD) techniques.

We have carried out syntheses and the characterization by spectroscopic and structural methods of a series of new derivatives $[M(RNCH_2CH_2)_3N]_n$ (M = B, Al, Ga; R = H, Me, $SiMe_3$, $SiMe_2$-*tert*-Bu; n = 1, 2). These azatranes were found to be monomeric or dimeric depending on the size of the substituents R and the nature of the central atom M. The structural determination of $Al(Me_3SiNCH_2CH_2)_3N$ was undertaken to establish the coordination environment around the central aluminum atom for which a rare trigonal monopyramidal (TMP) geometry was revealed. Only a handful of TMP-coordinated transition metals and one main-group element (Ga) derivative were previously structurally characterized. Three azatrane derivatives of Al and Ga were shown by NMR techniques to be dimeric in solution. The question whether these molecules possess a cis or trans configuration of the substituents on the central four-membered ring was answered by single-crystal X-ray diffraction studies which demonstrated the presence of curious cis isomers in the solid state. These compounds also constitute the first examples of group 13 elements pentacoordinated solely by nitrogens.

^{27}Al NMR chemical shifts are well-known to be characteristic for a particular coordination number of aluminum in the oxo and alkyl series. For aluminum compounds coordinated by nitrogen ligands only, values for octahedral and tetrahedral geometries were known. We have extended the AlN_x series by establishing values of chemical shifts featuring an upfield trend from trigonal planar to trigonal monopyramidal (TMP) to trigonal bipyramidal (TBP) geometries.

The attempts made in the past to prepare several transition metal azatranes by transamination reactions failed. We have found that both

azaalumatranes and the azaboratrane $B(MeNCH_2CH_2)_3N$ can undergo a complex multistep transmetallation reactions with transition metal or main-group alkoxides or $Ga(acac)_3$, thus affording transition metal or main-group azatranes, respectively.

The three-fold molecular symmetry of monomeric azatranes implies the presence of a pair of enantiomers. We have found in the case of $B(Me_3SiNCH_2CH_2)_3N$ that their interconversion proceeds via a concerted mechanism. This contrasts with a step-wise mechanism reported previously for silatranes.

A reinvestigation of the oligomeric properties of alumatrane, $Al(OCH_2CH_2)_3N$, was undertaken to clarify its degree of association in solution, which was reported in the literature in a rather broad range from monomeric to octameric. Our NMR studies unambiguously showed the presence of a tetramer in solution and moreover variable temperature ^{13}C NMR spectroscopy revealed a complex dynamic process including racemization and rotation of the alumatrane units in the tetramer.

PAPER I. **GROUP 13 AZATRANES: SYNTHETIC, CONFORMATIONAL, AND CONFIGURATIONAL FEATURES**

ABSTRACT

The monomeric azatranes $E(RNCH_2CH_2)_3N$ **7** (E = B, R = Me), **8** (E = B, R = $SiMe_3$), and **9** (E = Al, R = $SiMe_3$) can be synthesized from $E(NMe_2)_3$ and $(HRNCH_2CH_2)_3N$ in low yields (6-37%). The azatrane **10** (E = Al, R = Me), formed in 64% yield by the analogous reaction, is a stable dimer featuring a four-membered MeNAlNMeAl ring in which the aluminum is five-coordinate as shown by ^1H, ^{13}C, and ^{27}Al NMR spectroscopic techniques (including two-dimensional ones). Compound **7** can be made in 30% yield by reacting **10** with $B(OMe)_3$. Compound **8**, in contrast to **7** and **9**, exists as rigid enantiomers that interconvert slowly at room temperature on the NMR time scale owing to steric repulsion of the $SiMe_3$ groups. VT ^1H and ^{11}B NMR studies provide evidence for a concerted (rather than a stepwise) racemization mechanism ($\Delta H^{\ddagger}$, 61 ± 5 $kJ \cdot mol^{-1}$; $\Delta S^{\ddagger}$, -36 ± 13 $J \cdot mol^{-1} \cdot K^{-1}$) involving a symmetric (C_{3v}) transition state that retains the transannular bond.

INTRODUCTION

Azatrane structures such as **1-6** are members of an interesting class of compounds. Compounds of this type (including those wherein Z = OEt, for

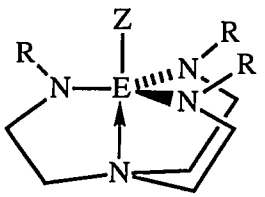

	E	Z	R
1[1]	Si	NMe_2	Me
2[2]	Ge	NMe_2	Me
3[3]	Sn	NMe_2	Me
4[4]	Ti	NMe_2	Me
5[3]	V	N-*t*-Bu	Me
6[5]	Mo	N	Me

example) offer an interesting opportunity to study relative reactivities of the upper axial and the equatorial substituents to protonation and methylation, for example.[6] By increasing the bulk of R in these compounds to $SiMe_3$ (when E = Si and Z = Me), the transannular bond can be essentially broken.[7] Compounds of type **1-6** are volatile and may therefore also be potential OMCVD precursors to nitride films of E, since carbon retention may be minimized by the absence of C-E bonds and by a higher number of N-E bonds than is required by the normal valence of E.

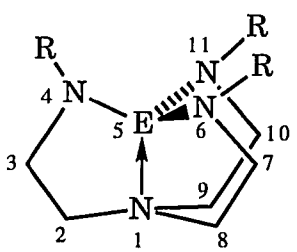

	E	R
7	B	Me
8	B	$SiMe_3$
9	Al	$SiMe_3$

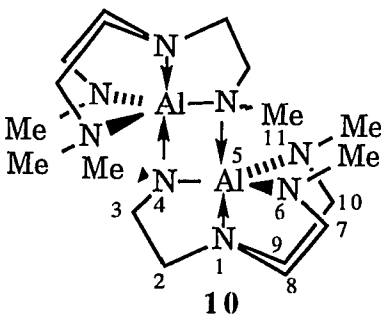

10

Here we report the synthesis of the novel azatranes **7-9** in which boron and aluminum are four-coordinate and **10** in which aluminum occurs in a five-coordinate dimeric structure.[8] We further demonstrate that whereas **7** and **9** are non-rigid in solution on the NMR time scale, **8** is rigid at room temperature. Moreover, as suggested by the configuration shown for **10**, we demonstrate by NMR spectroscopy that this compound does not possess a mirror plane.

EXPERIMENTAL SECTION

General Procedures. All reactions were carried out under argon with the strict exclusion of moisture using Schlenk or dry box techniques.[9] Solvents were dried over and distilled from Na/benzophenone under nitrogen. Deuterated benzene and toluene were dried over and distilled from CaH_2 under an argon atmosphere. The starting materials $(MeHNCH_2CH_2)_3N$,[10] **11**, and $(Me_3SiHNCH_2CH_2)_3N$,[11] **12**, were prepared using our procedures published earlier. $B(NMe_2)_3$ was purchased from Aldrich and was used as received. $[Al(NMe_2)_3]_2$, **13**, was prepared using the published procedure[12a] and was characterized by ^1H, ^{13}C, and ^{27}Al NMR spectroscopy.[12b] $B(OMe)_3$ was purchased from Aldrich and was purified by distillation from Na before using.

NMR spectra were recorded on a Varian VXR 300 with deuterated solvents as an internal lock. ^1H (299.949 MHz) spectra were referenced to the residual proton signal of the deuterated solvent (7.15 ppm for benzene-d_6 and 2.09 ppm for toluene-d_8). ^{13}C (75.429 MHz) spectra were also referenced to solvent signals (128.0 ppm in benzene-d_6 and 20.4 ppm in toluene-d_8). ^{11}B (96.233 MHz) spectra were referenced to $BF_3{\cdot}Et_2O$ in C_6D_6 (50% volume solution) as an external standard, ^{27}Al (78.157 MHz) spectra were measured at 25 and 70 °C and were referenced to the external standard 0.2M $Al(ClO_4)_3$/0.1M $HClO_4$ in H_2O with the coaxial capillary containing benzene-d_6 as a lock medium. ^{29}Si (59.591 MHz) spectra were referenced to a 30% volume solution of Me_4Si in benzene-d_6 as an external standard. Pulses of 90° and a relaxation delay of 25 s were used for acquisition of the ^{29}Si spectra. Variable temperature NMR spectra were measured in toluene-d_8 from -110 °C to +110

°C on Varian VXR 300 and Bruker WM 200 spectrometers with an accuracy of ± 1 °C. Coalescence temperatures were evaluated from a series of spectra taken with 1 °C increments.

Frequency differences $\Delta\nu_{AB}$ were measured at several (5-6) temperatures in the slow exchange region and were extrapolated to the corresponding T_c. ^1H, ^1H DQF COSY spectra were recorded on a Varian Unity 500 instrument.

Mass spectra were recorded on a Finnigan 4000 low-resolution (70 eV, EI; NH_3, CI) and a Kratos MS-50 high resolution instrument. The masses are reported for the most abundant isotope present. IR spectra were taken on an IBM IR-98 FTIR spectrometer (4000-400 cm^{-1}) using Nujol mulls between KBr discs or as KBr pellets.

Elemental analyses were carried out by Galbraith Laboratories or Desert Analytics. Melting points (uncorrected) were measured in sealed capillaries.

Trimethylboraazatrane,[13] 7. *Method A:* A solution of tetramine **11** (19 g, 0.10 mol) and $B(NMe_2)_3$ (16 g, 0.11 mol) in 350 mL of THF and a catalytic amount of vacuum dried $(NH_4)_2SO_4$ was refluxed for 99 h at which time the detectable evolution of $HNMe_2$ ceased. The yellowish solution was filtered and 3/4 of the solvent was removed under vacuum. The white crystalline solid was filtered, washed with 2 x 2.5 mL portions of THF and dried under vacuum. Further evaporation of the filtrate gave a second crop crystals providing a total yield of 7.4 g (37%). The product was further purified by sublimation at 65 °C at 5 x 10^{-3} Torr.

Method B: A solution of **10** (0.411 g, 0.970 mmol) and $B(OMe)_3$ (0.201 g, 1.93 mmol) in 50 mL of toluene was heated to 70-90 °C for 48 h with stirring. All volatiles were then removed under vacuum and the residue was sublimed at

70-80 °C at 5 x 10^{-3} Torr yielding 0.11 g (30%) of **7**: mp 135.0-135.5 °C; ^{1}H NMR (C_6D_6) δ 2.67 (s, 3 H, CH_3, $^{1}J_{CH}$ = 130.6 Hz, ^{13}C satellites), 2.58 (bt, 2 H, MeNCH_2, $^{3}J_{HH}$ = 5.6 Hz), 2.13 (t, 2 H, N(CH_2)$_3$, $^{3}J_{HH}$ = 5.6 Hz); ^{13}C NMR (C_6D_6) δ 37.1 (qt, CH_3, $^{1}J_{CH}$ = 130.3 Hz, $^{3}J_{CNCH}$ = 2.2 Hz), 52.4 (tqt, MeNCH_2, $^{1}J_{CH}$ = 134.2 Hz, $^{3}J_{CNCH}$ = 6.0 Hz, $^{2}J_{CCH}$ = 2.0 Hz), 57.1 (tm, N(CH_2)$_3$, $^{1}J_{CH}$ = 140.0 Hz); ^{11}B NMR (C_6D_6) δ 10.1 (bs, $\Delta\nu_{1/2}$ = 34 Hz); HRMS (EI): Calcd for $C_9H_{21}N_4B$ (M^+) *m/z* 196.18593, found 196.18605; LRMS (EI) *m/z* (ion, relative intensity) 196 (M^+, 58), 152 (100), 138 (87), 124 (58); CIMS (negative ion detection) *m/z* 195 ($M-H^-$, 36), 213 ($M+NH_3^-$, 100), 231 (43), 253 (15); CIMS (positive ion detection) *m/z* 197 ($M+H^+$, 100); IR (KBr pellet, 4000-400 cm^{-1}) ν 2987, 2949, 2919, 2872, 2856, 2830, 2769, 2646, 1474, 1455, 1444, 1411, 1357, 1341, 1325, 1274, 1265, 1233, 1208, 1188, 1163, 1151, 1098, 1040, 1005, 972, 960, 923, 867, 844, 768, 761, 609, 511, 444; Anal. Calcd for $C_9H_{21}N_4B$: C, 55.12; H, 10.79; N, 28.57. Found: C, 55.35; H, 10.65; N, 28.10.

Tris(trimethylsilyl)boraazatrane,[14] 8. A mixture of tetramine **12** (3.1 g, 8.5 mmol) and $B(NMe_2)_3$ (1.6 g, 11 mmol) and a catalytic amount of $(NH_4)_2SO_4$ was heated to 150 °C and the temperature held there for 40 h by which time the detectable evolution of $HNMe_2$ had ceased. Evacuation of residual volatiles under vacuum at room temperature was followed by sublimation at 100 °C at 5 x 10^{-3} Torr, yielding 0.2 g (6% yield) of a white solid: mp 82-85 °C; ^{1}H NMR (toluene-d_8) δ 0.23 (s, 9 H, $SiCH_3$, $^{1}J_{CH}$ = 117.3 Hz, ^{13}C satellites, $^{2}J_{SiH}$ = 6.3 Hz, ^{29}Si satellites), 1.72 (ddd, 1 H, N(CH_2)$_3$, $^{2}J_{HH}$ = $^{3}J_{HH(trans)}$ = 11.5 Hz, $^{3}J_{HH(gauche)}$ = 5.9 Hz), 2.16 (dd, 1 H, N(CH_2)$_3$, $^{2}J_{HH}$ = 11.2 Hz, $^{3}J_{HH(gauche)}$ = 3.9 Hz), 2.69 (b dd, 1 H, Me_3SiNCH_2, $^{2}J_{HH}$ = 12.2 Hz, $^{3}J_{HH(gauche)}$ = 5.9 Hz), 2.82 (ddd, 1 H, Me_3SiNCH_2, $^{2}J_{HH}$ = $^{3}J_{HH(trans)}$ = 12.2 Hz, $^{3}J_{HH(gauche)}$ = 3.8 Hz);

^{13}C NMR (APT, toluene-d_8) δ 1.7 ($SiCH_3$, $^1J_{CH}$ = 117.6 Hz, $^1J_{SiC}$ = 57.5 Hz, ^{29}Si satellites), 44.4 (Me_3SiNCH_2, $^1J_{CH}$ = 138 Hz), 60.2 ($N(CH_2)_3$, $^1J_{CH}$ = 137.9 Hz); ^{11}B NMR (C_6D_6) δ 16.1 (bs, $\Delta\nu_{1/2}$ = 100 Hz); ^{29}Si NMR (C_6D_6, 25 °C) δ -2.37; HRMS (EI) calcd for $C_{15}H_{39}N_4Si_3B$ (M^+) *m/z* 370.25757, found 370.25683; LRMS (EI) *m/z* (ion, relative intensity) 370 (M^+, 64), 355 ($M\text{-}CH_3^+$, 18), 268 (88), 254 (67), 240 (19), 180 (23), 73 ($SiMe_3^+$, 100), 59 (32); Anal. Calcd for $C_{15}H_{39}N_4Si_3B$: C, 48.62; H, 10.61; N, 15.12. Found: C, 49.74; H, 9.91; N, 16.49.

Tris(trimethylsilyl)alumaazatrane,[15] 9. A solution of tetramine **12** (39.76 g, 0.1096 mol) in 130 mL of toluene was added dropwise to a solution of $Al(NMe_2)_3$ (17.43 g, 0.1095 mol) in 350 mL of toluene. The reaction mixture was refluxed for 10 h with stirring. Removal of the solvent under vacuum left an amber-colored oil which solidified upon standing overnight. Although this material appeared to be pure **9** by ^1H NMR spectroscopy, the product was recrystallized from pentane to give 7.7 g (18% yield) of a white crystalline solid: mp 62-63 °C; ^1H NMR (C_6D_6) δ 0.24 (s, 9 H, $SiCH_3$, $^1J_{CH}$ = 117.0 Hz, ^{13}C satellites, $^2J_{SiC}$ = 6.3 Hz, ^{29}Si satellites), 2.00 (t, 2 H, $N(CH_2)_3$, $^3J_{HH}$ = 5.4 Hz, $^1J_{CH}$ = 137.3 Hz, ^{13}C satellites), 2.76 (t, 2 H, Me_3SiNCH_2, $^3J_{HH}$ = 5.3 Hz, $^1J_{CH}$ = 135.0 Hz); ^{13}C NMR (C_6D_6) δ 1.3 (q, $SiCH_3$, $^1J_{CH}$ = 116.6 Hz, $^1J_{SiC}$ = 55.3 Hz, ^{29}Si satellites), 41.4 (tt, Me_3SiNCH_2, $^1J_{CH}$ = 135 Hz, $^2J_{CH}$ = 2.2 Hz, $^1J_{CC}$ = 37 Hz, ^{13}C satellites), 58.7 (tm, $N(CH_2)_3$, $^1J_{CH}$ = 137 Hz, $^1J_{CC}$ = 37 Hz, ^{13}C satellites); ^{27}Al NMR (C_6D_6) δ 133 ($\Delta\nu_{1/2}$ = 3100 Hz at 25 °C, 1860 Hz at 70 °C); ^{29}Si NMR (C_6D_6, 25 °C) δ -1.24; HRMS (EI) calcd for $C_{15}H_{39}N_4Si_3Al$ (M^+) *m/z* 386.22979, found 386.22937; Anal. Calcd for $C_{15}H_{39}N_4Si_3Al$: C, 46.59; H, 10.16; N, 14.49. Found: C, 46.04; H, 10.19; N, 14.72.

Trimethylalumaazatrane Dimer, 10. A solution of tetramine **11** (7.71 g, 40.9 mmol) in 50 mL of THF was added dropwise to a solution of $Al(NMe_2)_3$ (6.26 g, 39.3 mmol) in 350 mL of THF. The reaction mixture was heated at 90 °C with stirring for 8 h. After cooling to room temperature, the solvent was removed under vacuum to give a solid product which was recrystallized from THF to give 10.4 g (64% yield) of **10**: mp 104-106 °C; ^{1}H NMR (500 MHz, C_6D_6).δ 1.88 (dd, 1 H, J = 13.2, 4.9 Hz), 2.12 (dd, 1 H, J = 13.1, 5.0 Hz), 2.24 (m, 1 H), 2.31 (m, 1 H), 2.44 (ddd, J = 13.3, 13.3, 5.1 Hz), 2.56-2.67 (m, 2 H), 2.65 (s, 3 H, CH_3), 2.78-2.85 (m, 2 H), 2.87 (s, 3 H, CH_3), 2.91 (s, 3 H, CH_3), 2.96 (m, 1 H), 3.04 (m, 1 H), 3.42 (ddd, 1 H, J = 13.1, 13.1, 4.9 Hz); ^{13}C NMR (C_6D_6) δ 39.8 (qdd, CH_3, $^1J_{CH}$ = 133.8 Hz, $^3J_{CH}$ = 10.2, 4.5 Hz), 40.8 (qdd, CH_3, $^1J_{CH}$ = 129.1 Hz, $^3J_{CH}$ = 4.3, 2.7 Hz), 41.9 (qdd, CH_3, $^1J_{CH}$ = 129.1 Hz, $^3J_{CH}$ = 3.6, 2.2 Hz), 52.5, 53.2, 53.6, 53.7, 54.3, 56.0 (CH_2 groups); ^{27}Al NMR (C_6D_6) δ 83 ($\Delta\nu_{1/2}$ = 950 Hz at 25 °C, 560 Hz at 70 °C); HRMS (EI) calcd for $C_{18}H_{42}N_8Al_2$ (M^+) *m/z* 424.31630, found 424.31628; calcd for $C_9H_{21}N_4Al$ ($M^+/2$) *m/z* 212.15815, found 212.15808; LRMS (EI) *m/z* 424 (M^+, 2), 409 (M-CH_3^+, 5), 368 (61), 337 (6), 311 (15), 267 (7), 232 (4), 213 (M/2 + H^+, 98), 212 ($M^+/2$, 74), 211 (23), 197 (17), 168 (65), 156 (29), 140 (70), 126 (100); Anal. Calcd for $C_{18}H_{42}N_8Al_2$: C, 50.92; H, 9.97; N, 26.39. Found: C, 50.44; H, 10.05; N, 25.59.

DISCUSSION

Syntheses. The synthesis of trimethylboraazatrane, **7**,occurs in 37% and 30% yield according to reaction 1 and 2, respectively. The small amount of

Reactions 1 and 2:

$$\underset{\mathbf{11}}{(MeHNCH_2CH_2)_3N} + B(NMe_2)_3 \xrightarrow[\substack{\text{reflux}\\ (NH_4)_2SO_4}]{\text{THF}} \underset{\mathbf{7}}{B(MeNCH_2CH_2)_3N} + 3HNMe_2$$

$$n\,\mathbf{10} + 2nB(OMe)_3 \xrightarrow[70\text{-}90\,^{\circ}C]{\text{toluene}} \underset{\mathbf{7}}{2nB(MeNCH_2CH_2)_3N} + [Al(OMe)_3]_{2n}$$

white precipitate formed during reaction 1 and the substantial amount of oily (polymeric?) residue remaining after sublimation of the crude product were not investigated further. Reaction 2 is an example of a novel type of transmetallation in which the rigid dimeric structure of **10** is disassembled and the ligand is reassembled around a new neutral atom. The driving force of this reaction is the formation of insoluble polymeric $[Al(OMe)_3]_n$ possessing strong polar Al-O bonds. By-products in reaction 2, probably containing partially transmetallated products, are currently under investigation. In the absence of moisture, **7** is stable for months in the solid and solution state and it is quite soluble in THF, toluene and pentane.

Tris(trimethylsilyl)boraazatrane, **8**, was synthesized via reaction 3. The large amount of glassy residue left upon sublimation of **8** in low yield (6%) from the reaction product suggests that a polymer formed during the reaction

Reaction 3:

$$(Me_3SiHNCH_2CH_2)_3N + B(NMe_2)_3 \xrightarrow[(NH_4)_2SO_4]{150\,^\circ C} \overline{B(Me_3SiNCH_2CH_2)_3N} + 3HNMe_2$$

12 **8**

rather than upon sublimation, since the former process occurred at a higher temperature (150 °C) than the latter (100 °C). Polymer formation may be favored over cage formation by the bulky $SiMe_3$ groups (see later). The solubility properties of **8** are similar to those of **7**. The transmetallation reaction of **9** with $B(OMe)_3$ did not yield the expected product **8**, suggesting that the bulk of the Me_3Si groups also disfavors a reaction analogous to reaction 2.

In contrast to the low yield of **8**, **9** is formed in essentially quantitative yield

Reaction 4:

$$(Me_3SiHNCH_2CH_2)_3N + 1/2[Al(NMe_2)_3]_2 \xrightarrow[\text{reflux}]{\text{toluene}} \overline{Al(Me_3SiNCH_2CH_2)_3N} + 3HNMe_2$$

12 **13** **9**

in reaction 4 without benefit of catalyst. The absence of polymer in this preparation is due at least in part to reduced steric hindrance among the $SiMe_3$ groups in **9** (see later). Compound **9** is soluble in non-polar hydrocarbon solvents and it was recrystallized in 18% yield from pentane, although the crystals were not suitable for X-ray analysis.

The highly ordered rigid dimer of trimethylalumaazatrane, **10**, is easily assembled in reaction 5, giving a 64% yield.

Reaction 5:

$$2(MeHNCH_2CH_2)_3N + 2Al(NMe_2)_3 \xrightarrow[\text{reflux}]{THF} \left[\overline{Al(MeNCH_2CH_2)_3N}\right]_2 + 6HNMe_2$$

11 **13** **10**

Structural Considerations. The monomeric nature of **7-9** is supported by their ^{1}H and ^{13}C NMR spectra which reflect the 3-fold symmetry of these molecules. There is also considerable precedent for transannular tricyclic structures of this type in the literature (Table I), two of which (**15a**[16] and **16a**[17]) have been established by X-ray diffraction. The single ^{11}B resonance for **7** at 10.1 ppm is also consistent with a monomeric transannulated structure (see Table I) possessing a tetracoordinated boron atom.[18] The possibility of head-to-tail oligomeric structures involving an extended sigma-type overlap of p-orbitals in solutions of a closely related compound **14** was disproven by an IR study[19] in various solvents. Association of **14** in solution is ascribed to dipolar attractions involving the transannulated structure.

Compound **7** is an adduct of the type $(R_2N)_3BNR_3$. No examples of such an adduct could be found in the literature, though the related salt $Li[B(NHMe)_4]$ was reported[20] as well as several adducts of the type $(RO)_3BNR_2H$.[21] The upfield ^{11}B chemical shift of $Li[B(NHMe)_4]$ (0.2 ppm) relative to **7** may reflect the shielding effect of the negative charge on the $B(NHMe)_4^-$ ion. Also consistent with a stable monomeric tricyclic cage structure for **7** is its stability to cleavage of the transannular bond via nucleophilic attack on boron by diisopropylamine, F^- and *tert*-BuO^-, as judged by the constancy of its ^{1}H and ^{11}B NMR spectra in the presence of these bases. The ^{1}H NMR spectrum of **7** consists of a methyl singlet and two methylene triplets. The breadth of the singlet and the downfield triplet is approximately twice that of the highfield triplet. We attribute this broadening to quadrupolar interactions of the CH_3N and the $MeNCH_2$ protons with the ^{11}B nucleus.[22] Although the $N(CH_2)_3$ as well as the $MeNCH_2$ protons are separated from the

Table I. ^{11}B NMR Chemical Shifts for Selected Boron Compounds

compound	δ ^{11}B(ppm)	solvent	ref
$B(CH_2CH_2CH_2)_3N$, **14**	9.40	CS_2	22
$B(OCHRCH_2)_3N$			
15a, R = H	14.2	[a]	40
	10.7	H_2O	39
	11.2	$CHCl_3$	39
15b, R = Me	14.2	[a]	40
$B(CHCXCH_2)_3N$			
16a, X = Cl	14.6	CH_2Cl_2	17
16b, X = Br	12.1	CH_2Cl_2	17
$B(NRCH_2CH_2)_3N$			
7, R = Me	10.1	C_6D_6	this work
8, R = $SiMe_3$	16.1	C_6D_6	this work

[a]No solvent given.

boron nucleus by an equal number of bonds, the latter protons are connected to the boron by essentially planar NR_2 groups[23] which possess a higher degree of s-character in their bonds (sp^2) then the $N(CH_2)_3$ nitrogen (sp^3).

The value of $^3J_{HH}$ in the methylene proton triplets (5.6 Hz) is consistent with conformational mobility of the five-membered rings of **7** on the NMR time scale even down to -110 °C, although some peak broadening occurs at lower temperatures. This broadening occurs more rapidly with decreasing temperature for the $N(CH_2)_3$ protons than for the $MeNCH_2$ protons, suggesting

that the latter (as expected) have greater motional freedom owing to their position on the "flap" carbon of a five-membered ring as in **15a**.[16] The ^{13}C APT NMR spectrum allows the assignment of the CH_3 versus the CH_2 carbons. Moreover the ^{13}C-H coupled spectrum reveals that the highfield CH_2 carbon peak is split into a quartet by scalar interaction with the CH_3 protons ($^3J_{CH}$) while the low-field CH_2 carbon resonance is split into an unresolved multiplet by protons on other $N(CH_2)_3$ carbons. The highfield position of the $MeNCH_2$ carbons relative to the $N(CH_2)_3$ carbons may result from the lone-pair electron density present on the (sp^2) nitrogen of the former which is absent on the latter (sp^3), thus rendering the $N(CH_2)_3$ nitrogen more electronegative. This is also demonstrated in the magnitudes of the $^1J_{CH}$ coupling constants. Greater s-character in the CH bonds of $N(CH_2)_3$ is manifested as a larger coupling constant of 140.0 Hz in contrast to smaller value of 134.2 Hz observed for $MeNCH_2$. Finally, the CH_2 proton and carbon NMR assignments were rendered consistent by sequential irradiation of the proton triplets, leading to the collapse of the corresponding ^{13}C resonances to singlets. Two vibrations in the IR spectrum of **7** at 1098 and 1040 cm^{-1} (intensity ratio roughly 1:4) can be tentatively assigned to the ^{10}B-N and ^{11}B-N stretch, respectively.[19]

The room temperature ^1H NMR spectrum of **8** contrasts that of **7** in that the protons on each of the CH_2 groups are diastereotopic (Figure 1). The four multiplets of equal intensity for these hydrogens in **8** indicate that the conformational mobility of the three five-membered rings of **7** is suppressed in **8** by the steric hindrance imposed by the presence of the $SiMe_3$ groups. Thus racemization of the two enantiomers is slow at room temperature on the NMR (300 MHz) time scale. At elevated temperatures, racemization is accelerated

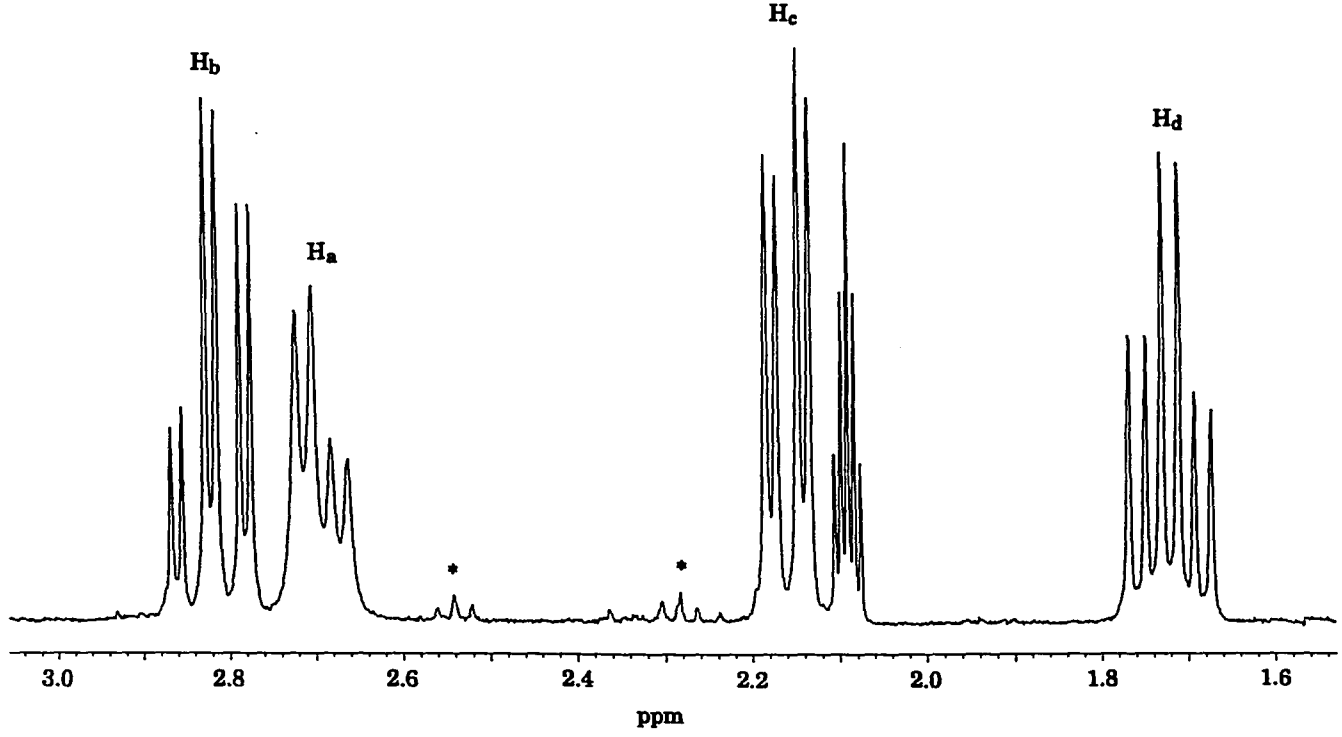

Figure 1. The methylene region of the ^{1}H NMR spectrum of **8** at room temperature. Asterisks denote impurities and the quintet at 2.09 ppm comes from the solvent, toluene-d_8.

and the two downfield multiplets coalesce at 81 °C while the two higher field ones do so at 100 °C. The broadening of one of the pair of downfield multiplets in Figure 1 (probably caused by quadrupolar and unresolved scalar interactions with the ^{11}B nucleus) and the lower coalescence temperature for this pair of multiplets strongly suggests their assignment to Me_3SiNCH_2 protons. The higher coalescence temperature for the upfield pair of multiplets corresponds to the slower narrowing of the $N(CH_2)_3$ proton resonance in **7** (compared with its $MeNCH_2$ protons) upon raising the temperature from -100 °C. Thus the $N(CH_2)_3$ methylene groups in both **7** and **8** possess less motional freedom than the methylene moieties residing at the "flap" positions of the five-membered rings.

The rigidity on the NMR time scale of the enantiomers of **8** at room temperature undoubtedly arises from steric repulsions of the $SiMe_3$ groups, which distort the structure from the nearly eclipsed conformation (as viewed down the B-N axis in Figure 2a) encountered in the crystallographically determined structures of $B(OCH_2CH_2)_3N$[16] and $ClV[(Me_3SiNCH_2CH_2)_3N]$[24] to a more staggered one (Figure 2b). This process (shown as a clockwise twist in Figure 2) reduces the congestion among the $SiMe_3$ groups by increasing the distance between them, and it changes the conformation of the five-membered rings from one in which the Me_3SiNCH_2 methylene carbon is in the "flap" position (Figure 2a) to one in which the $N(CH_2)_3$ nitrogen occupies this position. The latter location of the flap is not obvious from Figure 2b, but becomes clear in Figure 3.

Some pyramidalization of the Me_3SiN nitrogens may also result from the repulsions of the $SiMe_3$ groups. In order for the enantiomer in Figure 2b to

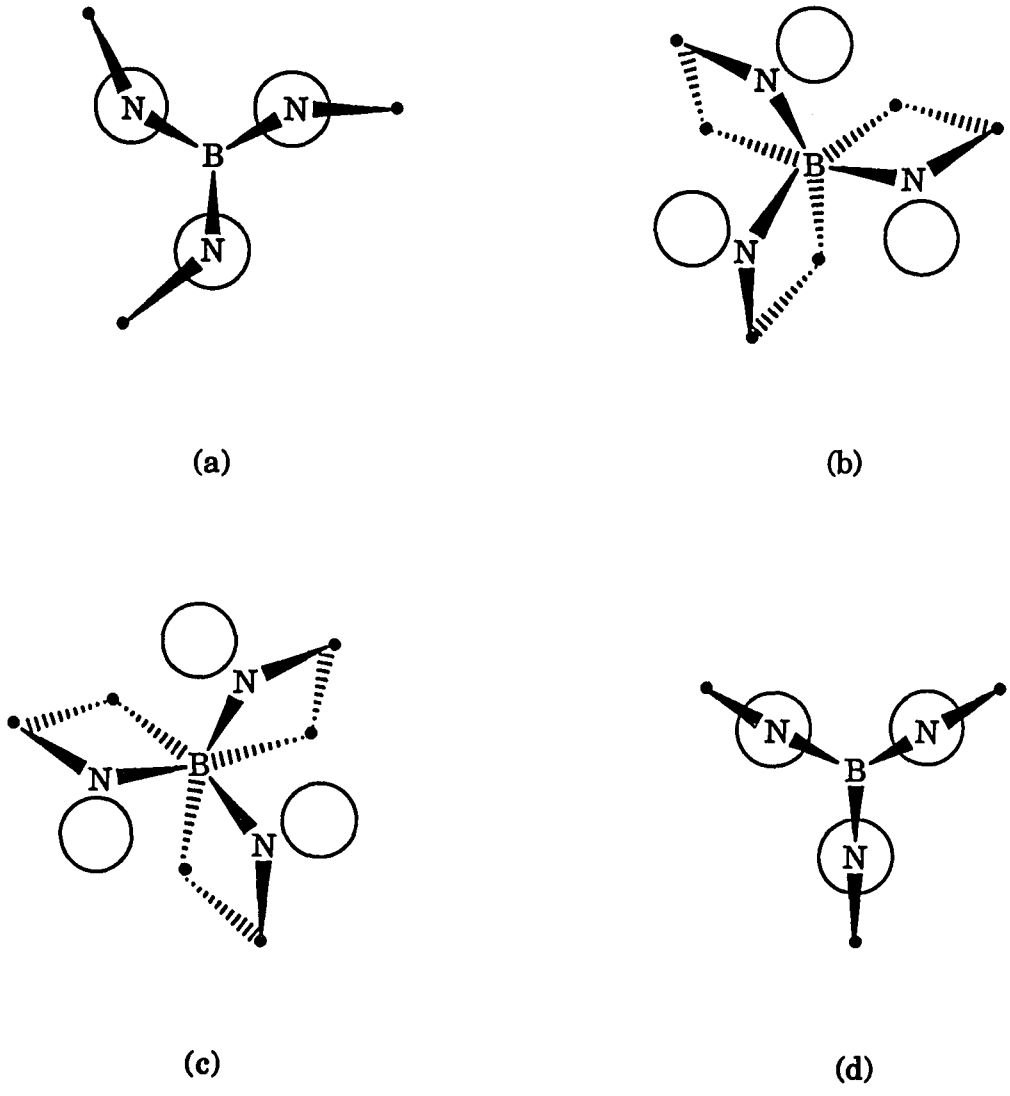

Figure 2. View down the B-N transannular bond axis of **8** showing an eclipsed conformation of the bonds on these atoms (a), enantiomeric staggered conformation (b) and (c), and a proposed transition state in which all the atoms in the framework of the five-membered rings are coplanar (d). The circles represent the $SiMe_3$ groups bonded to the adjacent trigonal nitrogens.

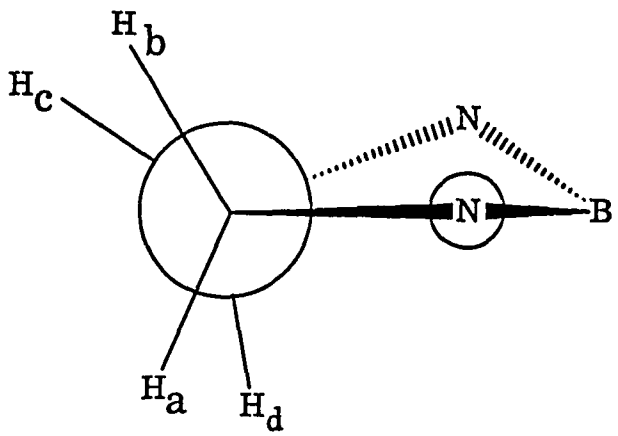

Figure 3. Newman projection of the ethylene portion of the five-membered rings in one of the enantiomers **8** revealing the four different environments of the protons and showing the axial nitrogen in the "flap" position. The circle represents the $SiMe_3$ group.

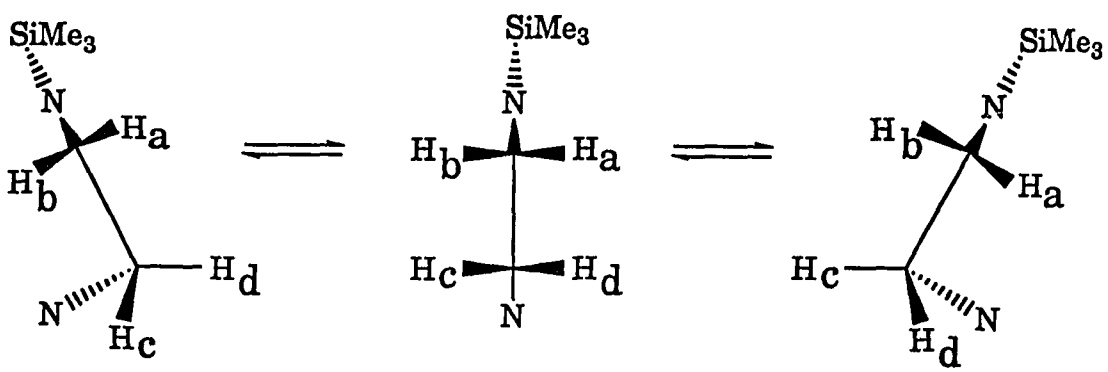

Figure 4. Depiction of a portion of the five-membered rings in **8** showing the four different methylene proton environments in the two enantiomers (a) and (c) and the two environments expirienced by these protons during the racemization process.

racemize to that in Figure 2c, a counterclockwise twist around the B-N axis is required, during which the $SiMe_3$ groups must temporarily crowd one another in an eclipsed conformation of the cage (Figure 2d) before separating again as conformation c in Figure 2 is approached. As depicted in Figure 4b and 4c, the protons on each methylene carbon exchange environments during racemization. At higher temperatures this exchange becomes rapid on the NMR time scale, providing an averaged spectrum of two signals.

The free energies of activation $\Delta G_{Tc}^{\ddagger}$ for racemization at the coalescence (Table II) were calculated from both the Me_3SiNCH_2 and the $N(CH_2)_3$ ^1H NMR coalescence temperatures at two different magnetic fields.[25] The higher values of $\Delta G_{Tc}^{\ddagger}$ than those for azastannatranes (33-36 $kJ \cdot mol^{-1}$) or for azametallatranes **6** and **17** (40.8 and 41.0 $kJ \cdot mol^{-1}$[5]) can be attributed to steric repulsions among the $SiMe_3$ groups. Thus the absence of π-bonding in the three BN amido bonds is in contrast to that likely to be of importance in favoring a structure resembling that in Figure 2d for azametallatranes **6** and **17**. Not unexpectedly, a rather low value of $\Delta G_{Tc}^{\ddagger}$ (8.4 $kJ \cdot mol^{-1}$) was measured for substituted boratranes[26] and the same value was calculated for **14**.[19]

A stepwise mechanism for ring flipping during racemization was substantiated by a ^1H NOESY experiment in the case of substituted

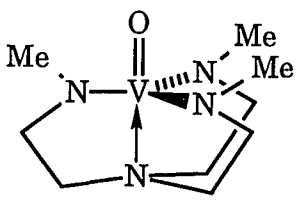

17

$[MeAlN(2,6\text{-}i\text{-}Pr_2C_6H_3)]_3$

18

Table II. Free Energies of Activation for Racemization of **8**

^{1}H resonance	T_c(K)	$\Delta\nu_{AB}{}^{T_c}$(Hz)	$\Delta G_{T_c}^{\ddagger}$ (kJ·mol^{-1})
Me_3SiNCH_2	350[a]	21.2[c]	73.4
	354[b]	33.9[c]	73.7
$N(CH_2)_3$	366[a]	94.8[d]	74.0
	373[b]	139.5[d]	74.3

[a]At 200 MHz. [b]At 300 MHz. [c]Treated as an AB spin system: J_{AB} = 12.2 Hz, $k_c = \pi(\Delta\nu_{AB}{}^2 + 6J_{AB}{}^2)^{1/2}/2^{1/2}$. [d]$k_c = \pi\Delta\nu_{AB}/2^{1/2}$.

silatranes.[27] On the other hand, a very small energy difference (8.4 kJ·mol^{-1}) between a stepwise and concerted pathway was calculated for **14**.[19] Owing to the bulkiness of the $SiMe_3$ groups, the synchronous mechanism is more plausible for azaboratrane **8**. Synchronous processes in polycyclic systems are known to possess higher barriers to interconversion, and this factor may also contribute to the high value of $\Delta G_{T_c}^{\ddagger}$ for **8**. For a series of 1,5-diazabicyclo[3.3.3]decane derivatives, the energy barriers increase as the bridgehead atoms are pushed further apart.[28] This can be accomplished in molecule **8** if breakage of the transannular B-N bond is involved in the racemization process. But as can be seen from the variable temperature ^{11}B NMR spectra,[29] the chemical shift is rather temperature insensitive (shifting 0.4 ppm downfield from 25 °C to 110 °C) and remains in the region characteristic for tetracoordinated boron[18] (16.2 ppm in toluene-d_8). Supporting evidence for a concerted racemization mechanism is the negative value of the activation entropy $\Delta S^{\ddagger}$ (-36±13 J·mol^{-1}·K^{-1}) which was evaluated together with the activation enthalpy $\Delta H^{\ddagger}$ (61±5 kJ·mol^{-1}) by the linear

regression of the plot $\Delta G_{Tc}^{\ddagger}$ versus T_c (r = 0.984) (Table II). The negative value of $\Delta S^{\ddagger}$ is expected if the transition state in the racemization process is more symmetrical than both enantiomers. This can be accomplished, for example, if a C_3 enantiomer passes through the C_{3v} transition state shown in Figure 2d.

Analysis of the coupling patterns and magnitudes in the ^1H NMR spectrum of **8** permits an assignment of each of the four multiplets in Figure 1. The presence of only two coupling constants in the two doublet of doublets at 2.16 and 2.69 ppm indicates that the vicinal coupling constant between them is close to zero owing to a dihedral angle of approximately 90°. Based on the assignment of the broadened multiplet (2.69 ppm) to one of the protons in the $Me_3SiNC\mathit{H}_2$ methylene group, the signals at 2.69 and 2.16 ppm are assigned to H_a and H_c in Figure 3, respectively. The appearance of two larger coupling constants (geminal and trans vicinal) of very similar values, and a smaller one (gauche vicinal) in the apparent pseudo doublet of triplets at 1.72 and 2.82 ppm are confirmatory of the assignments of these protons to H_d and H_b, respectively, in Figure 3. Using selective proton decoupling techniques, the peaks at 44.4 and 60.2 ppm in the ^{13}C NMR spectrum of **8** were assigned to $Me_3SiN\mathit{C}H_2$ and $N(CH_2)_3$, respectively.

The ^{11}B NMR chemical shift of **8** at 16.1 ppm is shifted 6 ppm downfield from that of **7**. This may be ascribed to competition for the lone pair density on the adjacent nitrogens by the Lewis acidic $SiMe_3$ groups, which deshield the boron nucleus. This phenomenon is also manifested in the series $B(NMe_2)_3$, $B(NMe_2)_2(NMeSiMe_3)$, and $B(NMeSiMe_3)_3$ in which δ ^{11}B increases from 27.3 to 28.7 to 33.8 ppm, respectively.[30]

The ^{1}H NMR spectrum of **9** consists of two methylene triplets and a $SiMe_3$ singlet at 0.24 ppm.[31] Crowding of the $SiMe_3$ groups, causing the conformational rigidity observed for the boron derivative **8**, is relieved in the case of **9** by the larger size of the central aluminum atom. As for **7**, rapid racemization is observed in the ^{1}H spectrum down to -70 °C. By analogy with **7** and **8**, the upfield and downfield triplets were assigned to the $N(CH_2)_3$ and Me_3SiNCH_2 protons, respectively. In accord with the corresponding assignments for **7** and **8**, the selectively decoupled ^{13}C NMR spectrum of **9** permitted ascribing the methylene signals at 41.4 and 58.7 ppm to Me_3SiNCH_2 and $N(CH_2)_3$, respectively.

The ^{27}Al NMR chemical shift at 133 ppm confirmed the tetrahedral coordination of the central aluminum atom of **9** (Table III). The signal is at lower field than that for tetrahedral aluminum with four surrounding nitrogens as in **13**.[12b] The downfield shift of **9** can be attributed to the large size of the aluminum atom, which distorts the coordination sphere of the central atom in **9** from tetrahedral towards trigonal monopyramidal (TMP) with a weakened transannular Al-N bond (reaction 6). Such a TMP configuration has recently been observed by X-ray crystallographic means for a related V(III) analogue.[32] As expected, the ^{27}Al chemical shift for **9** is at higher field

Reaction 6:

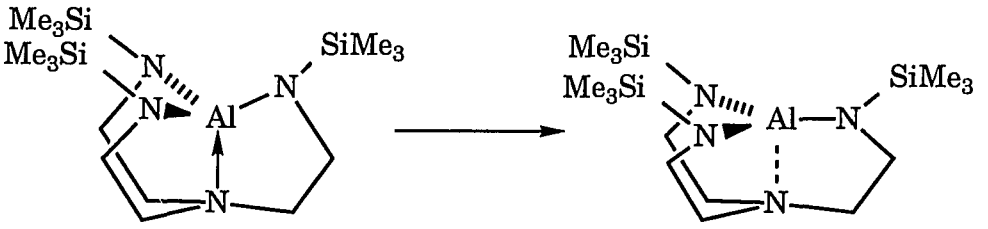

Table III. ^{27}Al NMR Chemical Shifts for Selected Aluminum Compounds

compound	$\delta^{27}Al$ (ppm)	coord. no.	$\Delta\nu_{1/2}$ (Hz)	ref
9	133[a]	4	3100 at 25 °C	this work
			1860 at 70 °C	
10	83[a]	5	950 at 25 °C	this work
			560 at 70 °C	
13	107[a]	4	840	12b
	107[a]		980 at 25 °C	this work
			620 at 70 °C	
18	168[a]	3	8800	33
19	112[b]	5	7200 at 27 °C	34
20	104[a]	5	broad[c]	35
	156[a]	4	broad[c]	
21	104[a]	5	broad[c]	35
	158[a]	4	broad[c]	
23	40.5[a]	6	sharp[c]	37
	159.5[a]	4	broad[c]	

[a]Benzene-d_6 solution. [b]Toluene-d_8 solution. [c]Value of $\Delta\nu_{1/2}$ not given; room temperature.

than that for alumazine **18**, which possesses trigonally coordinated aluminum.[33] On the other hand δ ^{27}Al for **9** is at lower field than those for compounds **19**,[34] **20**,[35] and **21**,[35] in which each possesses a pentacoordinate aluminum.

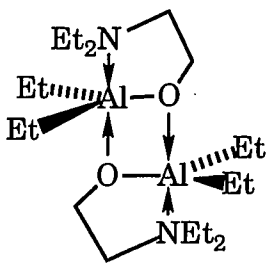

19

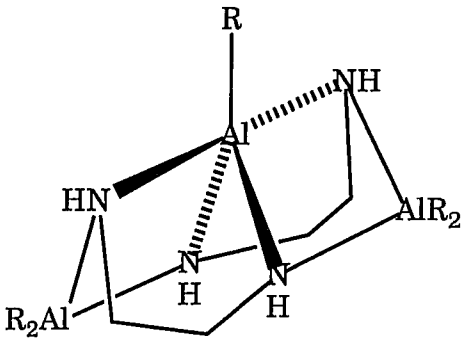

	R
20	Me
21	Et

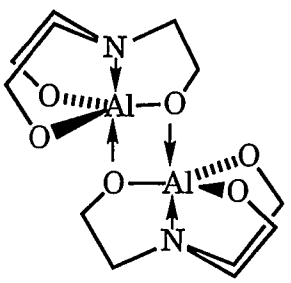

22

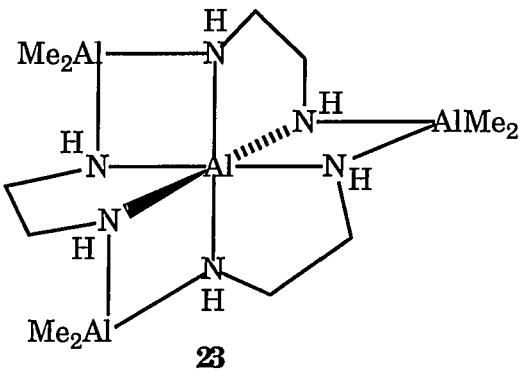

23

In contrast to the simple appearance of the ^{1}H NMR spectra of compounds **7-9**, twelve multiplets and three methyl singlets are observed in the case of **10** (Figure 5a). Moreover, six methylene and three methyl signals can be observed in its ^{13}C APT NMR spectrum. These results are consistent with a dimeric structure for **10**. Also, its HRMS gives evidence for a dimer stable in the gas phase, as is the case for alumatrane **22**.[36] The formation of the dimeric structure **10** renders three methyl groups and three CH_2CH_2 arms inequivalent. Moreover, all four methylene protons become diastereotopic.

Figure 5. ^{1}H NMR (500 MHz) spectrum of **10** showing twelve methylene multiplets A to L and three strong methyl singlets (a), the ^{1}H ^{1}H-DQF COSY 2D NMR spectrum (500 MHz) of **10** (b), and the ^{1}H ^{13}C-heterocorrelated 2D NMR spectrum (300 MHz) of **10** showing only methylene region (c).

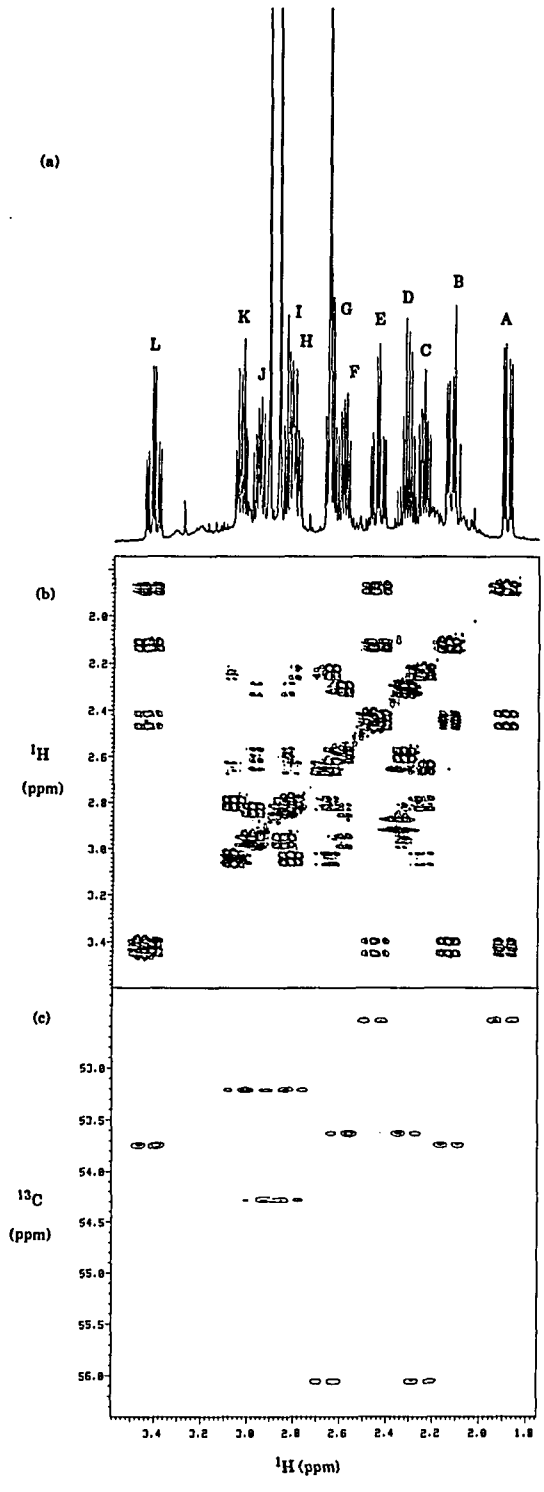
(a)
L
K
J
I
H
G
F
E
D
C
B
A
(b)
^{1}H
(ppm)
2.0
2.2
2.4
2.6
2.8
3.0
3.2
3.4
(c)
^{13}C
(ppm)
53.0
53.5
54.0
54.5
55.0
55.5
56.0
3.4
3.2
3.0
2.8
2.6
2.4
2.2
2.0
1.8
^{1}H (ppm)

There are two possible diastereomers for dimeric **10**. The diastereomer possessing an inversion center as the only symmetry element (schematically shown as **A**) features a trans configuration of the methyl groups on the central four-membered ring. The other diastereomer (**B**) exists as an enantiomeric pair, possesses a C_2 axis as the only symmetry element, and the configuration of the methyls on the central ring is cis. The ^1H NMR spectrum of **10** is clearly interpretable in terms of the presence of only one diastereomer. When an equimolar amount of the chiral shift reagent Eu(fod)$_3$ is added, the ^1H NMR spectrum in $CDCl_3$ shows broadening and some shifting of the peaks downfield. However no peak doubling is observed, even of peaks that have widths at half-heighth of only 4 Hz. This result militates against structure **B**, whose lack of a center of inversion gives rise to enantiomers, and favors structure **A** which possesses a center of inversion. The proposed conformation of the five-membered rings in **A** and **B** is based on the fact that barriers to ring flipping are generally low for [3.3.3] systems, and the conformation is governed

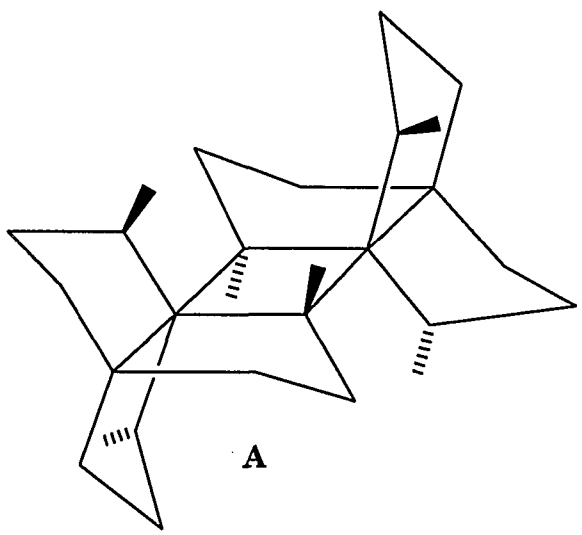

A

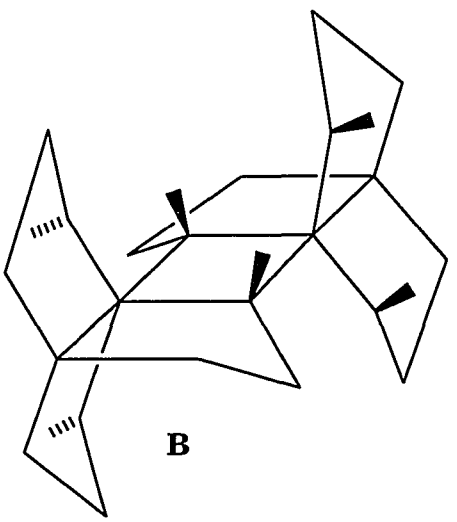

B

by a steric repulsion of substituents rather than by a mutual repulsion of rings.[36]

Distinguishing between the methyl group on the central Al_2N_2 ring (Me-4) and two other methyls (Me-6, 11) in **10** becomes possible from an analysis of its ^{13}C H-coupled NMR spectrum. The nitrogens of the central ring are tetracoordinated and each bears a formal positive charge, while the other four methyl-bearing nitrogens are tricoordinated and possess lone electron pairs. Thus, the nitrogen in the four-membered ring is relatively more electronegative than the other two, and attracts more p-character into the N-C(Me-4) bond. This in turn leaves more s character in the C-H bonds and increases the value of the $^1J_{CH}$ coupling to 133.8 Hz for the signal at 39.8 ppm in contrast to 129.1 Hz for the other two methyl groups at 40.8 and 41.9 ppm.

The analysis of the cross-peak pattern in the ^1H DQF COSY spectrum of **10** (Figure 5) allows the sorting of twelve CH_2 proton signals into three groups belonging to three inequivalent arms namely, A, B, E, L; C, G, H, K; and D, F, I, J. The ^1H-^{13}C heterocorrelated 2D spectrum shows the connectivities between the proton and carbon signals by crosspeaks (Table IV), and each methylene carbon signal is seen to bear two diastereotopic protons (Figure 5c). The information from both the COSY and ^1H-^{13}C correlated spectra completely identifies the three inequivalent CH_2CH_2 arms. The remarkable rigidity of the dimer **10** is preserved up to 110 °C in solution, as was judged from its variable temperature ^1H and ^{13}C NMR spectra. The ^{27}Al NMR chemical shift of 83 ppm (Table III) confirms pentacoordination of the aluminum atom even at 70°C. This value is at higher field than those for compounds **19**, **20**, and **21**, which are the closest examples of the few pentacoordinated aluminum

compounds whose ^{27}Al NMR spectra have been measured.[34,35] Alumaazatranes **9** and **10**, together with the amide **13** and compounds **22**[37] and **23**[37] possess only nitrogen atoms in their coordination spheres and they clearly display a trend in their ^{27}Al chemical shifts toward higher field in the order of increasing coordination numbers, namely, $AlN_4 < AlN_5 < AlN_6$ (Table III). This trend is analogous to that observed for oxo and alkyl aluminum species.[38]

Table IV. Results of ^{1}H-^{1}H and ^{1}H-^{13}C NMR Correlation Experiments with **10**

$\delta^{13}C$ (ppm)	$\delta^{1}H$ (ppm), assignment
39.8	2.65, Me-4
40.8	2.87, Me-6 or 11
41.9	2.92, Me-11 or 6
52.5	1.89, A; 2.45, E
53.7	2.12, B; 3.42, L
53.2	2.78-2.82, H; 3.04, K
56.0	2.24, C; 2.62-2.67, G
53.6	2.56-2.62, F; 2.31, D
54.3	2.82-2.85, I; 2.96, J

CONCLUSIONS

Azatranes of boron and aluminum are stable transannulated molecules. In the case of boron they are monomeric (**7** and **8**) whereas for aluminum they can be monomeric (**9**) or dimeric (**10**), depending upon the size of the substituent on the nitrogen in the three bridging moieties of the transannulated cage structure. Steric crowding among the $SiMe_3$ groups in **8** leads to enantiomers sufficiently long-lived to be observed at room temperature on the NMR time scale. These enantiomers apparently racemize by a concerted mechanism rather than the step-wise process found for silatranes.[27]

ACKNOWLEDGMENT

The authors are grateful to the National Science Foundation for a grant in support of this work, to the Iowa State Center for Advanced Technology Development and to the W. R. Grace Company for a research sample of $(H_2NCH_2CH_2)_3N$.

REFERENCES

(1) Wan, Y.; Verkade, J. G., ms in progress.

(2) Wan, Y.; Verkade, J. G. *Inorg. Chem.*, accepted for publication.

(3) Plass, W.; Verkade, J. G., ms in progress.

(4) Naiini, A. A.; Menge, W.; Verkade, J. G. *Inorg. Chem.*, **1991**, *30*, 5009.

(5) Plass, W.; Verkade, J. G. *J. Am. Chem. Soc.* **1992**, *114*, 2275.

(6) (a) Garant, R. J.; Daniels, L. M.; Das, S. K.; Janakiraman, M. N.; Jacobson, R. A.; Verkade, J. G. *J. Am. Chem. Soc.*, **1991**, *113*, 5728. (b) Woning, J.; Daniels. L. M.; Verkade, J. G. *J. Am. Chem. Soc.* **1990**, *112*, 4601. (c) Woning, J.; Verkade, J. G. *J. Am. Chem. Soc.* **1991**, *113*, 944.

(7) Gudat, D.; Daniels, L. M.; Verkade, J. G. *J. Am. Chem. Soc.* **1989**, *111*, 8520.

(8) Presented at the 203rd ACS National Meeting: Plass, W.; Pinkas, J.; Gaul, B.; Verkade, J. G. Abstracts, 203rd National ACS Meeting, **1992**, INOR 758.

(9) Shriver, D. F.; Drezdzon, M. A. The Manipulation of Air-Sensitive Compounds; Wiley-Interscience: New York, 1986.

(10) Schmidt, H.; Lensink, C.; Xi, S.-K.; Verkade, J. G. *Zeitschr. Anorg. Allg. Chem.* **1989**, *578*, 78.

(11) Gudat, D.; Verkade, J. G. *Organometallics* **1989**, *8*, 2772.

(12) (a) Ruff, J. K. *J. Am. Chem. Soc.* **1961**, *83*, 2835. (b) Waggoner, K. M.; Olmstead, M. M.; Power, P. P. *Polyhedron* **1990**, *9*, 257.

(13) 4,6,11-trimethyl-1,4,6,11-tetraaza-5-boratricyclo[3.3.3.$0^{1,5}$]undecane

(14) 4,6,11-tris(trimethylsilyl)-1,4,6,11-tetraaza-5-boratricyclo[3.3.3.$0^{1,5}$]undecane

(15) 4,6,11-tris(trimethylsilyl)-1,4,6,11-tetraaza-5-alumatricyclo[3.3.3.$0^{1,5}$]undecane

(16) (a) Taira, Z.; Osaki, K. *Inorg. Nucl. Chem. Letters* **1971**, *7*, 509. (b) Kemme, A.; Bleidelis, J. *Latv. PSR. Zinat. Akad. Vestis, Khim. Ser.* **1971**, *5*, 621; *Chemical Abstracts* **1972**, *76*, 64773f. (c) Mattes, R.; Fenske, D.; Tebbe, K.-F. *Chem. Ber.* **1972**, *105*, 2089. (d) Follner, H. *Monatsh. Chemie* **1973**, *104*, 477. (e) Bonczek, M.; Follner, H. *Monatsh. Chemie* **1976**, *107*, 283.

(17) Meller, A.; Hirninger, F. J.; Noltemeyer, M.; Maringgele, W. *Chem. Ber.* **1981**, *114*, 2519.

(18) Nöth, H.; Wrackmeyer, B. NMR Spectroscopy of Boron Compounds, in NMR Basic Principles and Progress, Vol. 14; Springer-Verlag: New York, 1978.

(19) Lee, K.-J.; Livant, P. D.; McKee, M. L.; Worley, S. D. *J. Am. Chem. Soc.* **1985**, *107*, 5901.

(20) Nöth, H.; Vahrenkamp, H. *Chem. Ber.* **1966**, *99*, 1049.

(21) Landesman, H.; Williams, R. E. *J. Am. Chem. Soc.* **1961**, *83*, 2663.

(22) Greenwood, N. N.; Morris, J. H.; Wright, J. C. *J. Chem. Soc.* **1964**, 4753.

(23) Schmid, G.; Boese, R.; Bläser, D. *Z. Naturforsch.* **1982**, *37b*, 1230.

(24) Cummins, C. C.; Schrock, R. R.; Davis, W. M. *Organometallics* **1992**, *11*, 1452-1454.

(25) Kemp, W. NMR in Chemistry: a Multinuclear Introduction; MacMillan Education Ltd.: London, 1986, 165 and Martin, M. L.;

Delpuech, J.-J.; Martin, G. J. Practical NMR spectroscopy; Heyden: London, 1980, 291.

(26) Tandura, S. N.; Pestunovich, V. A.; Voronkov, M. G.; Zelchan, G. I. Baryshok, V. P.; Lukina, Y. A. *Dokl. Akad. Nauk SSSR* **1977**, *235*, 406.

(27) Kupche, E. L.; Liepinsh, E. E.; Lukevits, E. *Khim. Geterotsikl. Soed.* **1987**, *1*, 129.

(28) Glass, R. S. Conformational Analysis of Medium-Sized Heterocycles; VCH Publishers, Inc.: New York, 1988, 128.

(29) Contreras, R.; Garcia, C.; Mancilla, T.; Wrackmeyer, B. *J. Organometal. Chem.* **1983**, *246*, 213.

(30) (a) Nöth, H.; Sprague, M. J. *J. Organometal. Chem.* **1970**, *22*, 11. (b) Nöth, H.; Tinhof, W.; Wrackmeyer, B. *Chem. Ber.* **1974**, *107*, 518.

(31) For $Al[N(SiMe_3)_2]_3$ δ (^1H) is 0.244 ppm in CCl_4 (Pump, J.; Rochow, E. G.; Wannagat, U. *Angew. Chem. Int. Ed. Engl.* **1963**, *5*, 264).

(32) Cummins, C. C.; Lee, J.; Schrock, R. R.; Davis, W. M. *Angew. Chem.* **1992**, *104*, 1510.

(33) Waggoner, K. M.; Hope, H.; Power, P. P. *Angew. Chem. Int. Ed. Engl.* **1988**, *27*, 1699.

(34) Benn, R.; Rufinska, A.; Lehmkuhl, H.; Janssen, E.; Krüger, C. *Angew. Chem. Int. Ed. Engl.* **1983**, *22*, 779.

(35) Jiang, Z.; Interrante, L. V.; Kwon, D.; Tham, F. S.; Kulling, R. *Inorg. Chem.* **1991**, *30*, 995.

(36) Lacey, M. J.; Macdonald, C. G. *Aust. J. Chem.* **1976**, *29*, 1119.

(37) Jiang, Z.; Interrante, L. V.; Kwon, D.; Tham, F. S.; Kulling, R. *Inorg. Chem.* **1992**, *31*, 4815.

(38) (a) NMR and the Periodic Table; Harris, R. K.; Mann, B. E., Eds.; Academic Press: New York, 1978. (b) Multinuclear NMR; Mason, J., Ed.; Plenum Press: New York, 1987.

(39) Onak, T. P.; Landesman, H.; Williams, R. E.; Shapiro, I. *J. Phys. Chem.* **1959**, *63*, 1533.

(40) Onak, T. P.; Williams, R. E.; Swidler, R. *J. Phys. Chem.* **1963**, *67*, 1741.

PAPER II. AZAALUMATRANES EXHIBITING UNUSUAL COORDINATION MODES OF THE CENTRAL ALUMINUM

ABSTRACT

The new monomeric azaalumatrane $Al(tert\text{-}BuMe_2SiNCH_2CH_2)_3N$, **6**, was prepared by the reaction of $[Al(NMe_2)_3]_2$, **7**, and $(tert\text{-}BuMe_2SiNHCH_2CH_2)_3N$, **11**, and was characterized by ^1H, ^{13}C, ^{27}Al, and ^{29}Si NMR, MS and IR spectroscopies. Its analogue $Al(Me_3SiNCH_2CH_2)_3N$, **3**, was structurally characterized and shown to contain a trigonal monopyramidal aluminum center. The dimeric azaalumatrane $[Al(Me_3SiNCH_2CH_2)_2(HNCH_2CH_2)N]_2$, **5**, possesses an unusual cis configuration of the central four-membered ring and the aluminum atoms display a distorted trigonal bipyramidal coordination sphere. Crystal data: **3**, a = 13.503(5) Å, b = 10.621(4) Å, c = 17.840(6) Å, β = 93.29(3)°, V = 2554(2) Å^3, Z = 4, space group $P2_1/c$, R = 5.2%; **5**, a = 12.134(3) Å, b = 17.049(4) Å, c = 18.297(5) Å, β = 100.02(2)°, V = 3726(2) Å^3, Z = 4, space group $P2_1/n$, R = 4.6%. ^{27}Al NMR chemical shifts for a series of Al-N compounds with aluminum coordination numbers ranging from three to six show increased shielding with increasing coordination number.

INTRODUCTION

The chemistry of compounds containing Al-N bonds has been flourishing in the past several years, mainly due to increasing interest in developing optimum AlN precursors.[1-5] Recently we reported the preparation and characterization of group 13 azatranes[6] such as **1-4**. These compounds exhibit monomeric or dimeric behavior, depending on the nature of the central atom and on the bulkiness of the pseudo-equatorial substituents, rendering the central atom in the monomers or dimers four- or five-coordinate, respectively. Compound **2** was shown by ^{1}H VT NMR spectroscopy to undergo an interesting dynamic process in solution, which is a concerted interconversion of two enantiomers ($\Delta \rightleftharpoons \Lambda$). Azaalumatrane **4** was also shown to be able to take part in a novel complex transmetallation reaction.[6] Azatranes such as these

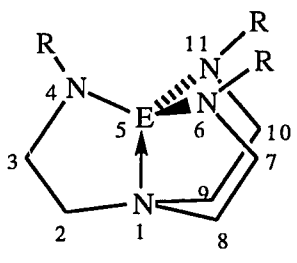

	E	R	R'
1	B	Me	–
2	B	$SiMe_3$	–
3	Al	$SiMe_3$	–
4	Al	Me	Me
5	Al	$SiMe_3$	H
6	Al	$SiMe_2$-*tert*-Bu	–

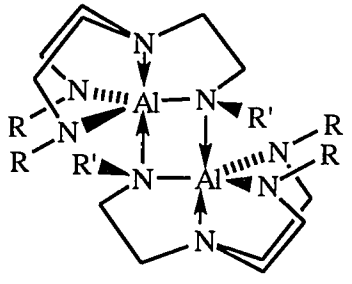

are sublimable solids, thus making them attractive to evaluate as OMCVD precursors for nitride films.

Here we report on the group 13 azatrane **5** which is dimeric and **6** which is monomeric. Surprisingly, the configuration of the substituents at the central four-membered Al_2N_2 ring in **5** is cis rather than trans as shown by X-ray crystallography. Compound **5** constitutes the first example of a

pentacoordinate aluminum surrounded exclusively by nitrogen ligands. Monomeric **3** and **6** containing four-coordinate atoms are rare examples of the trigonal monopyramidal (TMP) coordination environment for aluminum, and the main-group elements in general. A comparison of ^{27}Al NMR chemical shifts among compounds in which the central aluminum is coordinated only by nitrogens clearly reveals an upfield trend with increasing coordination number of the aluminum. As will also be shown, azaalumatranes **3** and **6**, despite the very bulky ligands at the equatorial nitrogens, are freely fluxional in solution even down to -95 °C in contrast to the boron analogue **2**.

EXPERIMENTAL SECTION

General Procedures. All reactions were carried out under argon with the strict exclusion of moisture using Schlenk or dry box techniques.[7] Solvents were dried over and distilled from Na/benzophenone under nitrogen. Deuterated benzene and toluene were dried over and distilled from CaH_2 under an argon atmosphere.

$[Al(NMe_2)_3]_2$, **7**, was prepared using the published procedure.[8a] $AlCl_3$, LiN-*iso*-Pr_2, $LiN(SiMe_3)_2$, Me_3SiCl, and *tert*-$BuMe_2SiCl$ were purchased from Aldrich and were used as received.

NMR spectra were recorded at 25 °C, unless otherwise stated, on a Varian VXR 300 with deuterated solvents as an internal lock using sealed 5 mm NMR tubes. ^1H (299.949 MHz) and ^{13}C (75.429 MHz) spectra were internally referenced to the corresponding Me_4Si signals. ^{27}Al (78.157 MHz) spectra were measured at 70 °C to decrease the line width of the signals and were referenced to the external standard 0.2M $Al(ClO_4)_3$/0.1M $HClO_4$ in D_2O. The chemical shifts were corrected for the difference in chemical shift between D_2O and the lock solvent used. The background signal, which was found as a broad peak at ~61 ppm ($\Delta\nu_{1/2}$ = 4100 Hz at 30 °C), did not interfere with our spectra owing to its low intensity when concentrated sample solutions were used. ^{29}Si (59.591 MHz) spectra were referenced to a 30% volume solution of Me_4Si in benzene-d_6 as an external standard. Pulses of 90° and a relaxation delay of 25 s were used for acquisition of the ^{29}Si spectra.

Mass spectra were recorded on a Finnigan 4000 low-resolution (70 eV, EI; NH_3, CI) and a Kratos MS-50 high resolution instrument. The masses are

reported for the most abundant isotope present. IR spectra (4000-400 cm^{-1}) were taken on an IBM IR-98 and a DigiLab FTS-7 FTIR spectrometer using Nujol mulls between KBr discs or as KBr pellets. Wave numbers were calibrated with a 0.05 mm polystyrene film. Intensities are noted as very strong (vs), strong (s), medium (m), weak (w), and very weak (vw). Elemental analyses were carried out by Desert Analytics, Knoxville, TN. Melting points (uncorrected) were measured in sealed capillaries.

Tris(di*iso*-propylamino)aluminum,[8a,9] 8a. The preparation of **8a** was reported in 1961 by Ruff[8a] using *iso*-Pr_2NH and $Me_3N{\cdot}AlH_3$ as starting materials. Because no spectral data were published, we report them here. We also report the synthesis of **8a** by a different method. A slurry of Li*N*-*iso*-Pr_2 (4.96 g, 46.3 mmol) in 70 mL of degassed pentane was added slowly to a stirred ice-cooled suspension of $AlCl_3$ (2.25 g, 50.6 mmol) in 150 mL of pentane and then stirred at room temperature for 70 h. All volatiles were removed in vacuum and the resulting solid was sublimed at 70-90 °C at 5 x 10^{-3} torr giving 0.20 g (4.1%) of a white solid **8a**: mp 60-61 °C (lit.[8a] 58-59 °C); ^1H NMR (benzene-d_6) δ 1.25 (d, 6 H, CH_3, $^3J_{CH}$ = 6.5 Hz, $^1J_{CH}$ = 124.0 Hz, ^{13}C satellites), 3.41 (sept., 1H, CH, $^3J_{CH}$ = 6.5 Hz, $^1J_{CH}$ = 131.5 Hz, ^{13}C satellites); ^{13}C NMR (benzene-d_6) δ 25.6 (CH_3), 46.2 (CH); ^{27}Al NMR (benzene-d_6, 70 °C) δ 143 ± 1 ($\Delta\nu_{1/2}$ = 3600 Hz); LRMS (EI) *m/z* (ion, relative intensity) 327 (M^+, 2), 312 (M-CH_3^+, 1), 226 (M-NH-*iso*-Pr_2^+, 28), 211 (45), 183 (20), 169 (9), 142 (10), 128 (29), 127 (19), 126 (40), 112 (9), 100 (N-*iso*-Pr_2^+, 10), 98 (6), 86 (34), 84 (19), 70 (11), 58 (10), 57 (29), 44 (100); CIMS (positive ion detection) *m/z* (ion, relative intensity) 327 (M^+, 0.2), 226 (M-HN-*iso*-Pr_2^+, 13), 211 (13), 183 (6), 139 (6), 124 (3), 100 (N-*iso*-Pr_2^+, 100).

Tris[bis(trimethylsilyl)amino]aluminum,[9,10] 8b. The reaction of $AlCl_3$ with $LiN(SiMe_3)_2$ as described in the literature[10a] was employed. Because only a melting point and ^1H NMR spectrum was reported, the product was more completely characterized by spectroscopic techniques. **8b** was purified by sublimation at 110-120 °C at 5 x 10^{-3} Torr yielding a white solid: mp 187-190 °C (lit.[10a] 188 °C); ^1H NMR (toluene-d_8) δ 0.33 (s, 54 H, CH_3, $^1J_{CH}$ = 117.9 Hz, ^{13}C satellites, $^2J_{SiCH}$ = 6.4 Hz, ^{29}Si satellites) (lit.[10a,b] δ 0.25 in CCl_4); ^{13}C NMR (toluene-d_8) δ 6.03 (q sept., $^1J_{CH}$ = 118.0 Hz, $^3J_{CH}$ = 1.8 Hz, $^1J_{SiC}$ = 55.6 Hz, ^{29}Si satellites); ^{27}Al NMR (toluene-d_8, 70 °C) δ 136 ± 1 ($\Delta\nu_{1/2}$ = 8200 Hz); ^{29}Si NMR (toluene-d_8) δ 0.34; HRMS (EI) calcd for $C_{18}H_{54}N_3Si_6Al$ (M^+) *m/z* 507.27488, found 507.27614; calcd for $C_{17}H_{51}N_3Si_6Al$ ($M\text{-}CH_3^+$) *m/z* 492.25140, found 492.25108; LRMS (EI) *m/z* (ion, relative intensity) 507 (M^+, 1), 492 ($M\text{-}CH_3^+$, 8), 404 (3), 347 ($M\text{-}N(SiMe_3)_2^+$, 10), 331 (14), 291 (4), 275 (23), 259 (5), 202 (75), 186 (6) 146 (25), 130 (43), 73 ($SiMe_3^+$, 100).

Tris(trimethylsilyl)tren,[11] 9. *Method A.* The reaction of lithiated tetramine tren $N(CH_2CH_2NH_2)_3$, **10**, with Me_3SiCl as described earlier in a paper from our laboratory[11a] was used, improving the reported yield of 54% to 75%. Here we also report complete spectroscopic data for **9**: bp 110 °C at 5 x 10^{-3} Torr; ^1H NMR (benzene-d_6) δ 0.13 (s, 9H, $Si(CH_3)_3$, $^1J_{CH}$ = 117.9 Hz, ^{13}C satellites, $^2J_{SiH}$ = 6.6 Hz, ^{29}Si satellites), 0.80 (bt, 1H, NH, $^3J_{HNCH}$ = 7 Hz), 2.36 (t, 2H, $N(CH_2)_3$, $^3J_{HH}$ = 6.2 Hz), 2.76 (td, 2H, $SiNCH_2$, $^3J_{HCCH}$ = 6.3 Hz, $^3J_{HNCH}$ = 7.4 Hz); ^{13}C NMR (benzene-d_6) δ 0.3 (q bm, $Si(CH_3)_3$, $^1J_{CH}$ = 117.8 Hz, $^1J_{SiC}$ = 56.4 Hz, ^{29}Si satellites), 40.2 (tq, $SiNCH_2$, $^1J_{CH}$ = 132.6 Hz, $^2J_{CNH}$ = $^2J_{CCH}$ = 2.3 Hz), 58.9 (tm, $N(CH_2)_3$, $^1J_{CH}$ = 130.8 Hz); ^{29}Si NMR (benzene-d_6) δ 2.55; LRMS (EI) *m/z* (ion, relative intensity) 363 ($M+H^+$, 64), 347 ($M\text{-}CH_3^+$, 32), 260 (M-

$CH_2NHSiMe_3^+$, 42), 229 (9), 171 (100), 157 (24), 116 ($CH_2CH_2NHSiMe_3^+$, 36), 102 ($CH_2NHSiMe_3^+$, 31), 73 ($SiMe_3^+$, 78); IR (neat, KBr discs, 4000-400 cm^{-1}) ν 3384 m (νNH), 2955 vs (ν_{as} CH_3), 2898 s ($\nu_s CH_3$), 2841 s ($\nu_{as} CH_2$), 2806 s ($\nu_s CH_2$), 2734 w, 1449 m, 1398 vs ($\delta_{as} CH_3$), 1248 vs ($\delta_s CH_3$), 1125 vs, 1110 vs (νNC), 1050 s, 990 w, 932 vs, 874 sh ($\rho_{as} CH_3$), 836 vs ($\rho_{as} CH_3$), 744 s ($\rho_s CH_3$), 679 s (νSiC), 613 m. *Method B.* Me_3SiCl (13 mL, 0.10 mol) was added dropwise to a solution of tren **10** (4.9 g, 0.033 mol) and Et_3N (16 mL) in 350 mL of Et_2O at 0 °C. After stirring over night at room temperature, the solution was filtered, the solvent was removed, and vacuum distillation afforded 5.67 g (46.8%) of **9**.

Tris(trimethylsilyl)azaalumatrane,[12] 3. Compound **3** prepared according to our procedure[6] was purified by sublimation at 70-80 °C at 1 x 10^{-2} Torr. Single crystals suitable for X-ray diffraction experiments were grown from a pentane solution stored in a refrigerator for several weeks. The characterization of **3** by NMR techniques was reported previously.[6] IR (KBr pellet, 4000-400 cm^{-1}) ν 2953 m ($\nu_{as} CH_3$), 2888 m, 2834 m, 1465 w, 1449 w, 1400 w, 1359 w, 1340 w, 1331 w, 1265 m, 1246 vs ($\delta_s CH_3$), 1143 w, 1087 s (νCN), 1066 m, 1049 m, 1031 m, 969 vs, 832 vs ($\rho_{as} CH_3$), 744 s ($\rho_s CH_3$), 726 w, 669 m, 663 w, 641 vw, 621 vw, 579 m, 576 m, 533 m; LRMS (EI) *m/z* (ion, relative intensity) 386 (M^+, 51), 371 ($M\text{-}CH_3^+$, 71), 358 ($M\text{-}CH_2CH_2^+$, 5), 284 ($M\text{-}CH_2NSiMe_3\text{-}H^+$, 100), 256 (9), 242 (5), 227 (5), 215 (7), 188 (6), 185 (7), 183 (8), 178 (10), 171 (19), 157 (7), 116 (11), 102 (11), 73 ($SiMe_3^+$, 68), 59 (14); CIMS (positive ion detection) *m/z* (ion, relative intensity) 387 ($M+H^+$, 100), 363 (18), 291 (18), 200 (5), 116 (21), 107 (46), 90 (70).

Tris(*tert*-butyldimethylsilyl)tren, 11. *Method A.* Tren, **10** (4.82 g, 33.0 mmol) in 150 mL of THF was lithiated with 48 mL of a 2.1M solution of *n*-BuLi

at -60 °C and then stirred overnight at room temperature. This suspension was quenched with a solution of *tert*-$BuMe_2SiCl$ (14.91 g, 98.94 mmol) in 150 mL of THF at -40 °C and then stirred overnight at room temperature. THF was removed under vacuum and 250 mL of pentane was added. The precipitate of LiCl was filtered off, pentane was removed under vacuum and the product was vacuum distilled giving 7.30 g (45.3%) of **11**: bp 170 °C at 0.1 Torr; ^1H NMR (benzene-d_6) δ 0.03 (s, 6H, $Si(CH_3)_2$, $^1J_{CH}$ = 118.0 Hz, ^{13}C satellites, $^2J_{SiH}$ = 6.2 Hz, ^{29}Si satellites), 0.73 (t, 1H, NH, $^3J_{HNCH}$ = 7.2 Hz), 0.93 (s, 9H, $C(CH_3)_3$, $^1J_{CH}$ = 124.5 Hz, ^{13}C satellites, $^3J_{SiH}$ = 5.6 Hz, ^{29}Si satellites), 2.31 (t, 2H, $N(CH_2)_3$, $^3J_{HH}$ = 6.2 Hz, $^1J_{CH}$ = 132.3 Hz, ^{13}C satellites), 2.75 (dt, 2H, $SiNCH_2$, $^3J_{HCCH}$ = 6.2 Hz, $^3J_{HNCH}$ = 7.3 Hz, $^1J_{CH}$ = 131.8 Hz, ^{13}C satellites); ^{13}C NMR (benzene-d_6) δ -4.7 (qqd, $Si(CH_3)_2$, $^1J_{CH}$ = 118.0 Hz, $^3J_{CSiCH}$ = $^3J_{CSiNH}$ = 1.8 Hz, $^1J_{SiC}$ = 55.3 Hz, ^{29}Si satellites), 18.7 (s, $C(CH_3)_3$, $^1J_{CC}$ = 31.2 Hz, ^{13}C satellites, $^1J_{SiC}$ = 60.7 Hz, ^{29}Si satellites), 26.8 (q sept., $C(CH_3)_3$, $^1J_{CH}$ = 124.6 Hz, $^3J_{CH}$ = 5.6 Hz, $^1J_{CC}$ = 31.2 Hz, ^{13}C satellites), 41.0 (ttd, $SiNCH_2$, $^1J_{CH}$ = 133.1 Hz, $^2J_{CCH}$ = $^2J_{CNH}$ = 2.5 Hz, $^1J_{CC}$ = 39.2 Hz, ^{13}C satellites), 59.4 (tm, $N(CH_2)_3$, $^1J_{CH}$ = 132.3 Hz, $^1J_{CC}$ = 38.7 Hz, ^{13}C satellites); ^{29}Si NMR (benzene-d_6) δ 7.50; LRMS (EI) *m/z* (ion, relative intensity) 489 ($M+H^+$, 0.05), 473 ($M-CH_3^+$, 0.3), 431 (M-*tert*-Bu^+, 0.1), 344 (11), 226 (5), 213 (35), 199 (11), 187 (38), 158 (34), 144 (29), 129 (6), 115 ($SiMe_2$-*tert*-Bu^+, 7), 100 (13), 88 (10), 73 ($SiMe_3^+$, 100), 59 (18), 58 ($SiMe_2^+$, 7), 57 (*tert*-Bu^+, 11), 44 (10), 43 (10); CIMS (positive ion detection) *m/z* (ion, relative intensity) 489 ($M+H^+$, 100), 375 (10), 344 (12), 332 (8), 299 (11), 261 (4); IR (neat, KBr discs, 4000-400 cm^{-1}) ν 3691 s (νNH), 2954 vs ($\nu_{as}CH_3$), 2930 vs, 2885 s (ν_sCH_3), 2856 vs, 1470 vs, 1464 vs, 1449 sh, 1401 vs, 1389 s, 1360 m, 1279 w, 1253 vs (δ_sCH_3), 1209 w, 1127 vs, 1114 vs, 1048 s, 1005 s, 988 vw, 936 s, 906 sh, 853 sh, 830 vs, 808 s, 770 vs, 724

sh, 678 w, 658 s, 570 w. Anal. Calcd for $C_{24}H_{60}N_4Si_3$: C, 58.95; H, 12.37; N, 11.46. Found C, 59.41; H, 12.80; N, 11.41.

Method B.[13a] A solution of *tert*-$BuMe_2SiCl$ (10.5 g, 69.8 mmol) in 100 mL of Et_2O was added dropwise to an ice cooled solution of tren, **10**, (3.3 g, 2.3 mmol) and Et_3N (10 mL, 72 mmol) in 250 mL of Et_2O with stirring. The white suspension was further stirred at room temperature overnight and solid Et_3NHCl was filtered off and then all volatiles were removed under vacuum. Further workup and characterization was identical to that in *Method A*, yielding 4.45 g (40.3%) of **11**.

Tris(*tert*-butyldimethylsilyl)azaalumatrane,[14] 6. A solution of **7** (0.93 g, 5.8 mmol) in 80 mL of toluene was added dropwise to a stirred solution of tetramine **11** (2.86 g, 5.84 mmol) in 100 mL of toluene over a period of 15 minutes. The reaction mixture was heated at 100 °C with stirring for 24 h. After cooling to room temperature, a small amount of a fine (probably polymeric) precipitate was filtered off. The volume of the filtrate was reduced under vacuum to 1/3 and the resulting precipitate was collected and washed with 2 x 1.5 mL of toluene giving 1.55 g (52%) of **6** as a white solid which was further purified for characterizational purposes by sublimation at 130 °C at 2 x 10^{-3} Torr: mp 163-164 °C; ^{1}H NMR (toluene-d_8) δ 0.18 (s, 6H, $SiCH_3$, $^1J_{CH}$ = 116.4 Hz, ^{13}C satellites, $^2J_{SiH}$ = 6.1 Hz, ^{29}Si satellites), 1.01 (s, 9H, $C(CH_3)_3$, $^1J_{CH}$ = 124.3 Hz, ^{13}C satellites, $^3J_{SiH}$ = 5.4 Hz, ^{29}Si satellites), 2.12 (t, 2H, $N(CH_2)_3$, $^3J_{HH}$ = 5.3 Hz, $^1J_{CH}$ = 138.4 Hz, ^{13}C satellites), 2.85 (t, 2H, $SiNCH_2$, $^3J_{HH}$ = 5.3 Hz, $^1J_{CH}$ = 135.0 Hz, ^{13}C satellites); ^{13}C NMR (toluene-d_8) δ -2.9 (qm, $SiCH_3$, $^1J_{CH}$ = 117.3 Hz, $^1J_{SiC}$ = 54.8 Hz, ^{29}Si satellites), 20.6 (s, $C(CH_3)_3$, $^1J_{SiC}$ = 59.3 Hz, ^{29}Si satellites, $^1J_{CC}$ = 31.0 Hz, ^{13}C satellites), 27.7 (q sept., $C(CH_3)_3$,

$^1J_{CH}$ = 124.3 Hz, $^3J_{CH}$ = 5.7 Hz, $^1J_{CC}$ = 31.0 Hz, ^{13}C satellites), 42.6 (tt, $SiNCH_2$, $^1J_{CH}$ = 135.2 Hz, $^2J_{CH}$ = 1.8 Hz), 58.8 (tm, $N(CH_2)_3$, $^1J_{CH}$ = 136.4 Hz); ^{27}Al NMR (toluene-d_8, 80 °C) δ 131 ± 1 ($\Delta\nu_{1/2}$ = 3030 Hz); ^{29}Si NMR (toluene-d_8) δ 3.91; HRMS (EI) calcd for $C_{24}H_{57}N_4Si_3Al$ (M^+) *m/z* 512.37064, found 512.37033; LRMS (EI) *m/z* (ion, relative intensity) 512 (M^+, 7), 497 ($M-CH_3^+$, 3), 455 (M-*tert*-Bu^+, 100), 397 (M-$SiMe_2$-*tert*-Bu^+, 1), 368 (3), 344(1), 341 (1), 325 (5), 298 (1), 283 (3), 199 (5), 178 (5), 169 (3), 158 (3), 144 (3), 73 ($SiMe_3^+$, 61), 59 (10), 57 (*tert*-Bu^+, 25); CIMS (positive ion detection) *m/z* 513 ($M+H^+$, 100), 489 (18), 455 (M-*tert*-Bu^+, 18); CIMS (negative ion detection) *m/z* 529 ($M+NH_3^-$, 17), 511 ($M-H^-$, 82), 487 (100); IR (KBr pellet, 4000-400 cm^{-1}) ν 2955 vs, 2930 vs, 2895 s, 2887 s, 2857 vs, 2817 s, 1472 s, 1465 s, 1404 m, 1400 m, 1388 w, 1361 w, 1251 s ($\delta_s CH_3$), 1127 m, 1112 m, 1080 w, 1060 w, 1048 m, 1006 w, 968 s, 937 m, 828 vs, 768 s, 668 w, 660 w, 599 w, 570 w, 527 w. Anal. Calcd for $C_{24}H_{57}N_4Si_3Al$: C, 56.19; H, 11.20; N, 10.92. Found: C, 55.65; H, 11.38; N, 10.57.

***Cis*-Bis(trimethylsilyl)azaalumatrane Dimer,[15] 5.** Compound **5** was prepared during attempts to grow single crystals of **3** from a pentane solution at -20 °C (see discussion for details). Clear plates of **5** were washed with pentane and dried in vacuum for 45 min: mp 160-165 °C dec.; ^{1}H NMR (benzene-d_6) δ 0.253, 0.255 (s, 18H, $Si(CH_3)_3$ groups, $^1J_{CH}$ = 117.9 Hz, ^{13}C satellites, $^2J_{SiCH}$ = 6.2 Hz, ^{29}Si satellites), 2.05 (ddd, 1H, *J* = 5.0, 12.4, 12.4 Hz), 2.20 (ddd, 1H, *J* = 1.5, 4.2, 12.2 Hz), 2.28-2.44 (m, 3H), 2.46-2.56 (m, 1H), 2.56-2.66 (m, 1H), 2.70-2.97 (m, 4H), 3.23-3.35 (m, 1H); ^{13}C NMR (benzene-d_6) δ 1.9, 2.0 (s, $Si(CH_3)_3$ groups, $^1J_{SiC}$ = 55 Hz, ^{29}Si satellites), 42.0, 43.8, 44.1 (s, $RNCH_2$ groups), 57.8, 62.6, 62.9 (s, $N(CH_2)_3$); ^{27}Al NMR (benzene-d_6) δ 86 ($\Delta\nu_{1/2}$ = 1930 Hz 25 °C, 1080 Hz at 70 °C); ^{29}Si NMR (benzene-d_6) δ -1.30, -2.94; HRMS (EI)

calcd for $C_{24}H_{62}N_8Si_4Al_2(M^+)$ *m/z* 628.38052, found 628.37925; LRMS (EI) *m/z* (ion, relative intensity) 628 (M^+, 2), 613 ($M-CH_3^+$, 1), 573 (1), 513 ($M-CH_2CH_2NSiMe_3^+$, 4), 511 (2), 471 (1), 411 (1), 398 (5), 315 (4), 313 (2), 260 (1), 188 (21), 171 (25), 159 (11), 157 (12), 147 (10), 143 (6), 117 (11), 116 (93), 115 (19), 102 (25), 100 (17), 99 (99), 87 (16), 85 (10), 75 (28), 74 (12), 73 ($SiMe_3^+$, 100), 70 (15), 59 (16), 58 (14), 56 (17), 45 (17), 44 (81), 43 (16), 42 (12); CIMS (positive ion detection) *m/z* (ion, relative intensity) 629 ($M+H^+$, 100), 363 (13), 291 (36), 219 (7); CIMS (negative ion detection) *m/z* (ion, relative intensity) 627 ($M-H^-$, 100); IR (KBr pellet, 4000-400 cm^{-1}) ν 3277 w (νNH), 3267 w (νNH), 2946 vs, 2891 vs, 2856 vs, 2829 s, 2799 m, 1477 w, 1461 m, 1451 vw, 1437 vw, 1396 w, 1370 w, 1353 m, 1332 m, 1300 m, 1257 sh, 1242 vs, 1209 m, 1153 m, 1116 s, 1074 vs, 1055 w, 1039 s, 1009 s, 969 vs, 952 vs, 925 w, 900 s, 845 vs, 833 vs, 799 s, 744 vs, 668 s, 643 s, 585 s, 549 vs, 508 vs, 481 s; Anal. Calcd for $C_{24}H_{62}N_8Si_4Al_2$: C, 45.82; H, 9.93; N, 17.81. Found C, 45.73; H, 9.48; N, 17.62.

Single-Crystal X-ray Diffraction Studies of 3 and 5. Colorless crystals of **3** and **5** were mounted in 0.5 mm glass capillaries in a nitrogen-filled glove box and flame-sealed. The diffraction intensity data for **3** and **5** were collected on Rigaku AFC6R and Siemens P4RA instruments, respectively, both equipped with low-temperature devices. Crystal data, experimental conditions for data collection, solution and structure refinement are listed in Table I. The intensity of three standard reflections remained constant within the errors of measurement throughout data collection for **3** while a decay correction was applied for **5**. Lorentz and polarization corrections were applied. Azimuthal scans of several reflections indicated no need for an absorption correction for **3** while a semi-empirical absorption correction based on a series of ψ-scans was

applied in the case of **5**. The structures of **3** and **5** were solved by direct methods and refined by a full-matrix least-squares method, using TEXSAN (VAX)[16] and SHELXTL PLUS (VMS),[17] respectively. All non-hydrogen atoms were refined with anisotropic thermal parameters. All hydrogens in **3** were placed and refined. For **5**, the C-H hydrogen atoms were fixed with distances of 0.96 Å. The N-H hydrogen atoms were allowed to refine isotropically with free positional parameters. Neutral atom scattering factors were taken from common sources.[18] Positional and thermal parameters are listed in the supplementary materials.

Table I. Crystal, Data Collection, Solution and Structure Refinement Parameters for **3** and **5**

	3	**5**
formula	$AlC_{15}H_{39}N_4Si_3$	$Al_2C_{24}H_{62}N_8Si_4$
fw	386.74	629.11
crystal size (mm)	0.2 x 0.4 x 0.5	0.3 x 0.2 x 0.2
crystal system	monoclinic	monoclinic
space group	$P2_1/c$ (no. 14)	$P2_1/n$ (no. 14)
a (Å)	13.503 (5)	12.134 (3)
b (Å)	10.621 (4)	17.049 (4)
c (Å)	17.840 (6)	18.297 (5)
β (deg)	93.29 (3)	100.02 (2)
volume (A^3)	2554 (2)	3726 (2)
Z	4	4
d_{calcd} (g/cm^3)	1.006	1.122
$F(000)$	812	1376
abs coeff (cm^{-1})	2.18	21.36
diffractometer	Rigaku AFC6R	Siemens P4RA
radiation	MoK_α (λ = 0.71069 Å)	CuK_α (λ = 1.54178 Å)
temperature (°C)	-20	-50
monochromator	graphite crystal	graphite crystal
2θ scan range (deg)	5.0-55.1	5.0-115.0
scan type	2θ-θ	2θ-θ
scan speed (deg/min)	16.0 (in ω)	11.7-35.2 (in ω)

Table I. Continued

scan range (deg)	1.05 + 0.30 tan θ	1.00 plus K_α-separation
collected reflcns	9762	10394
independent reflcns	4923	5006
R_{init} (%)	11.8	2.7
observed reflcns, n_{obs}	1528 (I > 3.0 σ (I))	4085 (I > 4.0 σ (I))
weighting scheme, w^{-1}	$[\sigma^2(F_o^2)]/4F_o^2]$	$\sigma^2(F_o) + 0.0003\ (F_o)^2$
no. of variables, n_{var}	208	412
data-to-parameter ratio	7.4:1	9.9:1
largest peak ($e \cdot A^{-3}$)	0.22	0.26
largest hole ($e \cdot A^{-3}$)	-0.19	-0.22
R(%)[a]	5.2	4.6
R_w(%)[b]	5.8	4.3
GOF[c]	1.8	1.4

[a] $R = \Sigma||F_o|-|F_c||/\Sigma|F_o|$. [b] $R_w = [\Sigma w(|F_o|-|F_c|)^2/\Sigma w(F_o)^2]^{1/2}$. [c] $GOF = [\Sigma w(|F_o|-|F_c|)^2/(n_{obs}-n_{var})]^{1/2}$.

RESULTS AND DISCUSSION

Syntheses. The synthesis of silylated tetramines **9** and **11**, which have attracted considerable attention recently,[19] was accomplished here by the reaction of a silylchloride with a lithium salt of a tetramine or by the direct reaction of tetramine with a silylchloride in the presence of a base, the former giving a slightly higher yield. The silylation of tripodal triamines by the latter method was reported recently.[13a]

The monomeric azaalumatrane **6** was synthesized by the transamination reaction of **7** with the tetramine **11** according to eqn. 1, in 52% yield. **6** can be

Reaction 1:

$$\underset{\mathbf{7}}{1/2[Al(NMe_2)_3]_2} + \underset{\mathbf{11}}{(tert\text{-}BuMe_2SiNHCH_2CH_2)_3N} \xrightarrow{\text{toluene}} 3\,Me_2NH + \mathbf{6}$$

purified by crystallization from toluene. The ^{1}H, ^{13}C, ^{27}Al and ^{29}Si NMR data are similar for **3** and **6** and they are consistent with a three fold symmetry of these molecules. The monomeric alumaazatranes **3** and **6** are moisture sensitive solids that are easily sublimed at reduced pressure. It is worthy of note that the transamination reaction of tetramine **11** with monomeric amide $Al[N(SiMe_3)_2]_3$, **8b**, even after several hours of reflux did not give any expected alumaazatrane **6** and by ^{1}H NMR spectroscopy only the starting compounds were observed in the reaction solution. For the sake of argument, let us assume that a proton transfer from the NH groups of the tetramines **9** and **11** to the nitrogen of the NR_2 groups of amides **8a** and **8b** is a more important step in the transamination than a nucleophilic attack of the lone electron pair of the

tetramine NHR groups on the aluminum center. This assumption gains credibility from the observed higher reactivity of the silylated tetramines in the transamination of $[Al(NMe_2)_3]_2$ compared with alkylated tetramines such as Me_3tren and *iso*-Pr_3tren. Moreover, the reactivity of metal amides with protic reagents increases with their pK_a.[3] Thus in silylated tetramines, the basicity of the NHR nitrogens is diminished by π-bonding to silicon and conversely the acidity of the NHR protons is enhanced. In contrast, the opposite electronic situation occurs in alkylated tetramines. The inertness of $Al[N(SiMe_3)_2]_3$ can thus be attributed to the diminished basicity of the nitrogen lone electron pairs due to their π-bonding to silicons and also to a steric shielding of the aluminum center by the bulky $SiMe_3$ groups. Similarly, the monomeric amide Al(N-*iso*-$Pr_2)_3$, **8a**, failed to react with $(Me_3SiNHCH_2CH_2)_3N$, **9**. In this case, steric blocking could be the major reason for its inertness.

Formation of the dimeric azaalumatrane **5** by a desilylation of **3** (summarized in reaction 2) is a novel example of the degree of oligomerization being influenced by the bulkiness of ligands on the equatorial nitrogens. Thus, relaxing the steric congestion in **3** by removal of one of the three $SiMe_3$ groups

Reaction 2:

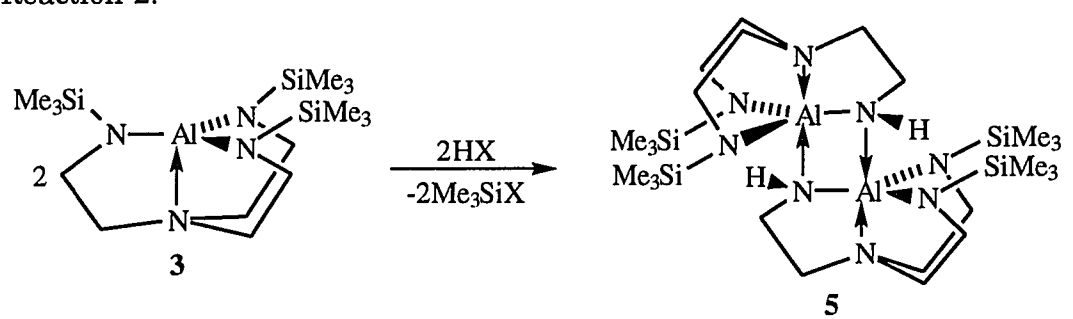

leads to dimerization and, as was confirmed by the X-ray diffraction study of **5** (vide infra) an unusual cis configuration at the central four-membered ring. The presence of the trans isomer in the mother liquor was ruled out by ^{13}C NMR spectroscopy. Heating a benzene-d_6 solution of **5** in a sealed NMR tube to 130° for 48 h caused no observable transformation of the cis-isomer to its trans counterpart.

The true nature of the desilylation process (reaction 2) remains unclear so far. One possibility is that adventious water caused a partial hydrolysis of **3**. Militating against this option are our consistent efforts to maintain anhydrous conditions throughout the reaction and workup, and also our inability to repeat the preparation by a controlled hydrolysis of **3** with 0.5 equivalent of water by several methods including the addition of the H_2O to a pentane solution of **3** at -78 °C, slow diffusion of water vapors from ice at -20 °C, and slow release of water of crystallization from $CuSO_4 \cdot 5H_2O$. In all cases, we observed by ^1H NMR spectroscopy a mixture of the parent amine **9** as a product of complete hydrolysis, and unreacted **3**. Also the amount of dimer is larger than what would be expected if only adventious water was present. Recently, a very

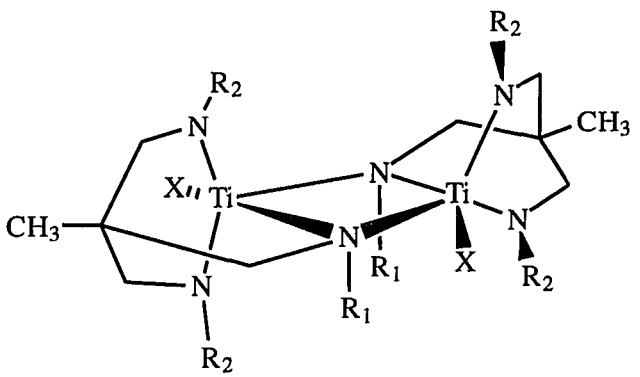

	R_1	R_2	X
12a	H	$SiMe_3$	Cl
12b	H	$SiMe_3$	Br
12c	Me	Me	Cl
12d	Me	Me	Br

similar observation was published[13b] for related compounds **12a,b** containing a tripodal ligand. The explanation for the formation of a desilylated dimer given by the authors involved a reaction with the solvent protons (THF) and excluded the hydrolytic pathway. Considering the coordinative unsaturation and Lewis acidity of the TMP aluminum center in **3** which might even be enhanced in the course of reaction by temporary breaking of the transannular Al-N(apical) bond (**3a** in Scheme I), a reaction of **3** with the activation of solvent molecules may emerge as a plausible explanation. The lengthening of the transannular bond as shown in the intermediate **3a** is made reasonable by the sterically

Scheme I

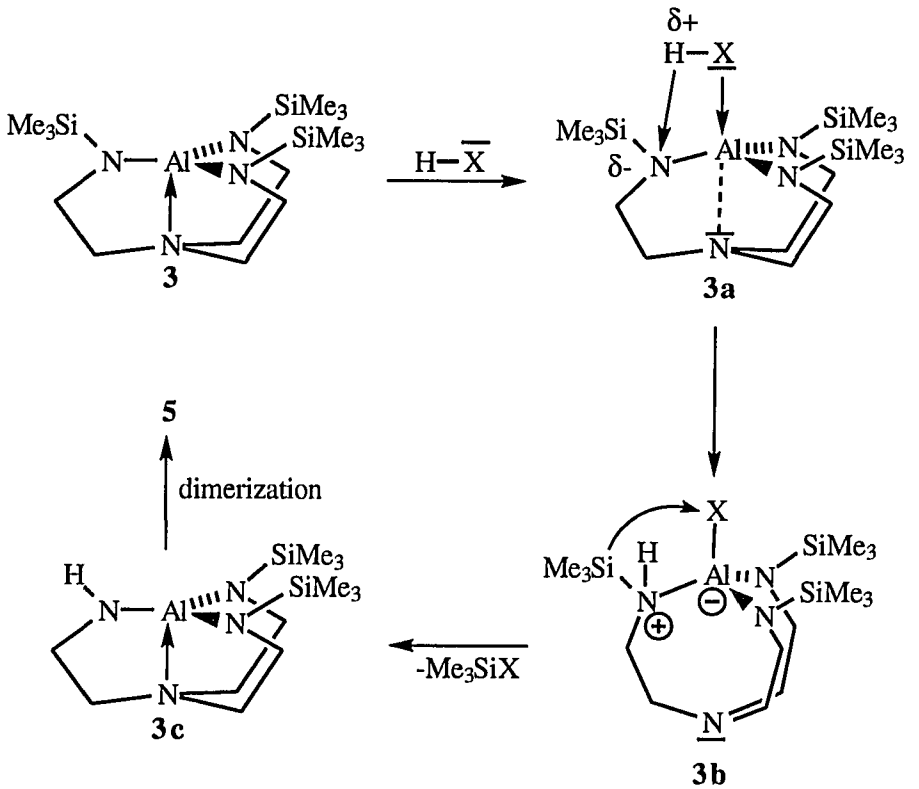

induced lengthening of the transannular interaction in the azasilatrane from **13** to **14** in reaction 3 by the bulky $SiMe_3$ groups.[20c] The suggested pathway in

Reaction 3:

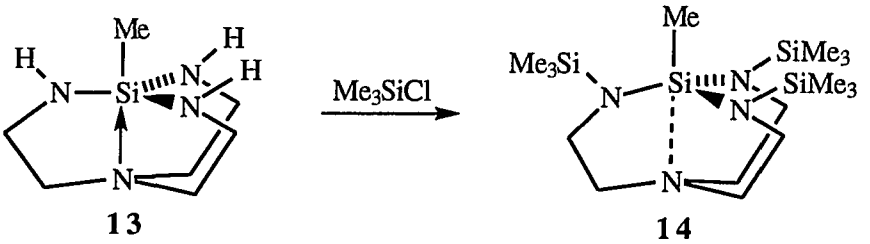

13 **14**

Scheme I involves intermediate **3b** with a protonated equatorial nitrogen. Such species have been characterized by X-ray diffraction methods in the case of azasilatranes **15a,b**.[20a,b] An example of the tendency of aluminum to increase

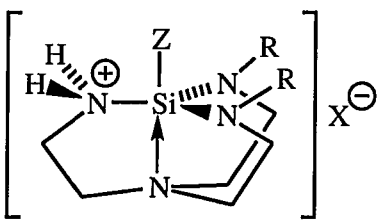

	R	Z	$X^{\ominus}$
15a	$SiMe_3$	H	$SCN^{\ominus}$
15b	H	H	$N_3^{\ominus}$

its coordination number was realized in the reaction of $AlMe_3$ with tren, **10**, using CH_3CN as a solvent.[21] The reaction resulted in dimerization of CH_3CN and its coupling with tren. The aluminum atom attained the coordination number of 6 in the product **16**.

Structural Considerations. The molecular structure of the monomeric azaalumatrane **3** shown in Figure 1 features a central aluminum atom which is in a TMP coordination geometry. This structure represents the first example of the TMP coordination mode for aluminum and it is one of few for the main-group elements in general. Similar compounds reported so far are

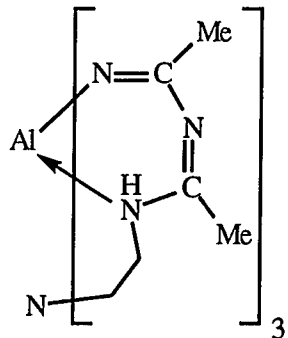

16

the 4,6,11-tricarbametallatranes **17a,b**, of which only the gallium derivative was structurally characterized.[22] For the transition metals, the first TMP complex verified by X-ray investigation was reported for nickel in $Ni(Ph_2PCH_2CH_2)_3N$.[23] Distorted TMP structures were found for Cu complexes[24] with unsymmetrical ligands. Recently, the molecular structure of the V(III) azatrane **18** with the TMP vanadium center was reported.[19c]

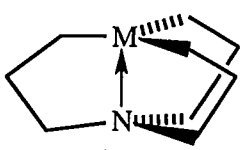

	M
17a	Al
17b	Ga

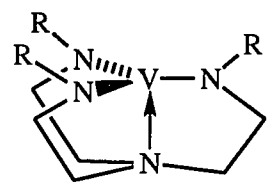

18

R = $SiMe_2$-*tert*-Bu

Compound **3** exists in a propeller-like conformation, possessing a pseudo-three fold symmetry with a pseudo C_3 axis through the Al and apical N atoms. This conformation implies the presence of Λ and Δ enantiomers in the solid state as depicted below. Two triangular units, AlN(2)N(3)N(4) and N(1)C(1)C(3)C(5), are nearly eclipsed with an average torsional angle of only 3.3(6)°. Three five-membered rings are in an envelope conformation with the

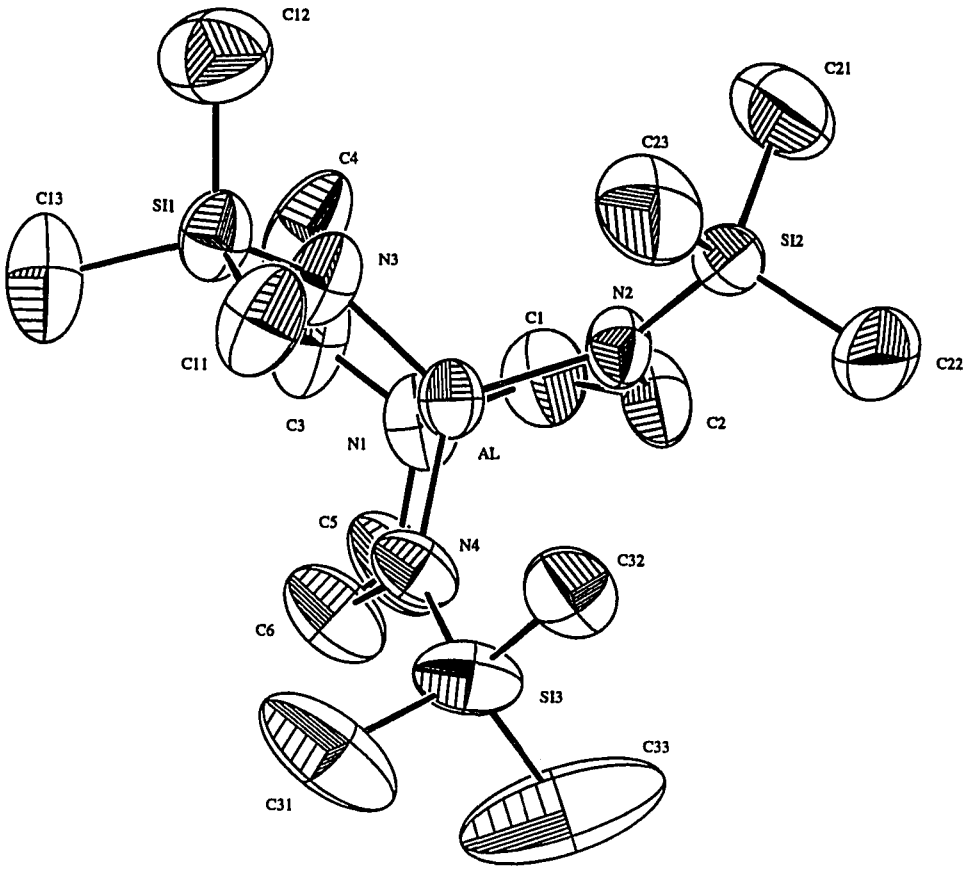

Figure 1. The molecular structure of monomeric $Al(Me_3SiNCH_2CH_2)_3N$, **3**, (a) top view showing the propeller-like conformation of the molecule.

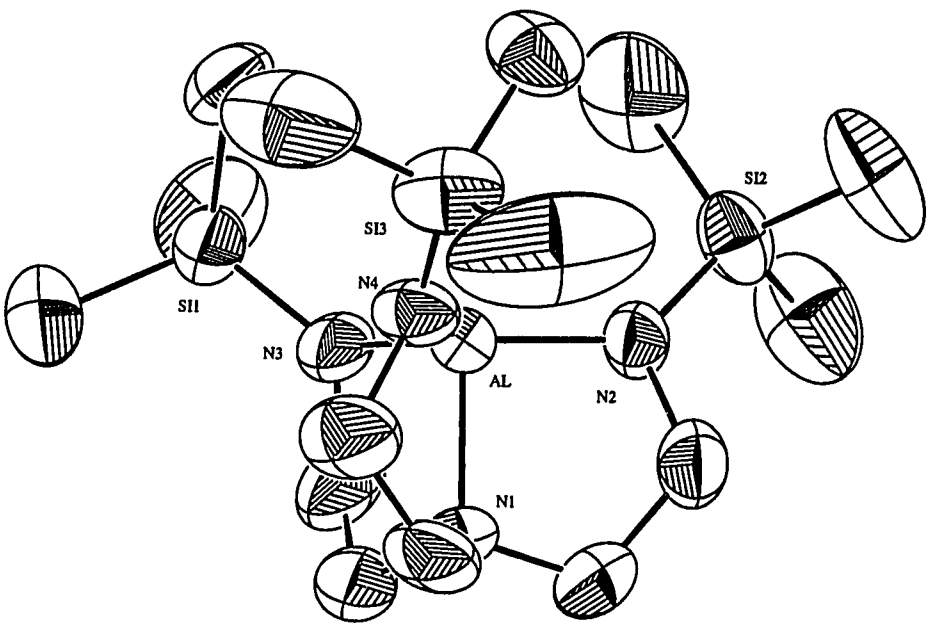

Figure 1. Continued (b) side view showing the TMP geometry around aluminum.

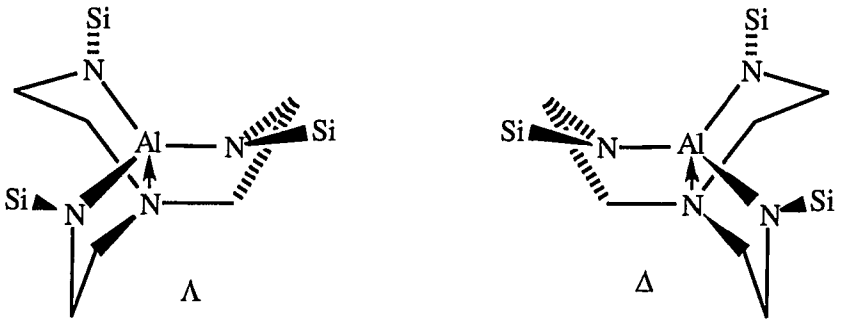

"flap" atoms C(2), C(4), and C(6) displaced out of the envelop plane by 0.59 Å. The equatorial nitrogens are planar, the average of the sum of angles around them being 359.5(5)°. Planarity of these nitrogens can be attributed to engagement of nitrogen electron lone pairs in 2p-3d π-bonding with the adjacent silicon. The lack of inversion at the equatorial nitrogens necessarily connects the movement of each bulky $SiMe_3$ groups with the conformational inversion of the five-membered ring to which it is attached. This structural feature supports our suggestion of a concerted mechanism of racemization ($\Delta \rightleftharpoons \Lambda$) for the closely related boron derivative **2**[6] from an analysis of its variable temperature ^1H NMR spectra. Unfortunately, similar experiments for **3** (and also **6** which has even bulkier substituents) revealed that these molecules are freely fluxional down to -95 °C on the NMR time scale. This prevented us from evaluating the activation entropy $\Delta S^{\ddagger}$ for the barriers to racemization, for which a negative value would substantiate the concerted mechanism. The less restricted fluxionality of **3** and **6** can be attributed to the substantially larger size of the aluminum atom in comparison with the smaller boron (tetrahedral covalent radii[25a] 1.230 and 0.853 Å, respectively). Hence, longer Al-N bonds (Table II) in comparison with B-N bonds render

azaalumatrane cage less sterically compact and relax the strain which was found in **2**.[6]

The coordination geometry of the aluminum center very closely approaches the ideal TMP geometry. Angles between nitrogens in the basal triangular face are the same (within 2σ) and their average is 119.9(3)° (Table II). The aluminum is drawn slightly below the plane of the basal nitrogens (0.07 Å) resulting in N(basal)-Al-N(apical) angles which lie within 2σ of each other and average 92.1(3)°. A similar angle of 91.3(1)° was found in the related compound **19**.[26a] The axial Al-N bond distance in **3** is 1.983(6) Å which

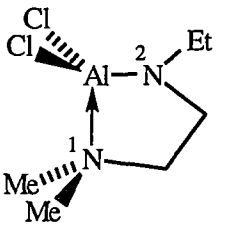

19

is slightly longer than the sum of tetrahedral covalent radii, 1.949 Å.[24a] Nevertheless, the axial Al-N distance is comparable to the Al-N(1) bond length of 1.963(2) Å in **19**.[26a] Moreover the values of the Al-N distances found in compounds in which both Al and N are four-coordinate span a remarkably wide range 1.83-2.13 Å.[1,2,4,8b,26-36] Typical values usually fall in the 1.91-1.97 Å range.[4] Bond distances in the basal AlN_3 triangle are the same (within 2σ) and their average is 1.809(6) Å. This is an example of a rather rare bonding situation in Al-N compounds, in which four-coordinate Al is bonded to three-coordinate N.[8b,26a,36,37] The change in the hybridization of N from sp^3 to sp^2 must largely account for the shortening of the Al-N bonds because 2p-3d

Table II. Selected Bond Distances (Å) and Angles (deg) for **3**[a]

Al-N(1)	1.983(6)	Si(1)-N(3)	1.697(6)
Al-N(2)	1.805(5)	Si(2)-N(2)	1.684(5)
Al-N(3)	1.812(6)	Si(3)-N(4)	1.690(6)
Al-N(4)	1.810(6)		
N(2)-Al-N(3)	119.6(3)	N(1)-Al-N(2)	92.3(3)
N(2)-Al-N(4)	120.2(3)	N(1)-Al-N(3)	92.3(3)
N(3)-Al-N(4)	119.9(3)	N(1)-Al-N(4)	91.8(3)
C(3)-N(1)-C(5)	114.9(7)	Si(2)-N(2)-Al	135.1(4)
C(1)-N(1)-C(5)	114.3(6)	Si(2)-N(2)-C(2)	118.9(5)
C(1)-N(1)-C(3)	112.5(6)	Al-N(2)-C(2)	105.9(4)
Si(1)-N(3)-Al	134.4(3)	Si(3)-N(4)-Al	133.7(3)
Si(1)-N(3)-C(4)	119.4(5)	Si(3)-N(4)-C(6)	120.2(5)
Al-N(3)-C(4)	105.4(4)	Al-N(4)-C(6)	105.6(5)

[a]Numbers in parentheses are estimated standard deviations in the least significant digits.

π-bonding between Al and N is apparently prevented by competitive π-bonding from N to Si and also by large twist angles (60-70°) between the basal AlN_3 plane and the Al-N(basal)-Si planes. Comparable values were found for the terminal Al-N distances in **7**[8b] (1.802(2) Å) and in an adamantane-like cage $Al_4Cl_4(NMe_2)_4(NMe)_2$ (1.79(3) Å[36]). The Al-N(2) bond length found in **19** is even shorter (1.770(2) Å[26a]). The Si-N bond distances in **3** (average 1.690(6) Å) are the same (within 3σ) and are slightly but significantly shorter than the Me_3Si-

N bond lengths in **14** (1.726(5) Å[20c]), $ClV(Me_3SiNCH_2CH_2)_3N$ (1.737(6) Å[19d]), **8b** (1.75(1) Å[10c]), and in **13a** (1.755(2) Å[20a]). The triptych structure of **3** can be contrasted with the previously mentioned **16**,[21] in which the aluminum atom does not interact with the apical nitrogen and instead satisfies its coordination needs by bonding to solvent moieties that have become incorporated into the chelating ligand by reaction. The present example **3** emphasizes the importance of the bulky $SiMe_3$ groups for stabilizing the transannular bond and tetracoordination of the aluminum center, and it also points to the potential possibility of the aluminum center to increase its coordination number (perhaps with a small ligand such as H^-) via the sterically crowded but vacant axial coordination site.

The molecular structures of **3** and **5** offer a rare opportunity to compare structural parameters in two closely related molecules with the aluminum atoms in two different coordination environments. The molecular structure of **5** is depicted in Figure 2 and selected bond distances and angles are collected in Table III. The heptacyclic dimer consists of two azaalumatrane units connected in an unusual cis fashion. The replacement of one $SiMe_3$ groups in **3** by hydrogen decreased the steric hindrance sufficiently to allow association of two units into a dimer. The bridging NH groups together with two aluminums form a puckered central four-membered ring in which the Al-N(4)-N(4') and Al'-N(4)-N(4') planes are separated by 149°. The aluminum atoms are in a distorted trigonal bipyramidal coordination sphere. This structure is to our knowledge the first example of five-coordinate aluminum ligated solely by nitrogens. In contrast to **3**, the Al atoms in **5** are

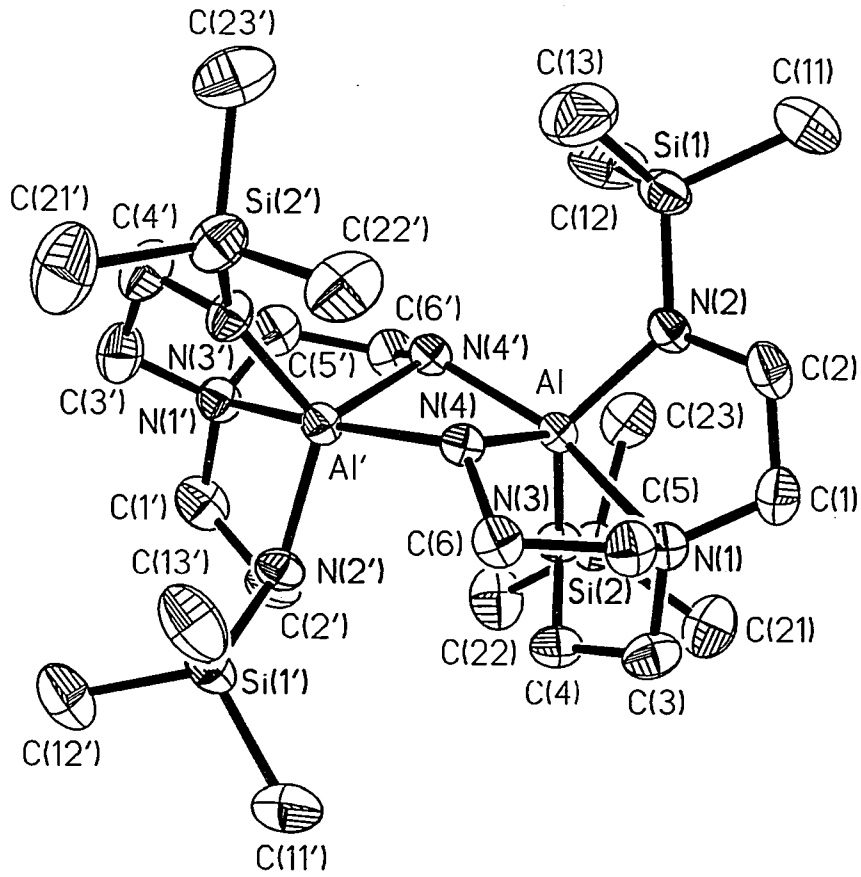

Figure 2. The molecular structure of $[Al(Me_3SiNCH_2CH_2)_2(HNCH_2CH_2)N]_2$, **5**, showing the atom labelling scheme.

Table III. Selected Bond Distances (Å) and Angles (deg) for **5**

Al-N(1)	2.161(2)	Al'-N(1')	2.174(2)
Al-N(2)	1.858(2)	Al'-N(2')	1.859(2)
Al-N(3)	1.858(2)	Al'-N(3')	1.853(2)
Al-N(4)	2.004(2)	Al'-N(4')	2.014(2)
Al-N(4')	1.968(2)	Al'-N(4)	1.967(2)
Si(1)-N(2)	1.712(2)	Si(1')-N(2')	1.705(2)
Si(2)-N(3)	1.705(2)	Si(2')-N(3')	1.720(2)
N(1)-Al-N(2)	86.2(1)	N(1')-Al'-N(2')	82.6(1)
N(1)-Al-N(3)	82.5(1)	N(1')-Al'-N(3')	86.6(1)
N(1)-Al-N(4)	81.6(1)	N(1')-Al'-N(4')	81.3(1)
N(1)-Al-N(4')	160.5(1)	N(1')-Al'-N(4)	159.8(1)
N(4)-Al-N(4')	80.3(1)	N(4')-Al'-N(4)	80.1(1)
Al-N(4)-Al'	95.3(1)	Al'-N(4')-Al	94.9(1)
N(2)-Al-N(3)	125.4(1)	N(2')-Al'-N(3')	124.4(1)
N(2)-Al-N(4)	111.3(1)	N(3')-Al'-N(4')	111.1(1)
N(3)-Al-N(4)	119.4(1)	N(2')-Al'-N(4')	120.7(1)

[a]Numbers in parentheses are estimated standard deviations in the least significant digits.

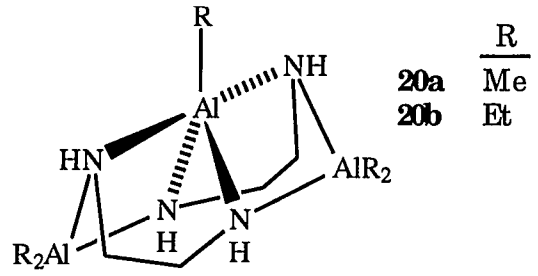

	R
20a	Me
20b	Et

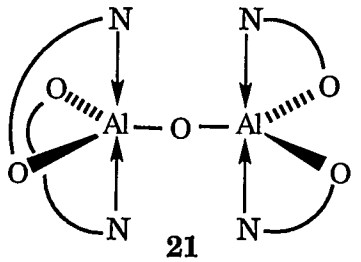

21

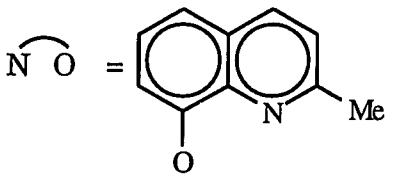

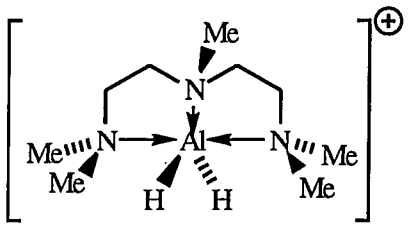

22

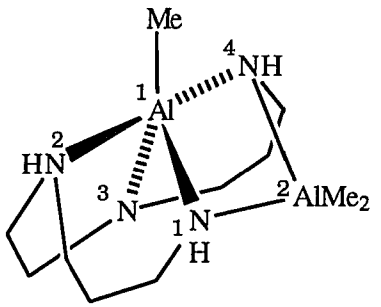

23

drawn out of the azatrane cages toward the bridging nitrogens. The axes of the trigonal bipyramids formed by the N(1)-Al-N(4') and N(1')-Al'-N(4) moieties are bent at 160.5(1)° and 159.8(1)° angles, respectively. This distortion is a result of steric strain imposed by the chelating tetradentate tripodal ligands. Comparable examples of distorted TBP geometries are found in **20**,[30a] **21**,[38] **22**,[39] and **23**[40] where the angles N_{ax}-Al-N_{ax} range from 149.2(1)° to 169.2(2)°.

The central Al_2N_2 array of **5** forms a puckered rectangle with a pseudo two-fold axis through its center. The hydrogen atoms of the NH groups were not located in the difference map, but the nitrogen atoms in the central ring are clearly pyramidal with angle sums of 335.7(2)° and 336.8(2)°. This

contrasts to a planar central ring in **12a**,[13b] in which NH hydrogens were not found by the X-ray experiment. The Al-N bonds connecting the two azaalumatrane units (Al-N(4') and Al'-N(4)) are shorter by approximately 2% (1.967(2) Å) than the Al-N(bridging) distances within the units (2.014(2) and 2.004(2) Å). This suggests strong bonding between the two units, which agrees with the rigidity of the dimer as observed by ^{1}H and ^{13}C NMR spectroscopies. A similar bonding pattern was reported for **12a-d**.[13b] Average angles within the Al_2N_2 ring are 80.2(1)° and 95.1(2)° on aluminums and nitrogens, respectively. Even more acute angles (73.0(2)°) on the Ti centers and considerably wider angles (107.0(2)°) on the nitrogens were found in **12c**.[13b] This difference in distortion of the central rings in **5** and **12c** can be explained by less strain exerted by the longer and more flexible arms of the ligand in **5**. By comparison, angles in the Al_2N_2 units of $[R_2Al\text{-}NR'_2]_2$ (a large class of compounds) are in general close to 90°, ranging from 85.3(1)° to 90.6(1)° at Al and from 89.4(2)° to 94.7(1)° at N.[1a,2,4a,8b,27a,c,29a,31]

The coordination environment of the nonbridging equatorial nitrogens is nearly planar, with the sum of angles around them ranging from 356.6(2)° to 360.0(2)°. This planarity reflects Si-N and Al-N π-bonding effects.

The Al-$NSiMe_3$ distances in **5** are the same (within 3σ) and their average length is 1.857(2) Å which is longer by ~3% than the corresponding bond lengths in **3**. This lengthening can be ascribed to the increase of the aluminum coordination number from four to five. A comparable bond distance (Al(1)-N(3)) of 1.826(2) Å was found in **23**.[40] The transannular bonds (Al-N(1), Al-N(1')) in the two units of **5** are slightly but significantly different (2.161(2) Å and 2.174(2) Å). This difference, which may be caused by packing

forces, demonstrates a certain flexibility of those bonds. The Al-N distances fall in the range for the analogous bond distances in other compounds containing a five-coordinate TBP aluminum and a four-coordinate axial nitrogen. The upper limit of the range is 2.18(1) Å for $AlH_3 \cdot 2NMe_3$[41] and other examples include **20a** (2.058(2), 2.073(2) Å[30a]), **21** (2.054(5)-2.110(5) Å[38]), **22** (2.158(7) Å[39]), and **23** (2.055(2), 2.135(2) Å[40]). In the related tetrameric alumatrane $[Al(OCH_2CH_2)_3N]_4$,[42] the axial Al-N distance in the five-coordinate units is 2.069(5) Å.[43] Comparison of the transannular Al-N(1) bond distance in **3** with the corresponding distances in **5** shows an approximately 10% lengthening upon increasing the TMP coordination sphere of aluminum to TBP. This considerably larger increase of the axial bond distances in **5** compared with the smaller increase of the pseudo-equatorial bonds demonstrates the substantial *trans* influence of an apical ligand along the TBP axis compared with its *cis* influence.

At this time, we have no convincing rationale for the unusual preferential formation of the cis diastereomer of **5** over the trans. The reasons offered for the exclusive cis arrangement of **12**[13b] suggest that a puckered central ring in the cis isomer can more easily accommodate the strain caused by the chelating tripodal ligand in contrast to a planar array implied for the trans configuration. However, we have no reason to believe that a trans arrangement of substituents necessitates a planar ring. Moreover, a planar ring can bear cis substituents as shown for $[R_2Al\text{-}NHBp]_2$ (R = Me, *iso*-Bu, Bp = 2-aminobiphenyl)[31c] by X-ray crystallography. As an additional example of an unusual cis configuration, the dimeric gallium derivative **24**[44] can be cited.

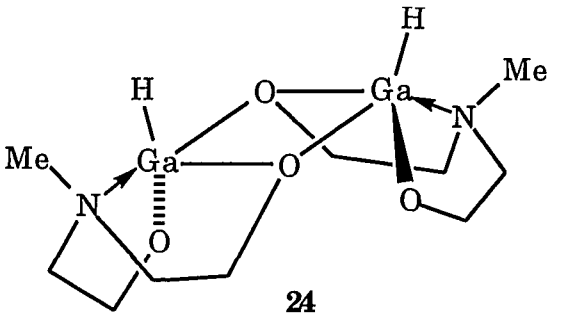

24

Mass Spectra. The EI mass spectra of the tetramines **9** and **11** are characteristic for amines in that no M^+ peaks are observed. However, **9** shows a strong and **11** exhibits a weak $M+H^+$ parent peak, which is also a base peak in the CI-NH_3 spectrum of **11**. Similarly to our previous observations for the group 13 azatranes[6], the molecular $M+H^+$ peak is a base peak in the CI-NH_3 spectrum of **6**. The dimer **5** gives a weak molecular peak in EI mass spectra while under milder NH_3 chemical ionization conditions, $M+H^+$ and M^+ are the most intense signals in the spectrum.

Infrared Spectra. The assignment of the Al-N stretching frequency in the IR spectra of **3**, **5**, and **6** is not a trivial task owing to strong mixing of the normal modes of the azatrane framework as was shown for analogous silatranes.[45] The presence of two stretching coordinates, Al-N_{ax} and Al-N_{eq} in **3**, and even more coordinates in **5**, together with coupling of the Al-N_{eq} and Si-N stretches (which are of a similar energy[46a]) complicate the spectral assignment. Furthermore, the values for Al-N stretching modes were observed in a rather broad region, namely, 392 cm^{-1} in $Al[N(SiMe_3)_2]_3$,[10a] 460 cm^{-1} in $(Me_3N)_2{\cdot}AlH_3$,[46b] 533 cm^{-1} in $Me_3N{\cdot}AlH_3$,[46b] 565 cm^{-1} in $Me_3N{\cdot}AlCl_3$,[46a] 582 cm^{-1} in $(Me_3Si)_3N{\cdot}AlCl_3$,[46a] 460-587 cm^{-1} in the six-membered ring compounds $(R_2AlNR_2')_3$,[27a,32] 652, 688 cm^{-1} in the tetrahedral

$Al(NH_2)_4^-$, and 726, 742 cm^{-1} in octahedral $[Al(NH_3)_4Cl_2]^+$.[3] In the IR spectra of **3** and **6**, there are several bands in the region 700-500 cm^{-1} of which some may have predominant contributions from the Al-N vibrations.

Several characteristic bands of the $SiMe_3$ group were tentatively assigned by comparison with literature data.[47] The presence of NH groups in **5** was confirmed by two weak bands at 3277 and 3267 cm^{-1} for the νNH mode.

NMR Spectra. The assignment of signals in the ^1H NMR spectra of silylated tetramines **9** and **11** was facilitated by the presence of a three-bond coupling (~7 Hz) between the NH protons and the adjacent CH_2 protons. This coupling cannot be seen in the spectra of alkylated tren derivatives such as Me_3tren[48] and *iso*-Pr_3 tren.[49] Silicon bonded to an NH group engages the lone electron pair on N in π-bonding, thus changing the hybridization of N from sp^3 to sp^2 which increases the s-character in the H-N-CH_2 bonds and results in an observable scalar coupling. The formation of transannulated azatrane frameworks **3** and **6** is accompanied by a small downfield shift of $SiNCH_2$ signals and by an upfield shift of $N(CH_2)_3$ signals with respect to the free amines. In all monomeric group 13 azatranes,[6] we found the $N(CH_2)_3$ protons at higher field relative to the $SiNCH_2$ protons. This accords with our observations in azasilatranes,[11a,20c] azastannatranes,[50] and transition azametallatranes.[51] As in the ^1H NMR spectra of **9** and **11**, silylation of the NH groups caused an appearance of a two-bond coupling H-N(Si)-CH_2 (~2.5 Hz) in the proton-coupled ^{13}C NMR spectra. This made an assignment of the ^{13}C signals straightforward revealing an upfield position of the $SiNCH_2$ carbon signals relative to the $N(CH_2)_3$ carbons. This order is retained upon the formation of azatranes.[6,11,20a,52] In monomeric azatranes **1**, **2**, **3** and **6**, the

$RNCH_2$ carbons appear at a lower field than in the parent tetramines, with boron causing larger downfield shifts in agreement with its higher electronegativity. A different situation is encountered for $N(CH_2)_3$ signals, wherein boron causes downfield shifts while aluminum moves them upfield.

The magnitude of the one-bond C-H coupling constant in methylene groups is a useful indicator of the formation of a transannulated cage structure. While in the free tetramines **9** and **11** the $^1J_{CH}$ coupling in the $SiNCH_2$ methylenes is higher than for $N(CH_2)_3$, in azatranes **3** and **6** these magnitudes are reversed. This reflects a change in the character of the nitrogens adjacent to methylene groups in question. The apical nitrogen acquires a formal positive charge upon the formation of the Al-N transannular bond. The positive charge increases the electronegativity of N which in turn attracts more *p*-character in the N-C bonds and leaves more s-character in the C-H bonds, thus raising the value of the C-H coupling constant. The nitrogen in the $SiNCH_2$ groups of **3** and **6** have more amidic character because of the lone-pair electron density on them. This partial negative character, by the same mechanism as explained above, causes a lower value of $^1J_{CH}$ in the $SiNCH_2$ groups. However, compared with the magnitudes of the $^1J_{CH}$ values in the parent tren derivatives **9** and **11**, both $N(CH_2)_3$ and $SiNCH_2$ couplings are larger in **3** and **6** thus manifesting transannular bonding involving an electronegative metal center. The magnitudes of the C-H coupling constants in **3** and **6** fall in the region observed for azaboratranes,[6] azasilatranes,[20a,11b] and silatranes.[52]

A dimeric structure for **5** in solution was confirmed by its ^1H, ^{13}C and ^{29}Si NMR spectra. It is not possible to decide on the basis of symmetry arguments

and the number and splittings of the signals whether the azaalumatrane **5** possesses a cis or a trans configuration in solution because both diastereomers would give the same number of signals. The ^{1}H NMR spectrum of **5** closely resembles that of **4**[6] in that 12 diastereotopic methylene proton signals show an array of partially overlapped multiplets. In spite of our efforts, the NH proton signals could not be located, probably due to an overlap with the CH_2 multiplets or due to an exchange broadening. Two inequivalent $SiMe_3$ groups display separate signals in the ^{1}H, ^{13}C, and ^{29}Si NMR spectra. A pattern of six singlets similar to that displayed by **4**[6] was observed for six inequivalent CH_2 carbons. The presence of only one set of signals in the NMR spectra, the absence of any dynamic process at elevated temperatures, and the invariance of the spectra to prolonged heating assured us that the diastereomer observed in the solution was the same as that found by the X-ray experiment in the solid state.

^{27}Al NMR chemical shifts are well known[53] to reflect the coordination number of the aluminum atom and characteristic regions have been established for different coordination numbers for Al-O and Al-C compounds.[54a] Much less attention was given to the ^{27}Al NMR spectroscopy of Al-N compounds, in spite of feverish activity in this area. Moreover, a majority of these compounds also contains carbon bonded to the aluminum centers. Table IV contains data for a series of compounds in which the aluminum center is coordinated solely by nitrogen ligands. This table shows that there is only a handful of such Al-N compounds for which both ^{27}Al chemical shifts and molecular structures are known. Two examples of an octahedral geometry are **25**,[55a] **26**,[55b,c] and **27**,[30b] and their chemical shifts are

in the high-field region. From the similar values of 83 and 86 ppm for **4**[6] and **5**, respectively both dimers can be deduced to possess five-coordinate aluminums. The tetrahedrally coordinated aluminum in **7**[8b] was reported to display its signal at 107 ppm. The monomeric azaalumatranes **3** and **6** with the four-coordinate trigonal monopyramidal aluminum atoms which show very similar shifts of 133[6] and 130 ppm,

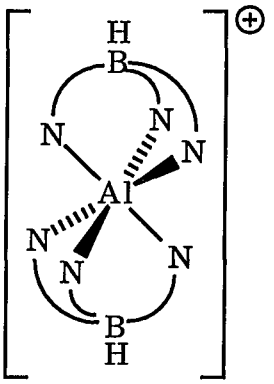

25

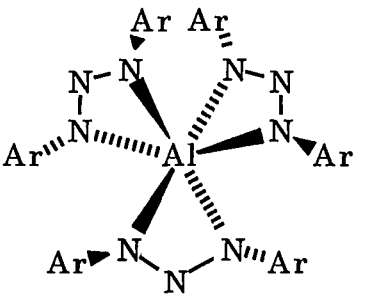

	Ar
26a	Ph
26b	2-MePh
26c	4-MePh
26d	4-MeOPh
26e	4-FPh
26f	4-ClPh
26g	4-BrPh
26h	C_6F_5

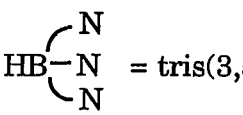

= tris(3,5-dimethyl-1-pyrazolyl)hydridoborate

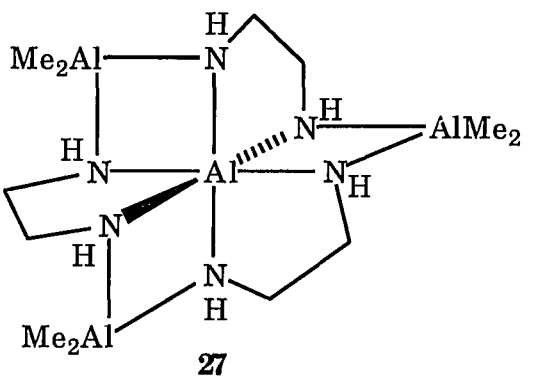

27

Table IV. ^{27}Al NMR chemical shifts of Aluminum Coordinated Solely by Nitrogens

compound	CN[a]	$\delta^{27}Al$ (ppm)	$\Delta\nu_{1/2}$ (Hz)	ref
25	6 (Oh)	6.2[b]	12 at 25 °C	55a
26	6 (Oh)[c]	25-34[d]	625-2460[e]	55b,c
27	6 (Oh)	40.5[f]	sharp[g]	30b
4	5 (TBP)	83[f]	560 at 70 °C	6
5	5 (TBP)	86[f]	1080 at 70 °C	this work
7	4 (Tet)	107[f]	840[e]	8b
3	4 (TMP)	133 ± 1[f]	1860 at 70 °C	6
6	4 (TMP)	131 ± 1[h]	3030 at 80 °C	this work
8a	3 (TPl)	143 ± 1[f]	3600 at 70 °C	this work
8b	3 (TPl)	136 ± 1[h]	8200 at 70 °C	this work

[a]Coordination number, geometry of the aluminum center given in parenthesis. Oh = octahedral, TBP = trigonal bipyramidal, Tet = tetrahedral, TMP = trigonal monpyramidal, TPl = trigonal planar. [b]Dichloromethane-d_2 solution. [c]Trigonally distorted. [d]Chloroform-d_1 solution. [e]Temperature not given. [f]Benzene-d_6 solution. [g]Value of $\Delta\nu_{1/2}$ not given; room temperature. [h]Toluene-d_8 solution.

respectively, are found in an intermediate region between the tetrahedral **7** and the trigonal planar monomeric amides **8a**,[1b,9] **8b**[9,10], for which chemical shifts were observed at 144 and 135, respectively.

This order of chemical shifts from high to low field reflects changes of the aluminum coordination geometry on going from a tetrahedral (Tet) to a trigonal monopyramidal (TMP) to a trigonal planar (TPl) environment as represented in Scheme II.

Scheme II

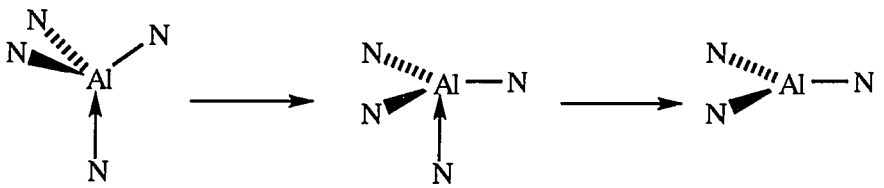

The overall sequence of chemical shifts in this complete series of Al-N compounds follows a general trend among the main-group elements wherein higher shielding is observed for higher coordination numbers and higher local symmetries.[54b] The low field chemical shifts of the monomeric amides **8a**, **8b** contrast the value of 3.2 ppm found for $Al(OAr)_3$, (Ar = 2,6-*tert*-Bu_2-4-MeC_6H_2) which possesses a trigonal planar AlO_3 array.[56] This high shielding was attributed to a p-p π-bonding between Al and O. A similar type of bonding is precluded in **8b**[10] owing to a large dihedral angle between the empty p_z orbital on Al and the lone electron pair in the p_z orbital of N and also by competitive π-bonding of nitrogen to silicon.

CONCLUSIONS

Compounds **3** and **5** demonstrate that the degree of oligomerization of azaalumatranes depends on the size of the substituents on the equatorial nitrogens. The monomeric compounds **3** and **6** are rare examples of trigonal monopyramidal coordination geometry as was confirmed by the X-ray diffraction analysis of **3**. This geometry is apparently imposed on the aluminum center by the steric influence of the tripodal tetradentate chelating ligands **9** or **11**. Dimeric **5** is the first example of a five-coordinate aluminum center coordinated exclusively by nitrogens. The X-ray diffraction study of **5** showed it to possess an unusual cis configuration of the substituents on the central Al_2N_2 ring. ^{27}Al NMR data were gathered on a series of Al-N compounds with the coordination numbers of the aluminum ranging from three to six. The observed trend in their chemical shifts clearly indicates increased shielding on going from a trigonal planar to trigonal monopyramidal to tetrahedral to trigonal bipyramidal and finally to an octahedral geometry.

ACKOWLEDGMENT

The authors are grateful to the National Science Foundation and the Iowa State Center for Advanced Technology Development for grants in support of this work and to the W. R. Grace Company for a research sample of $(H_2NCH_2CH_2)_3N$. We also thank Dr. Victor Young of Instrument Services at ISU and Tieli Wang and Dr. Robert A. Jacobson for the structural determinations of **5** and **3**, respectively.

REFERENCES

(1) (a) Waggoner, K. M.; Power, P. P. *J. Am. Chem. Soc.* **1991**, *113*, 3385. (b) Petrie, M. A.; Ruhlandt-Senge, K.; Power, P. P. *Inorg. Chem.* **1993**, *32*, 1135. (c) Waggoner, K. M.; Ruhlandt-Senge, K.; Wehmschulte, R. J.; He, X.; Olmstead, M. M.; Power, P. P. *Inorg. Chem.* **1993**, *32*, 2557.

(2) Riedel, R.; Schaible, S.; Klingebiel, U.; Noltemeyer, M.; Werner, E. *Zeitschr. Anorg. Allg. Chem.* **1991**, *603*, 119.

(3) (a) Jacobs, H.; Nöcker, B. *Zeitschr. Anorg. Allg. Chem.* **1992**, *614*, 25. (b) Jacobs, H.; Nöcker, B. *ibid* **1993**, *619*, 73. (c) Jacobs, H.; Nöcker, B. *ibid* **1993**, *619*, 381. (d) Lutz, H. D.; Lange, N.; Jacobs, H.; Nöcker, B. *ibid* **1992**, *613*, 83.

(4) (a) Janik, J. F.; Duesler, E. N.; Paine, R. T. *Inorg. Chem.* **1987**, *26*, 4341. (b) Janik, J. F.; Duesler, E. N.; Paine, R. T. *Inorg. Chem.* **1988**, *27*, 4335.

(5) Wade, T.; Park, J.; Garza, E. G.; Ross, C. B.; Smith, D. M.; Crooks, R. M. *J. Am. Chem. Soc.* **1992**, *114*, 9457.

(6) Pinkas, J.; Gaul, B.; Verkade, J. G. *J. Am. Chem. Soc.* **1993**, *115*, 3925.

(7) Shriver, D. F.; Drezdon, M. A. The Manipulation of Air-Sensitive Compounds; Wiley-Interscience: New York, 1986.

(8) (a) Ruff, J. K. *J. Am. Chem. Soc.* **1961**, *83*, 2835. (b) Waggoner, K. M.; Olmstead, M. M.; Power, P. P. *Polyhedron* **1990**, *9*, 257.

(9) Lappert, M. F.; Sanger, A. R.; Srivastava, R. C.; Power, P. P. Metal and Metalloid Amides; Ellis-Horwood: Chichester, U.K., 1980.

(10) (a) Bürger, H.; Cichon, J.; Goetze, U.; Wannagat, U.; Wismar, H. J. *J. Organomet. Chem.* **1971**, *33*, 1. (b) Pump, J.; Rochow, E. G.; Wannagat,

U. *Angew. Chem., Int. Ed. Engl.* **1963**, *2*, 264. (c) Sheldrick, G. M.; Sheldrick, W. S. *J. Chem. Soc. A* **1969**, 2279.

(11) (a) Gudat, D.; Verkade, J. G. *Organometallics* **1989**, *8*, 2772. (b) Kupce, E.; Liepins, E.; Zelcans, G.; Lukevics, E. *J. Organomet. Chem.* **1987**, *333*, 1.

(12) 4,6,11-Tris(trimethylsilyl)-1,4,6,11-tetraaza-5-alumatricyclo[3.3.3.$0^{1,5}$]undecane.

(13) (a) Gade, L. H.; Mahr, N. *J. Chem. Soc., Dalton Trans.* **1993**, 489. (b) Friedrich, S.; Gade, L. H.; Edwards, A. J.; McPartlin, M. *Chem. Ber.* **1993**, *126*, 1797.

(14) 4,6,11-Tris(*tert*-butyldimethylsilyl)-1,4,6,11-tetraaza-5-alumatricyclo[3.3.3.$0^{1,5}$]undecane.

(15) 4,6-Bis(trimethylsilyl)-1,4,6,11-tetraaza-5-alumatricyclo[3.3.3.$0^{1,5}$]undecane.

(16) TEXSAN-TEXRAY Structure Analysis Package; Molecular Structure Corporation: Woodlands, TX, 1985.

(17) SHELXTL PLUS; Siemens Analytical X-ray Instruemtns, Inc.: Madison, WI, USA.

(18) Cromer, D. T.; Waber, J. T. International Tables for X-ray Crystallography; Kynoch Press: Birmingham, U.K., 1974; Vol. IV.

(19) (a) Cummins, C. C.; Schrock, R. R.; Davis, W. M. *Angew. Chem., Int. Ed. Engl.* **1993**, *32*, 756. (b) Power, P. P. *Angew. Chem., Int. Ed. Engl.* **1993**, *32*, 850. (c) Cummins, C. C.; Lee, J.; Schrock, R. R.; Davis, W. M. *Angew. Chem., Int. Ed. Engl.* **1992**, *31*, 1501. (d) Cummins, C. C.; Schrock, R. R.; Davis, W. M. *Organometallics* **1992**, *11*, 1452.

(20) (a) Woning, J.; Verkade, J. G. *Organometallics* **1991**, *10*, 2259. (b) Woning, J.; Daniels, L. M.; Verkade, J. G. *J. Am. Chem. Soc.* **1990**, *112*, 4601. (c) Gudat, D.; Daniels, L. M.; Verkade, J. G. *J. Am. Chem. Soc.* **1989**, *111*, 8520.

(21) Moise, F.; Pennington, W. T.; Robinson, G. H. *J. Coord. Chem.* **1991**, *24*, 93.

(22) (a) Schumann, H.; Hartmann, U.; Dietrich, A.; Pickardt, J. *Angew. Chem., Int. Ed. Engl.* **1988**, *27*, 1077. (b) Schumann, H.; Hartmann, U.; Wassermann, W.; Just, O.; Dietrich, A.; Pohl, L.; Hostalek, M.; Lokai, M. *Chem. Ber.* **1991**, *124*, 1113.

(23) Mealli, C.; Sacconi, L. *J. Chem. Soc., Chem. Commun.* **1973**, 886.

(24) (a) Karlin, K. D.; Dahlstrom, P. L.; Stanford, M. L.; Zubieta, J. *J. Chem. Soc., Chem. Commun.* **1979**, 465. (b) Karlin, K. D.; Dahlstrom, P. L.; Hyde, J. R.; Zubieta, J. *J. Chem. Soc., Chem. Commun.* **1980**, 906.

(25) (a) Van Vechten, J. A.; Phillips, J. C. *Phys. Rev. B* **1970**, *2*, 2160. (b) Moeller, T. Inorganic Chemistry; J. Wiley & Sons: New York, 1982. (c) Adams, D. M. Inorganic Solids; J. Wiley & Sons: New York, 1978. (d) Huheey, J. E. Inorganic Chemistry; Harper & Row: New York, 1983.

(26) (a) Zaworotko, M. J.; Atwood, J. L. *Inorg. Chem.* **1980**, *19*, 268. (b) Whitt, C. D.; Parker, L. M.; Atwood, J. L. *J. Organomet. Chem.* **1971**, *32*, 291.

(27) (a) McLaughlin, G. M.; Sim, G. A.; Smith, J. D. *J. Chem. Soc., Dalton Trans.* **1972**, 2197. (b) Amirkhalili, S.; Hitchcock, P. B.; Smith, J. D. *J. Chem. Soc., Dalton Trans.* **1979**, 1206. (c) Amirkhalili, S.; Hitchcock, P. B.; Jenkins, A. D; Nyathi, J. Z.; Smith, J. D. *J. Chem. Soc., Dalton Trans.* **1981**, 377.

(28) Perego, G.; Dozz, G. *J. Organomet. Chem.* **1981**, *205*, 21.

(29) (a) Robinson, G. H.; Rae, A. D.; Campana, C. F.; Byram, S. K. *Organometallics* **1987**, *6*, 1227. (b) Robinson, G. H.; Zhang, H.; Atwood, J. L. *J. Organomet. Chem.* **1987**, *331*, 153. (c) Robinson, G. H.; Moise, F.; Pennington, W. T.; Sangokoya, S. A. *Polyhedron* **1989**, *8*, 1279.

(30) (a) Jiang, Z.; Interrante, L. V.; Kwon, D.; Tham, F. S.; Kullnig, R. *Inorg. Chem.* **1991**, *30*, 995. (b) Jiang, Z.; Interrante, L. V.; Kwon, D.; Tham, F. S.; Kullnig, R. *Inorg. Chem.* **1992**, *31*, 4815.

(31) (a) Robinson, G. H.; Pennington, W. T.; Lee, B.; Self, M. F.; Hrncir, D. C. *Inorg. Chem.* **1991**, *30*, 809. (b) Lee, B.; Pennington, W. T.; Robinson, G. H. *Inorg. Chim. Acta* **1991**, *190*, 173. (c) Byers, J. J.; Lee, B.; Pennington, W. T.; Robinson, G. H. *Polyhedron* **1992**, *11*, 967.

(32) Downs, A. J.; Duckworth, D.; Machell, J. C.; Pulham, C. R. *Polyhedron* **1992**, *11*, 1295.

(33) Bradford, A. M.; Bradley, D. C.; Hursthouse, M. B.; Motevalli, M. *Organometallics* **1992**, *11*, 111.

(34) Hill, J. B.; Eng, S. J.; Pennington, W. T.; Robinson, G. H. *J. Organomet. Chem.* **1993**, *445*, 11.

(35) Grant, D. F.; Killean, R. C. G.; Lawrence, J. L. *Acta Cryst.* **1969**, *B25*, 377.

(36) Thewalt, U.; Kawada, I. *Chem. Ber.* **1970**, *103*, 2754.

(37) Shearer, H. M. M.; Snaith, R.; Sowerby, J. D.; Wade, K. *J. Chem. Soc., Chem. Commun.* **1971**, 1275.

(38) Kushi, Y.; Fernando, Q. *J. Am. Chem. Soc.* **1970**, *92*, 91.

(39) (a) Atwood, J. L.; Robinson, K. D.; Jones, C.; Raston, C. L. *J. Chem. Soc., Chem. Commun.* **1991**, 1697. (b) Jones, C.; Koutsantonis, G. A.; Raston, C. L. *Polyhedron* **1993**, *12*, 1829.

(40) Robinson, G. H.; Sangokoya, S. A.; Moise, F.; Pennington, W. T. *Organometallics* **1988**, *7*, 1887.

(41) Heitsch, C. W.; Nordman, C. E.; Parry, R. W. *Inorg. Chem.* **1963**, *2*, 508.

(42) Pinkas, J.; Verkade, J. G. *Inorg. Chem.* **1993**, *32*, 2711, and references cited therein.

(43) Shklover, V. E.; Struchkov, Y. T.; Voronkov, M. G.; Ovchinnikova, Z. A.; Baryshok, V. P. *Dokl. Akad. Nauk SSSR (Engl. Transl.)* **1984**, *277*, 723.

(44) Rettig, S. J.; Storr, A.; Trotter, J. *Can. J. Chem.* **1974**, *52*, 2206.

(45) (a) Imbenotte, M.; Palavit, G.; Legrand, P.; Huvenne, J. P.; Fleury, G. *J. Mol. Spectrosc.* **1983**, *102*, 40. (b) Hencsei, P.; Sebestyen, A. *Main Group Metal Chem.* **1988**, *11*, 243.

(46) (a) Wiberg, N.; Schmid, K. H. *Zeitschr. Anorg. Allg. Chem.* **1966**, *345*, 93. (b) Fraser, G. W.; Greenwood, N. N.; Straughan, B. P. *J. Chem. Soc.* **1963**, 3742.

(47) (a) Goubeau, J.; Jiménez-Barberá, J. *Zeitschr. Anorg. Allg. Chem.* **1960**, *303*, 217. (b) Bürger, H.; Goetze, U.; Sawodny, W. *Spectrochimica Acta* **1970**, *26A*, 671.

(48) Schmidt, H.; Lensink, C.; Xi, S. K.; Verkade, J. G. *Zeitschr. Anorg. Allg. Chem.* **1989**, *578*, 75.

(49) Pinkas, J.; Verkade, J. G., manuscript in preparation.

(50) Plass, W.; Verkade, J. G. *Inorg. Chem.*, in press.

(51) Plass, W.; Verkade, J. G. *J. Am. Chem. Soc.* **1992**, *114*, 2275.

(52) Harris, R. K.; Jones, J.; Ng, S. *J. Magn. Res.* **1978**, *30*, 521.

(53) (a) Benn, R.; Rufin'ska, A.; Lehmkuhl, H.; Janssen, E.; Krüger, C. *Angew. Chem., Int. Ed. Engl.* **1983**, *22*, 779. (b) Benn, R.; Rufin'ska, A.; Janssen, E.; Lehmkuhl, H. *Organometallics* **1986**, *5*, 825. (c) Benn, R.; Rufin'ska, A. *Angew. Chem., Int. Ed. Engl.* **1986**, *25*, 861. (d) Benn, R.; Janssen, E.; Lehmkuhl, H.; Rufin'ska, A. *J. Organomet. Chem.* **1987**, *333*, 155. (e) Benn, R.; Janssen, E.; Lehmkuhl, H.; Rufin'ska, A.; Angermud, K.; Betz, P.; Goddard, R.; Krüger, C. *J. Organomet. Chem.* **1991**, *411*, 37.

(54) (a) Akitt, J. W. in Multinuclear NMR; Mason, J. Ed.; Plenum Press: New York, 1987. (b) Jameson, C. J.; Mason, J. *ibid.*

(55) (a) Cowley, A. H.; Carrano, C. J.; Geerts, R. L.; Jones, R. A.; Nunn, C. M. *Angew. Chem., Int. Ed. Engl.* **1988**, *27*, 277. (b) Leman, J. T.; Barron, A. R.; Ziller, J. W.; Kren, R. M. *Polyhedron* **1989**, *8*, 1909. (c) Lehman, J. T.; Braddock-Wilking, J.; Coolong, A. J.; Barron, A. R. *Inorg. Chem.* **1993**, *32*, 4324.

(56) Healy, M. D.; Barron, A. R. *Angew. Chem., Int. Ed. Engl.* **1992**, *31*, 921.

SUPPLEMENTARY MATERIAL

Table V. Atomic Coordinates and Thermal Parameters ($Å^2$) for **3**

atom	x	y	z	B(eq)
Si(1)	0.9837(2)	0.2606(2)	0.1380(1)	5.7(1)
Si(2)	0.7178(2)	-0.1045(2)	0.1057(1)	5.5(1)
Si(3)	0.6058(2)	0.3446(2)	0.1622(1)	7.1(1)
Al	0.7634(2)	0.1872(2)	0.0712(1)	4.2(1)
N(1)	0.7483(5)	0.2257(6)	-0.0376(3)	5.3(3)
N(2)	0.7109(4)	0.0320(5)	0.0576(3)	4.8(3)
N(3)	0.8967(4)	0.2075(5)	0.0730(3)	5.5(3)
N(4)	0.6849(4)	0.3183(5)	0.0939(3)	5.2(3)
C(1)	0.7098(6)	0.1076(8)	-0.0726(4)	6.2(4)
C(2)	0.6526(6)	0.0365(7)	-0.0140(5)	6.2(5)
C(3)	0.8499(7)	0.2557(9)	-0.0588(4)	7.8(6)
C(4)	0.9236(6)	0.189(1)	-0.0049(5)	8.2(6)
C(5)	0.6778(7)	0.3321(8)	-0.0432(4)	7.2(5)
C(6)	0.6886(7)	0.4062(7)	0.0300(5)	7.6(5)
C(11)	0.9250(6)	0.2776(8)	0.2277(4)	7.6(5)
C(12)	1.0894(6)	0.1505(9)	0.1507(5)	9.5(6)
C(13)	1.0360(7)	0.4139(8)	0.1104(5)	9.5(6)
C(21)	0.7702(7)	-0.2350(8)	0.0522(6)	10.7(7)
C(22)	0.5954(6)	-0.1570(8)	0.1333(6)	9.9(6)
C(23)	0.7973(7)	-0.0778(8)	0.1920(6)	10.7(7)
C(31)	0.638(1)	0.4933(8)	0.2145(5)	12.3(7)
C(32)	0.6166(6)	0.2149(7)	0.2297(4)	7.0(5)
C(33)	0.4766(8)	0.357(2)	0.1257(7)	19(1)

$B(eq) = 8\pi^2/3\ \Sigma_i\Sigma_j\ U_{ij}\ a_i^*a_j^*\ (\mathbf{a}_i.\mathbf{a}_j)$

Table VI. Bond Distances (Å) in **3**

SI1	N3	1.697(6)	AL	N2	1.805(5)
SI1	C11	1.836(8)	AL	N3	1.812(6)
SI1	C12	1.850(9)	AL	N4	1.810(6)
SI1	C13	1.851(8)	N1	C1	1.482(9)
SI2	N2	1.684(5)	N1	C3	1.48(1)
SI2	C21	1.846(9)	N1	C5	1.476(9)
SI2	C22	1.839(8)	N2	C2	1.463(8)
SI2	C23	1.85(1)	N3	C4	1.469(9)
SI3	N4	1.690(6)	N4	C6	1.475(9)
SI3	C31	1.87(1)	C1	C2	1.53(1)
SI3	C32	1.830(8)	C3	C4	1.52(1)
SI3	C33	1.83(1)	C5	C6	1.53(1)
AL	N1	1.983(6)			

Table VII. Bond Angles (deg) in **3**

N3	SI1	C11	108.2(3)	N3	AL	N4	119.9(3)
N3	SI1	C12	111.9(4)	AL	N1	C1	104.5(4)
N3	SI1	C13	111.8(4)	AL	N1	C3	104.4(5)
C11	SI1	C12	108.9(4)	AL	N1	C5	104.7(4)
C11	SI1	C13	109.5(4)	C1	N1	C3	112.5(6)
C12	SI1	C13	106.6(4)	C1	N1	C5	114.3(6)
N2	SI2	C21	113.2(4)	C3	N1	C5	114.9(7)
N2	SI2	C22	111.9(3)	SI2	N2	AL	135.1(4)
N2	SI2	C23	107.7(3)	SI2	N2	C2	118.9(5)
C21	SI2	C22	106.8(4)	AL	N2	C2	105.9(4)
C21	SI2	C23	108.9(5)	SI1	N3	AL	134.4(3)
C22	SI2	C23	108.1(5)	SI1	N3	C4	119.4(5)
N4	SI3	C31	111.3(4)	AL	N3	C4	105.4(4)
N4	SI3	C32	108.7(3)	SI3	N4	AL	133.7(3)
N4	SI3	C33	112.6(4)	SI3	N4	C6	120.2(5)
C31	SI3	C32	107.4(4)	AL	N4	C6	105.6(5)
C31	SI3	C33	107.6(6)	N1	C1	C2	108.0(6)
C32	SI3	C33	109.0(6)	N2	C2	C1	110.1(6)
N1	AL	N2	92.3(3)	N1	C3	C4	108.9(7)
N1	AL	N3	92.3(3)	N3	C4	C3	110.5(7)
N1	AL	N4	91.8(3)	N1	C5	C6	107.9(6)
N2	AL	N3	119.6(3)	N4	C6	C5	109.2(6)
N2	AL	N4	120.2(3)				

Table VIII. Anisotropic Displacement Coefficients ($Å^2$) for **3**

atom	U11	U22	U33	U12	U13	U23
Si(1)	0.070(2)	0.080(2)	0.065(1)	-0.020(1)	0.004(1)	-0.010(1)
Si(2)	0.057(1)	0.056(1)	0.095(2)	0.001(1)	0.005(1)	0.017(1)
Si(3)	0.102(2)	0.093(2)	0.076(2)	0.036(2)	0.014(1)	-0.004(2)
Al	0.061(2)	0.054(1)	0.047(1)	-0.010(1)	0.004(1)	0.003(1)
N(1)	0.094(5)	0.070(5)	0.036(4)	-0.019(4)	0.006(3)	-0.005(3)
N(2)	0.060(4)	0.055(4)	0.066(5)	-0.013(3)	-0.014(3)	0.011(3)
N(3)	0.068(4)	0.096(5)	0.047(4)	-0.022(4)	0.015(3)	-0.018(3)
N(4)	0.095(5)	0.052(4)	0.049(4)	0.013(4)	0.005(3)	0.006(3)
C(1)	0.092(6)	0.087(6)	0.056(5)	-0.012(5)	-0.017(5)	-0.006(5)
C(2)	0.090(6)	0.061(5)	0.084(7)	-0.021(5)	-0.016(6)	0.009(5)
C(3)	0.112(8)	0.133(9)	0.055(5)	-0.055(7)	0.028(5)	-0.017(6)
C(4)	0.068(6)	0.16(1)	0.081(7)	-0.041(6)	0.011(5)	-0.039(7)
C(5)	0.158(9)	0.056(6)	0.060(6)	0.002(6)	0.011(6)	0.020(5)
C(6)	0.150(8)	0.065(6)	0.075(7)	0.012(6)	-0.001(6)	0.010(5)
C(11)	0.089(6)	0.135(8)	0.062(5)	-0.032(6)	-0.007(5)	-0.019(5)
C(12)	0.098(7)	0.132(8)	0.129(8)	0.019(7)	-0.017(6)	-0.018(7)
C(13)	0.133(8)	0.115(8)	0.111(8)	-0.061(7)	-0.013(6)	0.015(6)
C(21)	0.147(9)	0.077(7)	0.19(1)	0.016(6)	0.061(8)	0.000(7)
C(22)	0.087(7)	0.098(7)	0.19(1)	-0.002(6)	0.046(7)	0.055(7)
C(23)	0.136(8)	0.105(8)	0.16(1)	0.006(7)	-0.052(7)	0.062(7)
C(31)	0.29(1)	0.079(7)	0.097(8)	0.042(8)	0.052(9)	-0.006(6)
C(32)	0.113(7)	0.080(6)	0.075(6)	0.004(5)	0.044(5)	-0.007(5)
C(33)	0.13(1)	0.44(2)	0.13(1)	0.15(1)	-0.020(8)	0.01(1)

Table IX. Atomic Coordinates ($x10^4$) and Equivalent Isotropic Displacement Coefficients ($Å^2x10^3$) for **5**

Atom	x	y	z	U_{eq}
Al	9423(1)	7861(1)	1820(1)	23(1)
Si(1)	10285(1)	8435(1)	3505(1)	39(1)
Si(2)	7951(1)	6247(1)	1747(1)	35(1)
N(1)	8023(2)	8580(1)	1327(1)	28(1)
N(2)	9318(2)	8365(1)	2706(1)	30(1)
N(3)	8497(2)	7056(1)	1394(1)	28(1)
N(4)	10216(2)	8531(1)	1175(1)	24(1)
C(1)	7520(2)	8784(2)	1979(2)	39(1)
C(2)	8432(2)	8967(2)	2624(2)	42(1)
C(3)	7281(2)	8085(2)	780(2)	40(1)
C(4)	7888(2)	7320(2)	670(1)	36(1)
C(5)	8469(2)	9266(2)	984(2)	34(1)
C(6)	9443(2)	8993(1)	629(1)	31(1)
C(11)	9708(4)	8963(3)	4255(2)	84(2)
C(12)	10788(4)	7453(2)	3864(2)	70(1)
C(13)	11525(3)	9028(3)	3364(2)	77(2)

Table IX. Continued

C(21)	6387(3)	6316(2)	1673(2)	56(1)
C(22)	8228(3)	5338(2)	1229(2)	57(1)
C(23)	8531(3)	6138(2)	2757(2)	49(1)
Al'	11301(1)	7721(1)	1012(1)	25(1)
Si(1')	10523(1)	7679(1)	-783(1)	36(1)
Si(2')	13263(1)	9106(1)	1276(1)	41(1)
N(1')	12157(2)	6597(1)	1072(1)	32(1)
N(2')	10602(2)	7332(1)	99(1)	29(1)
N(3')	12710(2)	8175(1)	1184(1)	33(1)
N(4')	10880(2)	7323(1)	1962(1)	26(1)
C(1')	11530(3)	6088(2)	486(2)	43(1)
C(2')	10426(3)	6481(1)	162(2)	38(1)
C(3')	13265(2)	6831(2)	921(2)	47(1)
C(4')	13623(3)	7586(2)	1310(2)	50(1)
C(5')	12196(2)	6277(2)	1825(2)	40(1)
C(6')	11110(2)	6479(1)	2079(2)	35(1)
C(11')	9054(3)	7672(3)	-1305(2)	66(1)

Table IX. Continued

C(12')	11362(3)	7086(2)	-1346(2)	59(1)
C(13')	11071(4)	8698(2)	-772(2)	59(1)
C(21')	14131(3)	9324(3)	547(2)	76(2)
C(22')	12183(3)	9895(2)	1215(2)	55(1)
C(23')	14195(3)	9235(2)	2197(2)	66(1)

Equivalent isotropic U defined as one third of the trace of the orthogonalized U_{ij} tensor.

Table X. Bond Distances (Å) in **5**

Al-N(1)	2.161 (2)	Al-N(2)	1.858 (2)
Al-N(3)	1.858 (2)	Al-N(4)	2.004 (2)
Al-Al'	2.934 (1)	Al-N(4')	1.968 (2)
Si(1)-N(2)	1.712 (2)	Si(1)-C(11)	1.875 (5)
Si(1)-C(12)	1.862 (4)	Si(1)-C(13)	1.868 (4)
Si(2)-N(3)	1.705 (2)	Si(2)-C(21)	1.883 (3)
Si(2)-C(22)	1.876 (3)	Si(2)-C(23)	1.869 (3)
N(1)-C(1)	1.473 (4)	N(1)-C(3)	1.487 (3)
N(1)-C(5)	1.475 (3)	N(2)-C(2)	1.475 (4)
N(3)-C(4)	1.471 (3)	N(4)-C(6)	1.472 (3)
N(4)-Al'	1.967 (2)	C(1)-C(2)	1.503 (4)
C(3)-C(4)	1.527 (4)	C(5)-C(6)	1.517 (4)
Al'-N(1')	2.174 (2)	Al'-N(2')	1.859 (2)
Al'-N(3')	1.853 (2)	Al'-N(4')	2.014 (2)
Si(1')-N(2')	1.705 (2)	Si(1')-C(11')	1.870 (3)
Si(1')-C(12')	1.867 (4)	Si(1')-C(13')	1.859 (3)
Si(2')-N(3')	1.720 (2)	Si(2')-C(21')	1.875 (5)

Table X. Continued

Si(2')-C(22')	1.867 (3)	Si(2')-C(23')	1.872 (4)
N(1')-C(1')	1.483 (3)	N(1')-C(3')	1.473 (4)
N(1')-C(5')	1.474 (3)	N(2')-C(2')	1.475 (3)
N(3')-C(4')	1.482 (4)	N(4')-C(6')	1.474 (3)
C(1')-C(2')	1.522 (4)	C(3')-C(4')	1.498 (4)
C(5')-C(6')	1.511 (4)		

Table XI. Bond Angles (deg) in **5**

N(1)-Al-N(2)	86.2(1)	N(1)-Al-N(3)	82.5(1)
N(2)-Al-N(3)	125.4(1)	N(1)-Al-N(4)	81.6(1)
N(2)-Al-N(4)	111.3(1)	N(3)-Al-N(4)	119.4(1)
N(1)-Al-Al'	117.3(1)	N(2)-Al-Al'	130.9(1)
N(3)-Al-Al'	101.2(1)	N(4)-Al-Al'	41.9(1)
N(1)-Al-N(4')	160.5(1)	N(2)-Al-N(4')	107.3(1)
N(3)-Al-N(4')	100.0(1)	N(4)-Al-N(4')	80.3(1)
Al'-Al-N(4')	43.2(1)	N(2)-Si(1)-C(11)	111.8(1)
N(2)-Si(1)-C(12)	111.9(1)	C(11)-Si(1)-C(12)	108.3(2)
N(2)-Si(1)-C(13)	111.6(2)	C(11)-Si(1)-C(13)	104.7(2)
C(12)-Si(1)-C(13)	108.2(2)	N(3)-Si(2)-C(21)	112.0(1)
N(3)-Si(2)-C(22)	111.2(1)	C(21)-Si(2)-C(22)	106.4(2)
N(3)-Si(2)-C(23)	110.5(1)	C(21)-Si(2)-C(23)	106.2(2)
C(22)-Si(2)-C(23)	110.4(1)	Al-N(1)-C(1)	101.7(1)
Al-N(1)-C(3)	107.4(1)	C(1)-N(1)-C(3)	113.1(2)
Al-N(1)-C(5)	107.9(2)	C(1)-N(1)-C(5)	113.1(2)
C(3)-N(1)-C(5)	112.7(2)	Al-N(2)-Si(1)	129.5(1)

Table XI. Continued

Al-N(2)-C(2)	113.1(2)	Si(1)-N(2)-C(2)	114.6(2)
Al-N(3)-Si(2)	133.3(1)	Al-N(3)-C(4)	108.8(2)
Si(2)-N(3)-C(4)	115.0(2)	Al-N(4)-C(6)	112.9(2)
Al-N(4)-Al'	95.3(1)	C(6)-N(4)-Al'	129.6(2)
N(1)-C(1)-C(2)	109.4(2)	N(2)-C(2)-C(1)	111.0(2)
N(1)-C(3)-C(4)	108.9(2)	N(3)-C(4)-C(3)	108.8(2)
N(1)-C(5)-C(6)	108.0(2)	N(4)-C(6)-C(5)	109.1(2)
Al-Al'-N(4)	42.9(1)	Al-Al'-N(1')	116.9(1)
N(4)-Al'-N(1')	159.8(1)	Al-Al'-N(2')	102.1(1)
N(4)-Al'-N(2')	100.0(1)	N(1')-Al'-N(2')	82.6(1)
Al-Al'-N(3')	130.9(1)	N(4)-Al'-N(3')	107.7(1)
N(1')-Al'-N(3')	86.6(1)	N(2')-Al'-N(3')	124.4(1)
Al-Al'-N(4')	41.9(1)	N(4)-Al'-N(4')	80.1(1)
N(1')-Al'-N(4')	81.3(1)	N(2')-Al'-N(4')	120.7(1)
N(3')-Al'-N(4')	111.1(1)	N(2')-Si(1')-C(11')	111.9(1)
N(2')-Si(1')-C(12')	112.8(1)	C(11')-Si(1')-C(12')	106.1(2)
N(2')-Si(1')-C(13')	110.6(1)	C(11')-Si(1')-C(13')	108.6(2)

Table XI. Continued

C(12')-Si(1')-C(13')	106.5(2)	N(3')-Si(2')-C(21')	111.8(2)
N(3')-Si(2')-C(22')	113.7(1)	C(21')-Si(2')-C(22')	106.8(2)
N(3')-Si(2')-C(23')	111.2(1)	C(21')-Si(2')-C(23')	106.9(2)
C(22')-Si(2')-C(23')	106.1(2)	Al'-N(1')-C(1')	107.4(2)
Al'-N(1')-C(3')	101.2(2)	C(1')-N(1')-C(3')	113.2(2)
Al'-N(1')-C(5')	108.1(2)	C(1')-N(1')-C(5')	112.9(2)
C(3')-N(1')-C(5')	113.1(2)	Al'-N(2')-Si(1')	131.9(1)
Al'-N(2')-C(2')	109.2(1)	Si(1')-N(2')-C(2')	115.5(2)
Al'-N(3')-Si(2')	137.3(1)	Al'-N(3')-C(4')	112.7(2)
Si(2')-N(3')-C(4')	110.0(2)	Al-N(4')-Al'	94.9(1)
Al-N(4')-C(6')	128.2(2)	Al'-N(4')-C(6')	112.6(2)
N(1')-C(1')-C(2')	109.3(2)	N(2')-C(2')-C(1')	109.5(2)
N(1')-C(3')-C(4')	110.1(3)	N(3')-C(4')-C(3')	111.1(2)
N(1')-C(5')-C(6')	108.4(2)	N(4')-C(6')-C(5')	109.3(2)

Table XII. Anisotropic Displacement Coefficients ($Å^2x10^3$) for **5**

Atom	U_{11}	U_{22}	U_{33}	U_{12}	U_{13}	U_{23}
Al	28(1)	19(1)	22(1)	1(1)	5(1)	2(1)
Si(1)	44(1)	45(1)	27(1)	-5(1)	5(1)	-5(1)
Si(2)	37(1)	24(1)	44(1)	-4(1)	10(1)	2(1)
N(1)	31(1)	24(1)	30(1)	1(1)	7(1)	4(1)
N(2)	37(1)	29(1)	25(1)	4(1)	8(1)	-3(1)
N(3)	34(1)	20(1)	29(1)	-1(1)	0(1)	1(1)
N(4)	31(1)	18(1)	23(1)	0(1)	3(1)	1(1)
C(1)	38(2)	37(2)	43(2)	9(1)	16(1)	5(1)
C(2)	52(2)	39(2)	38(2)	10(2)	17(1)	-6(1)
C(3)	38(2)	36(2)	42(2)	2(1)	-4(1)	5(1)
C(4)	38(2)	33(2)	35(2)	-3(1)	-2(1)	-1(1)
C(5)	39(2)	26(1)	37(2)	7(1)	9(1)	7(1)
C(6)	38(2)	24(1)	31(1)	3(1)	7(1)	9(1)
C(11)	80(3)	132(4)	39(2)	8(3)	4(2)	-30(2)
C(12)	91(3)	64(2)	45(2)	2(2)	-20(2)	8(2)
C(13)	61(3)	89(3)	78(3)	-28(2)	3(2)	-6(3)

Table XII. Continued

C(21)	46(2)	48(2)	76(3)	-8(2)	18(2)	5(2)
C(22)	68(3)	31(2)	76(3)	-10(2)	25(2)	-9(2)
C(23)	51(2)	45(2)	54(2)	0(2)	12(2)	16(2)
Al'	28(1)	23(1)	23(1)	3(1)	6(1)	1(1)
Si(1')	49(1)	35(1)	25(1)	6(1)	8(1)	1(1)
Si(2')	35(1)	38(1)	51(1)	-7(1)	8(1)	7(1)
N(1')	36(1)	28(1)	34(1)	7(1)	6(1)	-2(1)
N(2')	36(1)	26(1)	25(1)	1(1)	3(1)	1(1)
N(3')	28(1)	30(1)	42(1)	4(1)	8(1)	1(1)
N(4')	31(1)	21(1)	25(1)	2(1)	3(1)	3(1)
C(1')	60(2)	27(2)	43(2)	7(1)	10(2)	-4(1)
C(2')	51(2)	30(2)	32(2)	-2(1)	3(1)	-5(1)
C(3')	40(2)	44(2)	59(2)	15(2)	15(2)	2(2)
C(4')	34(2)	47(2)	68(2)	6(1)	9(2)	3(2)
C(5')	44(2)	32(2)	42(2)	15(1)	5(1)	8(1)
C(6')	44(2)	27(1)	35(2)	8(1)	8(1)	10(1)
C(11')	62(2)	93(3)	38(2)	12(2)	-7(2)	-2(2)

Table XII. Continued

C(12')	79(3)	58(2)	42(2)	11(2)	23(2)	-4(2)
C(13')	95(3)	41(2)	46(2)	-3(2)	29(2)	7(2)
C(21')	63(3)	80(3)	95(3)	-9(2)	37(3)	24(2)
C(22')	53(2)	32(2)	78(3)	-12(2)	6(2)	3(2)
C(23')	54(2)	59(2)	78(3)	-14(2)	-7(2)	-1(2)

The anisotropic displacement factor exponent takes the form:
$-2\pi^2(h^2a^{*2}U_{11} + k^2b^{*2}U_{22} + l^2c^{*2}U_{33} + 2hka^*b^*U_{12} + 2hla^*c^*U_{13} + 2klb^*c^*U_{23})$

PAPER III. GROUP 13 AZATRANES : STRUCTURE AND REACTIVITY

ABSTRACT

The new dimeric azagallatrane $[Ga(MeNCH_2CH_2)_3N]_2$, **14**, was prepared by two synthetic routes: (i) the transamination reaction of $[Ga(NMe_2)_3]_2$, with $(MeNHCH_2CH_2)_3N$, **2**, and (ii) the transmetallation reaction of $[Al(MeNCH_2CH_2)_3N]_2$, **12**, with $Ga(acac)_3$ (acac = penta-2,5-dienoate). Dimeric azaalumatrane **12**, monomeric azaalumatranes $Al(RNCH_2CH_2)_3N$ (R = $SiMe_3$, **8**; $SiMe_2$-*tert*-Bu, **9**), and azaboratrane $B(MeNCH_2CH_2)_3N$, **6**, react with a variety of alkoxides giving transition metal or main-group element azatranes. The molecular structures of **12** and **14** were established by X-ray diffraction experiments and both possess an unusual cis configuration of the substituents on the central four-membered $(M\text{-}N)_2$ ring. Crystal data: **12**, a = 37.3782(10) Å, b = 14.379(2) Å, c = 8.774(2) Å, V = 4677.2(1) Å^3, Z = 8, space group P_{bca}, R = 5.0%; **14**, a = 9.716(1) Å, b = 11.324(2) Å, c = 11.343(1), α = 110.36(2)°, β = 97.87(1)°, γ = 90.34(1)°, V = 1157.2(3) Å^3, Z = 2, space group $P\bar{1}$, R = 4.7%. Compound **14** is the first example of five-coordinate gallium surrounded solely by nitrogen ligands.

INTRODUCTION

The chemistry of compounds of the group 13 elements bonded to nitrogen is a large and vigorous research area owing to efforts in preparation of nitride ceramic materials and semiconductors.[1-6] There is a vast amount of literature on compounds of group 13 elements with multifunctional amine ligands, but comparatively few of them are highly symmetrical ones.[7] Recently we have focused our attention on the use of symmetrical tripodal tetramine ligands such as **1-5** for the synthesis of azatranes as potential nitride film precursors.

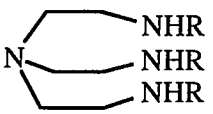

R = H, **1**; Me, **2**; *iso*-Pr, **3**; $SiMe_3$, **4**; $SiMe_2$-*tert*-Bu, **5**

We have reported syntheses and the characterization of four group 13 azatranes[8,9] which are monomeric, **6-9**, and two which are dimeric, **12** and **13**, depending on the size of the substituents on the equatorial nitrogens and the nature of the central atom. The monomeric azaalumatrane **8** was shown by the X-ray crystallography to possess a rare trigonal monopyramidal (TMP) coordination geometry at the aluminum center while the dimeric molecule **13** contains aluminums in a trigonal bipyramidal (TBP) environment. In addition, the central four-membered $(Al\text{-}N)_2$ ring of **13** features an unusual cis configuration of the substituents.[9] By comparing ^{27}Al NMR chemical shifts of the monomeric trigonal planar amides $Al(NR_2)_3$ (R = *iso*-Pr, $SiMe_3$) and azaalumatranes **8**, **9**, **12** and **13** with literature data for hexacoordinate and

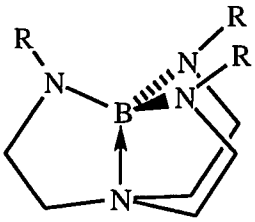

	R
6	Me
7	$SiMe_3$

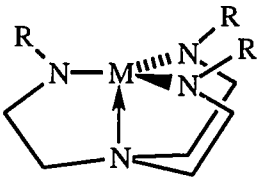

	M	R
8	Al	$SiMe_3$
9	Al	$SiMe_2$-*tert*-Bu
10	Ga	$SiMe_3$
11	Ga	$SiMe_2$-*tert*-Bu

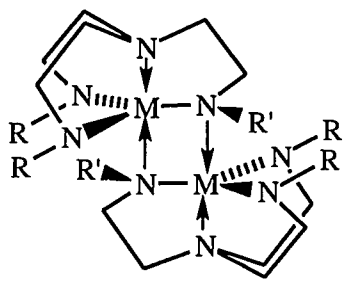

	M	R	R'
12	Al	Me	Me
13	Al	$SiMe_3$	H
14	Ga	Me	Me

tetracoordinate species, we demonstrated a trend toward higher shielding of the aluminum nucleus upon increasing its coordination by nitrogens, ($AlN_3 \rightarrow AlN_4 \rightarrow AlN_5 \rightarrow AlN_6$).[9] We also showed that alumaazatrane **12** takes part in an interesting transmetallation reaction with $B(OMe)_3$ to give **6**.[8] Here we report results of our further study of this reaction whose scope is now extended to the transmetallation of **6**, **8**, **9**, and **12** with other main-group and transition metal alkoxides and $Ga(acac)_3$, giving azatranes **11**, and **14-19**. Azatranes **8** and **12** were previously shown to transligate cleanly with

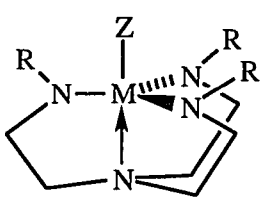

	MZ	R
15	SiMe	Me
16	V=NSiMe$_3$	Me
17	V=O	$SiMe_3$
18	V=O	Me
19	TiO-*iso*-Pr	Me

triethanolamine to give the tetrameric alumatrane $[Al(OCH_2CH_2)_3N]_4$, **20**.[10] Here we describe the analogous reaction for azaboratrane **6** and azasilatrane **15** giving boratrane $B(OCH_2CH_2)_3N$, **21** and silatrane $MeSi(OCH_2CH_2)_3N$, **22**,

respectively. The crystal and molecular structures of azaalumatrane **12** and azagallatrane **14** determined by single-crystal X-ray diffraction experiments feature the cis configuration at the central puckered four-membered ring, as was the case for **13**.[9]

EXPERIMENTAL SECTION

All reactions were carried out under argon with the strict exclusion of moisture using Schlenk or dry box techniques.[11] Solvents were dried over and distilled from Na/benzophenone under nitrogen. Deuterated benzene, toluene, and chloroform were dried over and distilled from CaH_2 under an argon atmosphere. The starting materials $(MeHNCH_2CH_2)_3N$, **2**[12] and $(Me_3SiHNCH_2CH_2)_3N$, **4**[13] were prepared using our procedures published earlier. $GaCl_3$, $B(NMe_2)_3$, $O{=}V(O\text{-}iso\text{-}Pr)_3$, $Ti(O\text{-}iso\text{-}Pr)_4$, $MeSi(OMe)_3$, and $Eu(hfc)_3$ were purchased from Aldrich and were used as received. $B(OMe)_3$ and $MeC(OMe)_3$ were distilled from Na before use. $Ga(acac)_3$ was purchased from Gelest. $[Al(NMe_2)_3]_2$,[14] $[Ga(NMe_2)_3]_2$,[14] $Me_3SiN{=}V(OSiMe_3)_3$,[15] and $Mo_2(O\text{-}tert\text{-}Bu)_6$[16] were prepared according to published procedures.

NMR spectra were recorded at 25 °C, unless otherwise stated, on Varian VXR 300 and Unity 500 spectrometers with deuterated solvents as an internal lock. ^1H (299.949 MHz) and ^{13}C (75.429 MHz) spectra were internally referenced to the corresponding Me_4Si signals. ^{11}B (96.233 MHz) spectra were referenced to $BF_3{\cdot}Et_2O$ in C_6D_6 (50% volume solution) as an external standard, ^{27}Al (78.157 MHz) spectra were measured at 70 °C and were referenced to the external standard 0.2 M $Al(ClO_4)_3$/0.1 M $HClO_4$ in D_2O. The background signal, which was found as a broad peak at ~61 ppm ($\Delta\nu_{1/2}$ = 4100 Hz at 30 °C), did not interfere with our spectra owing to its low intensity.[17] ^{29}Si (59.591 MHz) spectra were referenced to a 30% volume solution of Me_4Si in benzene-d_6 as an external standard. Pulses of 90° and a relaxation delay of 25 s were used for acquisition of the ^{29}Si spectra. ^{71}Ga (91.485 MHz) spectra were recorded at 70

°C and were referenced to the signal of $GaCl_4^-$/5 M HCl in D_2O which was set at 257 ppm in order that measured shifts are with respect to $Ga(H_2O)_6^{3+}$.[18] The chemical shifts were corrected for the difference in chemical shift between D_2O and the lock solvent used.

Mass spectra were recorded on a Finnigan 4000 low-resolution (70 eV, EI; NH_3, CI) and a Kratos MS-50 high resolution instrument. The masses are reported for the most abundant isotope present. IR spectra (4000-400 cm^{-1}) were taken on IBM/Bruker IR-98 and DigiLab FTS-7 FTIR spectrometers using Nujol mulls between KBr discs or as KBr pellets. Wavenumbers were calibrated with a 0.05 mm polystyrene film. Intensities are noted as vs (very strong), s (strong), m (medium), w (weak), vw (very weak), and sh (shoulder). Two specimens for IR experiments were always prepared by recrystallization and sublimation of a particular compound to assure consistency of data. Elemental analyses were carried out by Galbraith Laboratories or Desert Analytics. Melting points (uncorrected) were measured in sealed capillaries.

Trimethylazaboratrane, 6. This compound was prepared for HRMS study according to our previously published procedure[8] with the slight modification that after the reaction, all volatiles were removed under vacuum at room temperature and the residue was sublimed at 60-80 °C at 5 x 10^{-3} Torr giving an improved yield of 42% of white crystalline solid **6**. The ^1H NMR shifts of **6** in chloroform-d_1 are given here to demonstrate the aromatic solvent-induced shift effect by comparing them with values reported for a benzene-d_6 solution.[8] ^1H NMR (chloroform-d_1) δ 2.46 (s, 3 H, NMe), 2.78 (t, 2 H, $N(CH_3)_2$, $^3J_{HH}$ = 5.1 Hz), 2.93 (t, 2 H, $MeNCH_2$, $^3J_{HH}$ = 5.1 Hz).

Trimethylazaalumatrane Dimer, 12. This compound was prepared according to our previously published procedure[8] and further purified by sublimation at 120 °C at 2.5 x 10^{-3} Torr. Single crystals suitable for X-ray diffraction analysis were grown from a THF solution layered with pentane at -20 °C. For the purpose of comparison with azagallatrane **14**, we present here IR data for **12**: IR (KBr pellet, 4000-400 cm^{-1}) ν 2968 s, 2847 vs, 2797 vs, 2765 vs, 2747 s, 2675 m, 1478 sh, 1468 s, 1446 m, 1422 w, 1377 w, 1355 vs, 1342 m, 1307 w, 1272 s, 1262 w, 1238 vw, 1217 vw, 1197 sh, 1190 s, 1164 sh, 1155 vs, 1143 s, 1135 s, 1109 vs, 1082 s, 1061 vs, 1051 vs, 1035 m, 1011 w, 955 m, 944 s, 923 s, 880 vs, 856 m, 845 s, 768 vw, 751 vw, 647 s, 631 vs, 609 vs, 591 s, 575 vw, 563 m, 536 vs, 509 vw, 497 vw, 457 w, 436 s, 413 w.

Reaction of Trimethylazaalumatrane Dimer, 12, with $MeSi(OMe)_3$. Neat $MeSi(OMe)_3$ (0.75 mL, 5.3 mmol) was added dropwise to a stirred solution of **12** (1.11 g, 2.62 mmol) in 150 mL of toluene at room temperature. After refluxing the reaction mixture for 40 h, a clear solution was decanted from a gel-like precipitate of $[Al(OMe)_3]_n$ and all volatiles were removed under vacuum. A yellow waxy solid was sublimed at 60-75 °C at 5 x 10^{-3} Torr, yielding 0.50 g (42%) of **15**. The product possessed ^1H, ^{13}C, and ^{29}Si NMR spectra which compared well with data published earlier for this compound.[19] The ^1H NMR chemical shifts display ASIS effects, therefore the data for benzene-d_6 and chloroform-d_1 solutions of **15** are listed here: ^1H NMR (benzene-d_6) δ 0.43 (s, 3 H, $SiCH_3$, $^1J_{CH}$ = 114.9 Hz, ^{13}C satellites, $^2J_{SiH}$ = 5.7 Hz, ^{29}Si satellites), 2.24 (t, 6 H, $MeNCH_2$, $^3J_{HH}$ = 6.1 Hz), 2.66 (t, 6 H, $N(CH_2)_3$, $^3J_{HH}$ = 6.1 Hz), 2.69 (s, 9 H, NCH_3, $^1J_{CH}$ = 132 Hz, ^{13}C satellites); ^1H NMR (chloroform-d_1) δ 0.11 (s, 3 H,

$SiCH_3$), 2.55 (s, 9 H, NCH_3), 2.68 (t, 6 H, MeNCH_2, $^3J_{HH}$ = 6.0 Hz), 2.83 (t, 6 H, $N(CH_2)_3$, $^3J_{HH}$ = 6.0 Hz).

Reaction of Trimethylazaalumatrane Dimer, 12, with $Me_3SiN{=}V(OSiMe_3)_3$. Compounds **12** (0.42 g, 0.99 mmol) and $Me_3SiN{=}V(OSiMe_3)_3$ (0.78, 1.9 mmol) were dissolved in 50 mL of toluene. The reaction mixture was refluxed for 1 h during which its color changed to deep red. The solvent was removed under vacuum and the remaining dark brown solid was sublimed at 100-110 °C at 5 x 10^{-3} Torr, giving a red-brown solid, whose ^1H, ^{13}C, and ^{27}Al NMR spectra revealed the formation of **16**[20] and the presence of a substantial amount of the byproduct of $[Al(OSiMe_3)_3]_2$.[21]

Reaction of Tris(trimethylsilyl)azaalumatrane, 8, with O=V(O-*iso*-Pr)$_3$. To a solution of **8** (3.11 g, 8.05 mmol) in 70 mL of toluene, O=V(O-*iso*-Pr)$_3$ (2.01 g, 8.23 mmol) in 10 mL of toluene was added dropwise with stirring. The yellowish color of the solution slowly turned deep red. The reaction mixture was stirred and heated to 70 °C for 3 h. Attempts to separate products by sublimation, vacuum distillation and fractional crystallization from pentane were not successful. However, the presence of **17** in the mixture was indicated by its ^1H NMR spectrum: ^1H NMR (benzene-d_6) δ 0.46 (s, 9 H, $SiCH_3$), 2.32 (t, 2 H, $^3J_{HH}$ = 5.6 Hz, $N(CH_2)_3$), 3.29 (bs, 2 H, $SiNCH_2$).

Reaction of Trimethylazaboratrane, 6, with O=V(O-*iso*-Pr)$_3$. Neat O=V(O-*iso*-Pr)$_3$ (0.14 mL, 0.59 mmol) was added dropwise via a microsyringe to a solution of **6** (0.11 g, 0.56 mmol) in benzene-d_6, in an NMR tube and mixed thoroughly. The color of the solution changed from colorless to deep red. ^1H and ^{13}C NMR spectra of the reaction mixture were recorded and compared with literature data revealing the presence of **18**[22] and B(O-*iso*-Pr)$_3$.[23]

Reaction of 6 with Ti(O-*iso*-Pr)$_4$. A solution of Ti(O-*iso*-Pr)$_4$ (2.5 g, 8.8 mmol) in 60 mL of toluene was added with stirring to a solution of **6** (1.47 g, 7.50 mmol) in 120 mL of toluene and the mixture was refluxed for 40 h. Only starting materials were observed by ^{1}H NMR spectroscopy. An aliquot of the reactants was removed and sealed as a benzene-d_6 solution in an NMR tube. ^{1}H, ^{13}C and ^{11}B NMR spectra taken after 9 months revealed the presence of B(O-*iso*-Pr)$_3$,[23] **6**,[8] Ti(O-*iso*-Pr)$_4$ and **19**.

19: ^{1}H NMR (benzene-d_6) δ 1.44 (d, 6 H, $^3J_{HH}$ = 6.2 Hz, CH(CH_3)$_2$), 2.70 (t, 6H, $^3J_{HH}$ = 5.8 Hz, N(CH_2)$_3$), 3.16 (t, 6 H, $^3J_{HH}$ = 5.9 Hz, MeNCH_2), 3.39 (s, 9 H, NCH_3), 4.77 (sept, 1 H, $^3J_{HH}$ = 6.1 Hz, CH(CH$_3$)$_2$); ^{13}C NMR (benzene-d_6) δ 26.9 (qm, CH(*C*H$_3$)$_2$, $^1J_{CH}$ = 125.4 Hz, $^2J_{CH}$ = $^3J_{CH}$ = 4.5 Hz), 47.7 (qt, NCH$_3$, $^1J_{CH}$ = 131.5 Hz, $^3J_{CH}$ = 2.6 Hz), 52.9 (tm, N(CH$_2$)$_3$, $^1J_{CH}$ = 134.8 Hz), 58.3 (tqt, MeNCH_2, $^1J_{CH}$ = 131.8 Hz, $^3J_{CH}$ = 6.1 Hz, $^2J_{CH}$ = 2.2 Hz), 74.7 (d sept, *C*HMe$_2$, $^1J_{CH}$ = 141.4 Hz, $^2J_{CH}$ = 4.3 Hz).

Trimethylazagallatrane Dimer, 14. *Method A.* A solution of tetramine **2** (Me$_3$tren) (2.09 g, 11.1 mmol) in 75 mL of degassed toluene was added dropwise within 15 min to a solution of [Ga(NMe$_2$)$_3$]$_2$ (2.24 g, 11.1 mmol) in 75 mL of toluene with stirring at -40 °C. The reaction solution was left to warm to room temperature and stirred for 24 h. All volatiles were removed under vacuum giving 2.20 g (78%) of the crude product. Further purification was effected by sublimation at 110 °C at 5 x 10^{-3} Torr giving the white solid product **14**: mp 121-128° dec.; ^{1}H NMR (500 MHz, toluene-d_8) δ 2.10-2.17 (m, 6H), 2.37 (ddd, 2 H, $^2J_{HH}$ = 15.0 Hz, $^3J_{HH(trans)}$ = 9.7 Hz, $^3J_{HH(gauche)}$ = 5.4 Hz), 2.47-2.55 (m, 4H), 2.60-2.66 (m, 2H), 2.68 (s, 6 H, CH$_3$), 2.75 (s, 6 H, CH$_3$), 2.78 (ddd, 2 H, $^2J_{HH}$ = 11.8 Hz, $^3J_{HH(trans)}$ = $^3J_{HH(gauche)}$ = 4.0 Hz), 2.87-2.97 (m, 4H), 2.93 (s, 6 H,

CH_3), 3.16 (ddd, 2 H, $^2J_{HH}$ = 13.7 Hz, $^3J_{HH(trans)}$ = 10.0 Hz, $^3J_{HH(gauche)}$ = 4.0 Hz), 3.73 (ddd, 2 H, $^2J_{HH}$ = $^3J_{HH(trans)}$ = 13.2 Hz, $^3J_{HH(gauche)}$ = 5.1 Hz, $^1J_{CH}$ = 139.0 Hz, ^{13}C satellites); ^{13}C NMR (benzene-d_6) δ 40.50 (qdd, CH_3, $^1J_{CH}$ = 133.9 Hz, $^3J_{CH}$ = 10.3, 4.3 Hz), 41.85 (qdd, CH_3, $^1J_{CH}$ = 129.5 Hz, $^3J_{CH}$ = 6.9, 6.9 Hz), 42.22 (qdd, CH_3, $^1J_{CH}$ = 129.5 Hz, $^3J_{CH}$ = 3.0, 3.0 Hz), 54.03, 54.56, 54.83, 54.96, 56.15, 58.86, CH_2 groups; ^{71}Ga NMR (benzene-d_6, 70 °C) δ 255 ± 5 ($\Delta\nu_{1/2}$ = 12 kHz); HRMS (EI) calcd for $C_{18}H_{42}N_8{}^{69}Ga^{71}Ga$ (M^+) *m/z* 510.20384, found 510.20265, calcd for $C_{18}H_{42}N_8{}^{69}Ga_2$ (M^+) *m/z* 508.20464, found 508.20436, calcd for $C_{15}H_{36}N_7{}^{69}Ga_2$ *m/z* 452.15462, found 452.15475, calcd for $C_9H_{21}N_4{}^{69}Ga$ *m/z* 254.10232, found 254.10192; LRMS (EI) *m/z* (ions $^{69}Ga_2$, $^{69}Ga^{71}Ga$, $^{71}Ga_2$, relative intensities) 508, 510, 512 (M^+, ~0.04), 452, 454, 456 ($M\text{-}C_3H_6N^+$, 0.16, 0.24, 0.06), 323, 325, 327 (0.5, 0.7, 0.2), 255, 257 (7, 5), 155 (7), 144 (14), 132 (7), 114 (6), 113 (7), 99 (51), 72 (39), 71 (12), 70 (22), 69 (11), 58 (100), 57 (19), 56 (24); CIMS (positive ion detection) *m/z* (ions, relative intensities) 509, 511, 513 ($M+H^+$, 58, 70, 25), 452, 454, 456 (3, 3, 1), 314, 316, 318 (9, 11, 4), 291, 293, 295 (14, 13, 3), 255, 257 (6, 6), 203 (22), 189 (100); IR (KBr pellet, 4000-400 cm^{-1}) ν 2962 s, 2948 s, 2926 s, 2886 s, 2844 vs, 2800 vs, 2760 vs, 2746 s, 2674 m, 1465 m, 1456 m, 1449 m, 1413 vw, 1376 w, 1359 w, 1349 s, 1331 m, 1322 vw, 1304 m, 1279 m, 1263 m, 1240 vw, 1224 vw, 1195 m, 1182 m, 1162 vs, 1112 w, 1092 s, 1080 vs, 1040 vs, 1026 s, 1010 w, 977 s, 948 s, 912 s, 853 vs, 838 s, 803 w, 748 m, 634 vs, 593 m, 563 m, 541 s, 504 vs, 495 sh. Anal. Calcd for $C_{18}H_{42}N_8Ga_2$: C, 42.39; H, 8.30; N, 21.97. Found C, 43.15; H, 8.78; N, 21.06.

Crystals suitable for X-ray diffraction experiments were grown from a saturated pentane solution of **14** at -20 °C.

Method B. A solution of $Ga(acac)_3$ (0.546 g, 1.49 mmol) and **12** (0.320 g, 0.754 mmol) in 70 mL of toluene was stirred at room temperature and the conversion was monitored by ^1H NMR. The reaction was completed after 35 days. The separation of **14** from $Al(acac)_3$ failed owing to their similar volatility and solubility.

Tris(trimethylsilyl)gallazatrane, 10. A solution of tetramine **4** (5.67 g, 15.6 mmol) in 20 mL of degassed THF was added dropwise to a stirred solution of $[Ga(NMe_2)_3]_2$ (3.16 g, 15.6 mmol) in 125 mL of THF at room temperature. The reaction mixture was heated to reflux for 24 h. After the removal of all volatiles, 5.91 g (88%) of **10** was obtained as an oily liquid which solidified in a freezer. The crude product was sublimed at 80-90 °C at 5 x 10^{-3} Torr giving a white solid **10**: mp 43-45 °C; ^1H NMR (toluene-d_8) δ 0.21 (s, 9 H, $SiMe_3$, $^1J_{CH}$ = 113.8 Hz, ^{13}C satellites, $^2J_{SiCH}$ = 6.4 Hz, ^{29}Si satellites), 1.97 (t, 2 H, $N(CH_2)_3$, $^3J_{HH}$ = 5.3 Hz), 2.83 (t, 2 H, $SiNCH_2$, $^3J_{HH}$= 5.3 Hz); ^{13}C NMR (toluene-d_8) δ -1.6 ($SiMe_3$, $^1J_{SiC}$ = 55.3 Hz, ^{29}Si satellites), 43.6 ($SiNCH_2$), 57.7 ($N(CH_2)_3$); ^{29}Si NMR (toluene-d_8) δ 0.34; ^{71}Ga NMR (toluene-d_8) δ 304 ± 10 ($\Delta\nu_{1/2}$ = 40 kHz at 70 °C); HRMS (EI) calcd for $C_{15}H_{39}N_4Si_3{}^{69}Ga$ (M^+) *m/z* 428.17396, found 428.17301; LRMS (EI) *m/z* (ions ^{71}Ga, ^{69}Ga, relative intensities) 430, 428 (M^+,11,13), 415,413 ($M\text{-}CH_3^+$, 14, 18), 328, 326 ($M\text{-}Me_3SiNCH_2\text{-}H^+$, 76, 100), 260 (9), 213 (45), 211 (13), 187 (13), 171 (32), 157 (13), 69 (23).

Reaction of Tris(*tert*-butyldimethylsilyl)azaalumatrane, 9, with Ga(acac)$_3$. A solution of **9** (0.18 g, 0.35 mmol) and $Ga(acac)_3$ (0.13 g, 0.35 mmol) in 200 mL of toluene was stirred at room temperature and the reaction was monitored by ^1H NMR spectroscopy. After 1 month, 30% of **9** was converted to **11**: ^1H NMR

(benzene-d_6) δ 0.09 (s, 6 H, $SiMe_2$), 0.99 (s, 9 H, *tert*-Bu), 2.33 (t, 2 H, $^3J_{HH}$ = 6.3 Hz, $N(CH_2)_3$), 2.80 (t, 2 H, $^3J_{HH}$ = 6.0 Hz, $SiNCH_2$).

Reaction of Trimethylazaboratrane, 6, with Triethanolamine (TEA). An excess of TEA (0.1 mL, 0.8 mmol) was added to a stirred solution of **6** (0.14 g, 0.71 mmol) in 50 mL of toluene at room temperature and further stirred for 2 h until precipitation of a white solid was completed. Filtration followed by washing of the precipitate with 3 x 1 mL portions of Et_2O, and drying under vacuum for 45 minutes afforded 0.11 g (99%) of boratrane **21**[24]: mp 235.5-236.5, lit.[24] 236.5-237.5; ^1H NMR (chloroform-d_1) δ 3.11 (t, 6 H, NCH_2, $^3J_{HH}$ = 5.7 Hz, $^1J_{CH}$ = 141.4 Hz, ^{13}C satellites), 3.95 (t, 6 H, OCH_2, $^3J_{HH}$ = 5.7 Hz, $^1J_{CH}$ = 146.5 Hz, ^{13}C satellites), ^{13}C NMR (chloroform-d_1) δ 59.2 (tm, NCH_2, $^1J_{CH}$ = 141.3 Hz, $^1J_{CC}$ = 34 Hz , ^{13}C satellites), 62.0 (tt, OCH_2,$^1J_{CH}$ = 146.5 Hz, $^2J_{CH}$ = 1.7 Hz, $^1J_{CC}$ = 34 Hz, ^{13}C satellites); ^{11}B NMR (chloroform-d_1, 20 °C) δ 14.5 ($\Delta\nu_{1/2}$ = 70 Hz); LRMS (EI) *m/z* (ions ^{11}B, ^{10}B, relative intensities) 157, 156 (M^+, 11, 3), 127, 126 ($M\text{-}CH_2O^+$, 48, 100), 125 (24), 100 (20), 99 (11), 98 (5), 56 (21), 55 (21).

Reaction of Azasilatrane 15 with Triethanolamine (TEA). An excess of TEA (0.15 mL, 1.1 mmol) as added to a solution of **15** (0.179 g, 0.783 mmol) in 0.5 mL of benzene-d_6 in an NMR tube. Products **22** and **2** were characterized by favorable comparisons of their ^1H, ^{13}C and ^{29}Si NMR spectra with published data.[12,25]

Single-Crystal X-ray Diffraction Studies of 12 and 14. Colorless crystals of **12** were mounted in 0.5 mm glass capillaries in a nitrogen-filled glove box and flame-sealed, while crystals of **14** were covered with paraffin oil, attached to a glass fiber and quickly transferred into a stream of cold nitrogen on the diffractometer. Pertinent crystal data, experimental conditions for data

collection, solution and structure refinement are listed in Table I. Lorentz and polarization corrections were applied. A nonlinear correction based on the decay in the standard reflections and a semi-empirical absorption correction based on the azimuthal scans of several reflections were applied to the data. The structures of **12** and **14** were solved by direct methods and refined by a full-matrix least-squares method, using the TEXAN (VAX)[26] and SHELXTL-Plus (MicroVAX)[27] programs. All non-hydrogen atoms were placed directly from the E-map and refined anisotropically. Neutral atom scattering factors were taken from Cromer and Waber.[28] Atomic coordinates, thermal parameters, bond distances, and bond angles are listed in the supplementary materials.

Table I. Crystal Data, Data Collection, Solution and Refinement Parameters for **12** and **14**

	12	**14**
formula	$Al_2C_{18}H_{42}N_8$	$Ga_2C_{18}H_{42}N_8$
fw	424.55	510.02
crystal size (mm)	0.24 x 0.18 x 0.20	0.40 x 0.40 x 0.40
crystal system	orthorhombic	triclinic
space group	P_{bca} (no. 61)	$P\bar{1}$ (no. 2)
a (Å)	37.372(10)	9.716(1)
b (Å)	14.379(2)	11.325(2)
c (Å)	8.774(2)	11.343(1)
α (deg)	90	110.36(2)
β (deg)	90	97.87(1)
γ (deg)	90	90.34(1)
V (Å^3)	4677.2(1)	1157.2(3)
Z	8	2
d_{calc} (g/cm^3)	1.206	1.464
F(000)	2988	536
abs coeff (cm^{-1})	25.4	23.5
diffractometer	Hilger-Watts	Enraf-Nonius CAD4
radiation (Å)	MoK$_\alpha$ (λ = 0.71069)	MoK$_\alpha$ (λ = 0.71073)
temperature (°C)	23 ± 1	-50 ± 1
monochromator	graphite crystal	graphite crystal
2θ range (deg)	5.0-50.2	4.0-50.0
scan type	ω	2θ-θ

Table I. Continued

scan speed (deg/min)	3-15	0.5-2.0
scan range (deg)	0.80 + 0.50 tan θ	0.80 plus K_α separation
collected reflcns	6961	4336
independent reflcns	4350	4072
R_{init} (%)	7.8	1.3
observed reflcns, n_{obs}	1553	3032
	(I>4.0σ(I))	(I>3.0σ(I))
weighting scheme, w^{-1}	$[\sigma^2(F_o^2)]/4F_o^2$	$\sigma^2(F_o) + 0.0025\,(F_o)^2$
no. of variables, n_{var}	414	284
data-to-parameter ratio	8.3:1	10.7:1
largest peak (e.Å^{-3})	0.27	0.49
largest hole (e.Å^{-3})	-0.25	-0.30
R (%)[a]	5.0	4.7
R_w (%)[b]	5.7	5.4
GOF[c]	2.43	0.74

[a] $R = \Sigma||F_o|-|F_c||/\Sigma|F_o|$. [b] $R_w = [\Sigma w(|F_o|-|F_c|)^2/\Sigma w(F_o)^2]^{1/2}$. [c] $GOF = [\Sigma w(|F_o|-|F_c|)^2/(n_{obs}-n_{var})]^{1/2}$.

RESULTS AND DISCUSSION

Syntheses and Reactions. The metathetical reaction 1 between $[Al(NMe_2)_3]_2$ and trialkylborates was reported by Ruff in the early 60's.[29] Recently, we used a similar approach to prepare azaboratrane **6** from azaalumatrane **12** by the transmetallation reaction[8] as depicted in Scheme I.

Reaction 1:

$$[Al(NMe_2)_3]_2 + B(OR)_3 \longrightarrow B(NMe_2)_3 + Al(OR)_3$$

R = Me, Et, *n*-Bu

There are two major factors driving these redistribution reactions. The higher strength of Al-O bonds relative to B-O and Al-N bonds is responsible for an enthalpic advantage, while the conversion of dimeric **12** to monomeric **6** is favored entropically. Moreover, the formation of insoluble polymeric $[Al(OMe)_3]_n$ which precipitates from the reaction solution, forces the equilibrium completely towards the products. Another crucial factor in the case of azatrane compounds is the stabilization effect of a transannular bond as we demonstrated in the case of group 14 elements. Thus while $MeSi(OMe)_3$ reacts easily with dimeric azaalumatrane **12**, as shown in Scheme I, giving azasilatrane **15** in 42% yield, the analogous reaction of $MeC(OMe)_3$ with **12** failed to produce any pro-azacarbatrane **23** or polymeric $[Al(OMe)_3]_n$ even after several hours of refluxing in toluene. The metathetical reaction 2 of trialkyltin amides with carboxylic esters resulting in the transfer of the OR" group from carbon to tin and in the formation of a C-N bond was reported by Lappert and George.[30]

Scheme I

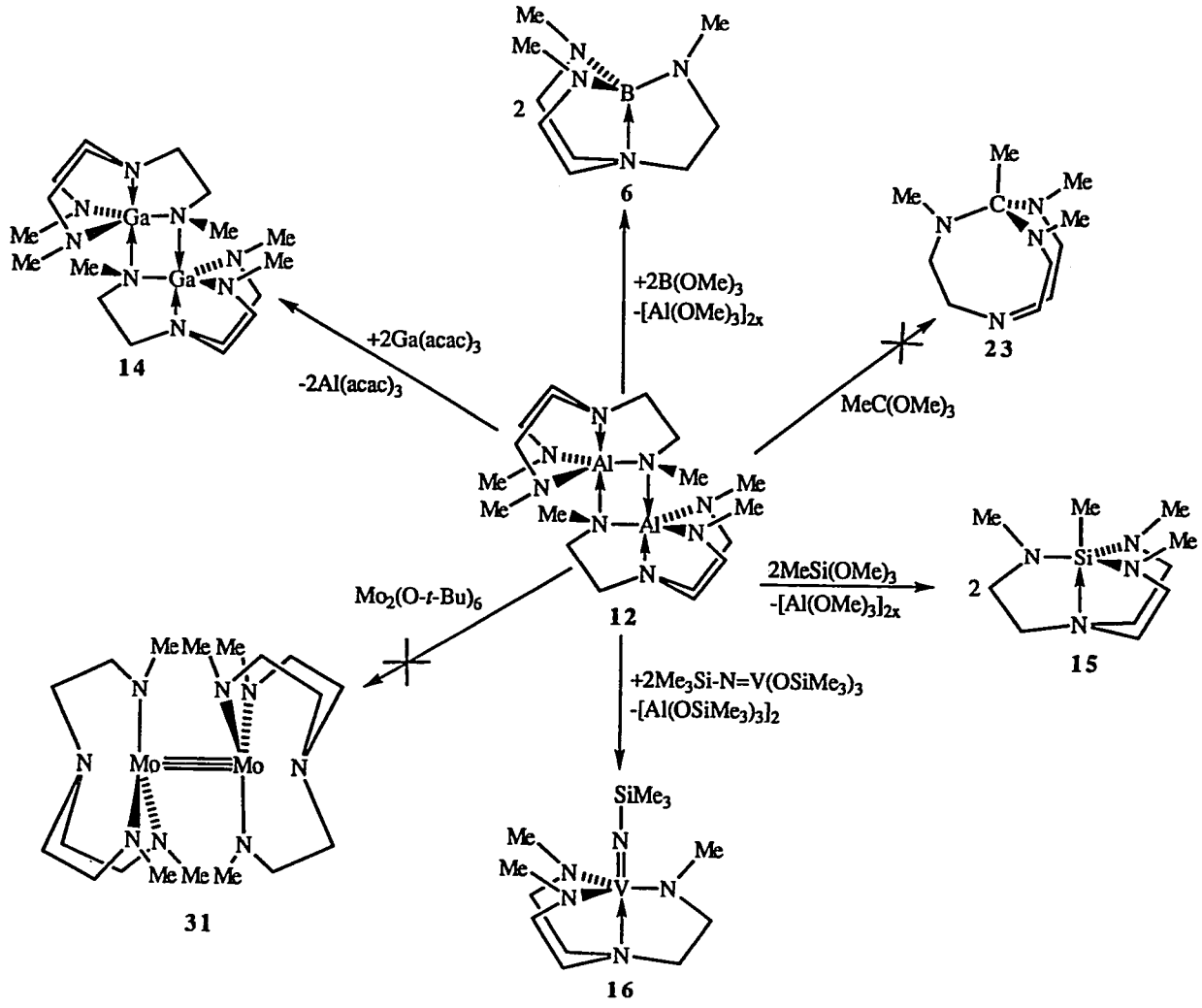
6
+2B(OMe)3
-[Al(OMe)3]2x
+2Ga(acac)3
-2Al(acac)3
14
MeC(OMe)3
23
12
2MeSi(OMe)3
-[Al(OMe)3]2x
15
Mo2(O-t-Bu)6
31
+2Me3Si-N=V(OSiMe3)3
-[Al(OSiMe3)3]2
16

Reaction 2:

$$R_3Sn\text{-}NMe_2 + R'C(O)\text{-}OR'' \rightarrow R_3Sn\text{-}OR'' + RC(O)\text{-}NMe_2$$

R = Me, *n*-Bu; R' = Me, CH_2=C(Me), $MeC(O)CH_2$; R'' = Me, Et

This shows that the formation of pro-azacarbatrane **23** might be feasible on bond energy grounds. However, we can consider two obstacles to this reaction. Assuming the initial step is a nucleophilic attack of the OMe group at aluminum and excluding the breakage of the M-O bond (M = C, Si) with the formation of a cation $MeM(OMe)_2^+$ as a pathway with a prohibitively high activation energy, we can envision structure **A** as a possible reaction intermediate. The formation of **A** requires an increase of the coordination

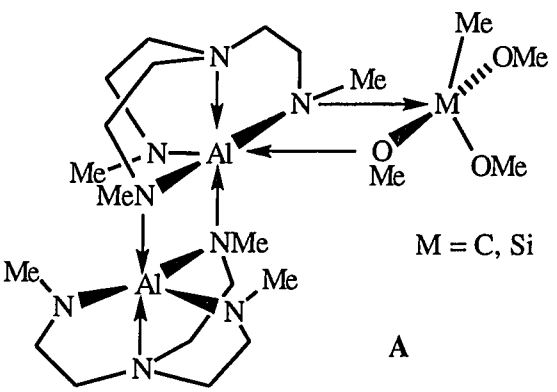

A

number of M in $MeM(OMe)_3$ from four to five. This is, of course, easily accomplished in the case of silicon but it is much more difficult for carbon. The same rationale accounts for the lack of stabilization of the desired product by a transannular N→C interaction, and hence contributes to the unreactivity of $MeC(OMe)_3$. Azasilatrane **15** was prepared previously in our laboratory by a transamination reaction 3 with a similar yield.[19]

Reaction 3:

$$MeSi(NMe_2)_3 + \underset{\mathbf{2}}{(MeNHCH_2CH_2)N} \longrightarrow 3Me_2NH + \underset{\mathbf{15}}{MeSi(MeNCH_2CH_2)_3N}$$

Two literature examples of transmetallation reactions involving atranes are worthy of note. The preparation of stibatrane from silatrane in reaction 4 makes use of the driving force of strong Si-F bonds in the by-product.[31] On the other hand, no striking energy difference between reactants and products

Reaction 4:

$$SbF_3 + R\text{-}Si(OCH_2CH_2)_3N \longrightarrow RSiF_3 + Sb(OCH_2CH_2)_3N$$
$$R = Me, Vinyl$$

is apparent in transesterification reaction 5 which uses aluminum ethoxide as a catalyst.[32]

Reaction 5:

$$B(OCH_2CH_2)_3N + HSi(OEt)_3 \xrightarrow{Al(OEt)_3} B(OEt)_3 + HSi(OCH_2CH_2)N$$

In analogy to the transmetallation of monomeric azastannatrane **24**[20,22] (reaction 6), we have shown that dimeric azaalumatrane **12** can serve as a useful starting material for the synthesis of azametallatranes among the transition metals. As summarized in Scheme I, $Me_3Si\text{-}N{=}V(OSiMe_3)_3$ reacts with **12** giving azavanadatrane **16**. This reaction proceeds smoothly upon mixing the reactants as is indicated by the color change from colorless to deep red. The ^1H and ^{13}C NMR spectra showed signals for azavanadatrane **16**[20] and dimeric $[Al(OSiMe_3)_3]_2$.[21] The latter was also identified as the only

aluminum-containing species by the ^{27}Al NMR signal at δ 59 ($\Delta\nu_{1/2}$ = 88 Hz at 20 °C). The separation of **16** from $[Al(OSiMe_3)_2]_2$ was precluded by their very

Reaction 6:

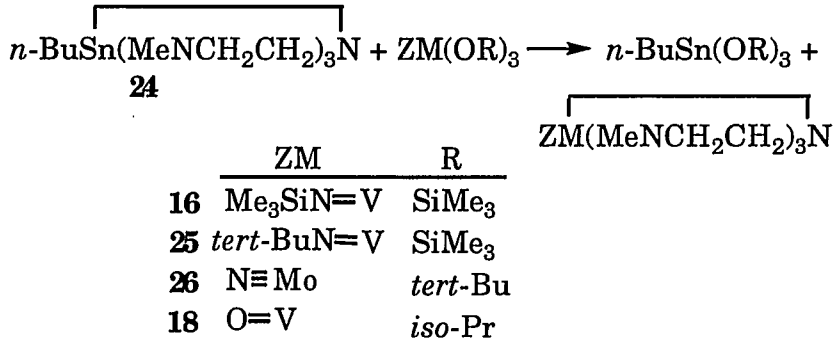

	ZM	R
16	$Me_3SiN{=}V$	$SiMe_3$
25	*tert*-BuN=V	$SiMe_3$
26	N≡Mo	*tert*-Bu
18	O=V	*iso*-Pr

similar volatilities and solubilities in hydrocarbon solvents. Recently, Schrock and coworkers[33] reported a series of azavanadatranes **27-30** possessing vanadium in the oxidation state three (**29**) and four (**27, 28, 30**). These species were synthesized by the reaction of lithiated tetramines with VCl_4·DME (eq 7) by a subsequent reduction with Na/Hg (eq 8), or by the reaction with an alkyllithium reagent (eq 9). The reaction of Ti(O-*iso*-Pr)$_4$ with **12**

Reactions 7-9:

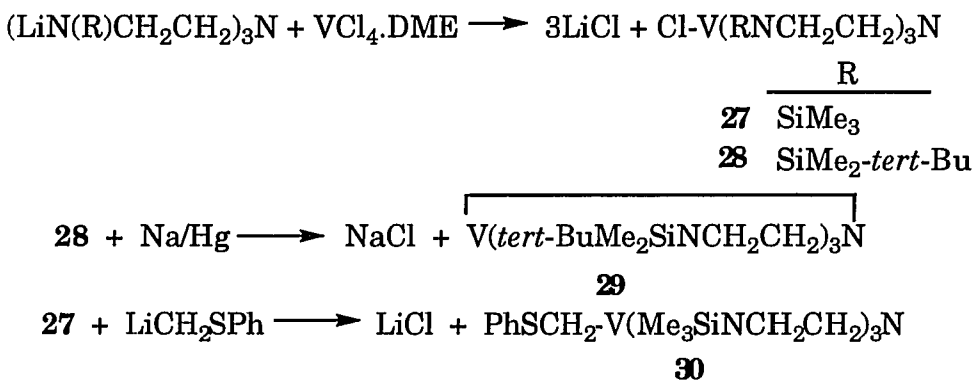

afforded an intractable mixture of products. The ^1H NMR spectrum showed the presence of more than seven isopropyl signals in the methine region which probably belong to partially transmetallated intermediates. Despite the complexity of the spectrum, the presence of a monomeric $M(MeNCH_2CH_2)_3N$ unit was clearly indicated by two triplets and a singlet for the CH_2 and CH_3 groups, respectively. An attempt to prepare azatrane **31** (Scheme I) with the central dimolybdenum unit failed since the ^1H and ^{13}C NMR spectra of the reaction mixture after 18 hours of reflux showed only the presence of unreacted starting materials **12** and $Mo_2(O\text{-}tert\text{-}Bu)_6$.[16]

Similarly to dimeric azaalumatrane **12**, monomeric **8**[8] reacts with the same facility with $O{=}V(O\text{-}iso\text{-}Pr)_3$ according to eq 10. The products **17** and $Al(O\text{-}iso\text{-}Pr)_3$[21] were identified by ^1H NMR spectroscopy but attempted separation by

Reaction 10:

$$\underset{\textbf{8}}{3Al(Me_3SiNCH_2CH_2)_3N} + 3O{=}V(O\text{-}iso\text{-}Pr)_3 \longrightarrow [Al(O\text{-}iso\text{-}Pr)_3]_3 + \underset{\textbf{17}}{+\ 3O{=}V(Me_3SiNCH_2CH_2)_3N}$$

sublimation or vacuum distillation failed due to the similar volatilities of these products. The fact that azaboratrane **6** is also capable of functioning as a reactant in the transmetallation reaction with transition metal alkoxides was demonstrated in its reactions with $O{=}V(O\text{-}iso\text{-}Pr)_3$ and $Ti(O\text{-}iso\text{-}Pr)_4$ which are shown in Scheme II. While the formation of azavanadatrane **18** proceeds to completion at room temperature nearly instantaneously, the reaction of

Scheme II

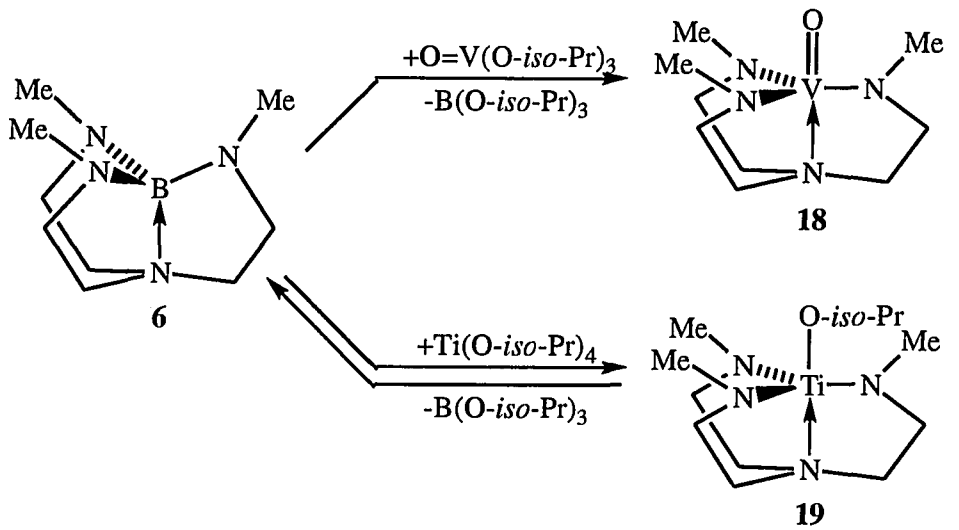

$Ti(O\text{-}iso\text{-}Pr)_4$ with **6** reaches equilibrium after it has been left for several months at room temperature. The ratio of reactants to products in the latter reaction was established both by ^{1}H and ^{11}B NMR spectroscopies to be 30:70. Azatitanatrane **19** was identified by a comparison of the similarity of cage ^{1}H and ^{13}C NMR chemical shifts to those of the previously reported *tert*-BuO derivative.[34]

Versatility of the transmetallation reaction was demonstrated by extending its scope to acac complexes (penta-2,5-dienoates). Both dimeric **12** (Scheme I) and monomeric azaalumatrane **9** (reaction 11) react slowly with $Ga(acac)_3$ and the central aluminum atom is replaced in a complex multistep reaction by gallium. The formation of $[Ga(MeNCH_2CH_2)_3N]_2$, **14**, (Scheme I) was completed after 35 days at room temperature as concluded from the ^{1}H, ^{13}C, ^{27}Al and ^{71}Ga NMR spectra of the reaction mixture. Elevated temperatures did not speed up the reaction but rather caused decomposition of the products. The conversion of only 30% after a month at room temperature

Reaction 11:

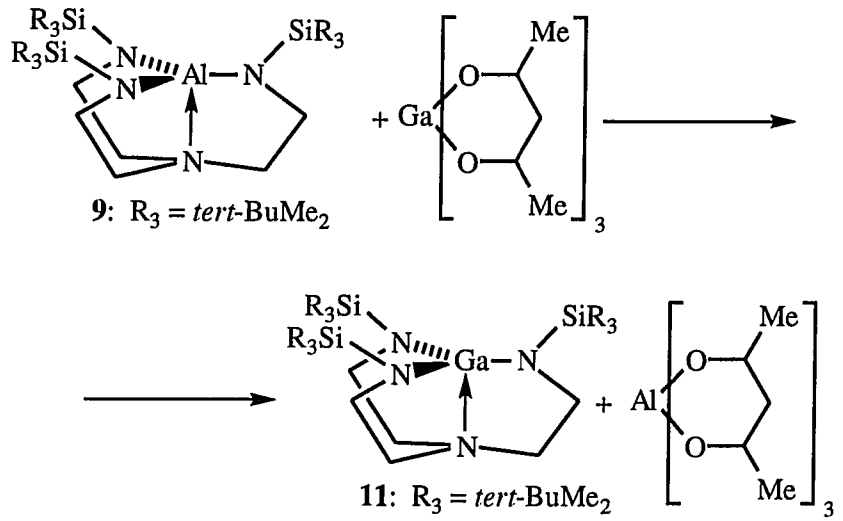

was observed by ^{1}H NMR spectroscopy for reaction 11.

A preparatively more useful route for synthesizing azagallatranes **14** and **10** is indicated in the transmetallation reaction 12. These facile transformations demonstrate that analogously to the situation for azaalumatranes,[9] the size of the substituents on the equatorial nitrogens governs the degree of oligomerization. The bulky $SiMe_3$ groups in **10** shield the gallium center and prevent dimerization, while smaller methyl groups in **14** allow gallium to increase its coordination number.

A close relationship between azatranes and atranes was recently demonstrated in a facile conversion of azagermatranes **32-35**[35] and azaalumatranes **8** and **12**[10] to atranes **36, 37** and **20**, respectively by the transligation reaction 13 with triethanolamine. In this metathesis, a triptych framework is retained despite the multiplicity of bonds that must be broken in the reactants and reformed in the products. This result emphasizes a remarkable stability of these multichelated structures. The ligand exchange

Reaction 12:

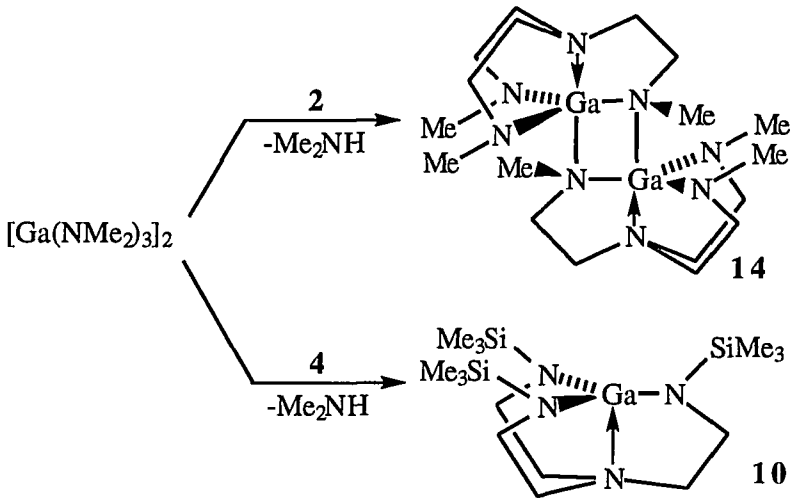

Reaction 13:

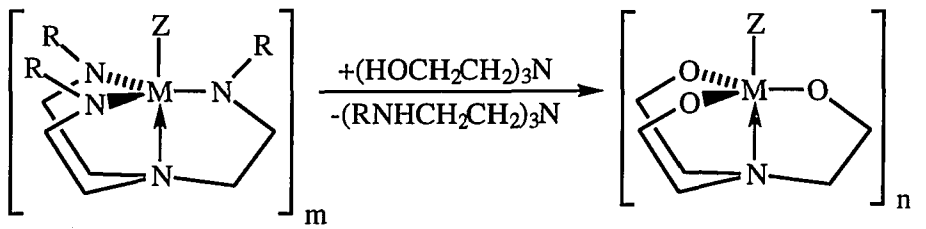

	m	M	Z	R	n	
32	1	Ge	Me	H	1	**36**
33	1	Ge	Me	Me	1	**36**
34	1	Ge	*tert*-Bu	H	1	**37**
35	1	Ge	*tert*-Bu	Me	1	**37**
12	2	Al	–	Me	4	**20**
8	1	Al	–	$SiMe_3$	4	**20**
6	1	B	–	Me	1	**21**
15	1	Si	Me	Me	1	**22**

is driven by the formation of strong oxygen-metal bonds. We have found, that azaboratrane **6** and azasilatrane **15** can also be converted to boratrane **21** and silatrane **22**, respectively, as shown in reaction 13. This extends and generalizes the scope of the transligation reaction. Boratrane **21** was isolated in quantitative yield and was characterized by ^{1}H, ^{11}B, ^{13}C NMR and MS spectroscopies.[24] Silatrane **22** was characterized by ^{1}H, ^{13}C and ^{29}Si NMR spectra in the reaction mixture.[25]

Structural Considerations. Recently we found that the molecular structure of dimeric azaalumatrane **13** features an unusual cis configuration of the substituents on the central four-membered ring.[9] Only two other similar examples could be found in the literature, namely, the gallium and titanium derivatives **38**[36] and **39**.[37]

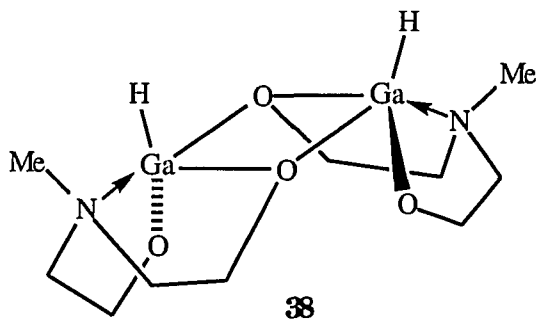

38

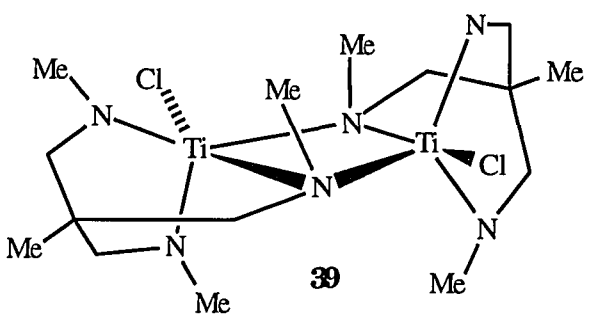

39

Here we present results of our single-crystal X-ray diffraction studies on azaalumatrane **12** and azagallatrane **14**. Their molecular structures are shown in Figures 1 and 2, respectively. Both molecules also possess the curious cis configuration of the substituent methyl groups on the central $(M\text{-}N)_2$ ring (M = Al, Ga). Structural data for **12** and **14** allow a detailed comparison between the Al and Ga atoms in an identical coordination environment and their influence on the surrounding ligands. The cis diastereomers, similarly to the situation found for **13**,[9] were the only species observed by ^1H and ^{13}C NMR spectroscopies in solutions of **12** and **14** . In fact, no interconversion of the cis isomers to the trans counterparts was observed after heating solutions of **12** and **14** for 60 h at 120 °C in sealed NMR tubes. Moreover, their spectra remain unchanged up to 100 °C in toluene-d_8 thus revealing no fluxionality which could be caused by a racemization process between two enantiomers of the cis species.

Both **12** and **14** contain an $(M\text{-}N)_2$ central array in the form of a puckered rectangle. The two planes of the puckered rectangle are canted with respect to one another by 146° and 148° in **12** and **14**, respectively, which closely corresponds to the value of 149° found in **13**. The central atoms in **12** and **14** are contained in a distorted trigonal bipyramidal coordination sphere and they are displaced approximately 0.2 and 0.3 Å, respectively, from the plane formed by the equatorial nitrogens toward the bridging nitrogens. The axial nitrogens are pyramidal and they are drawn toward the metal atoms by a transannular interaction. The distortion is reflected in a bending of the TBP axis to 160.6(2)° and 161.9(2)° for the N_{ax}-Al-N_{bridge} angles in **12** and to 161.8(1)° and 162.7(1)° for the N_{ax}-Ga-N_{bridge} angle in **14**, as shown in Tables II and III, respectively.

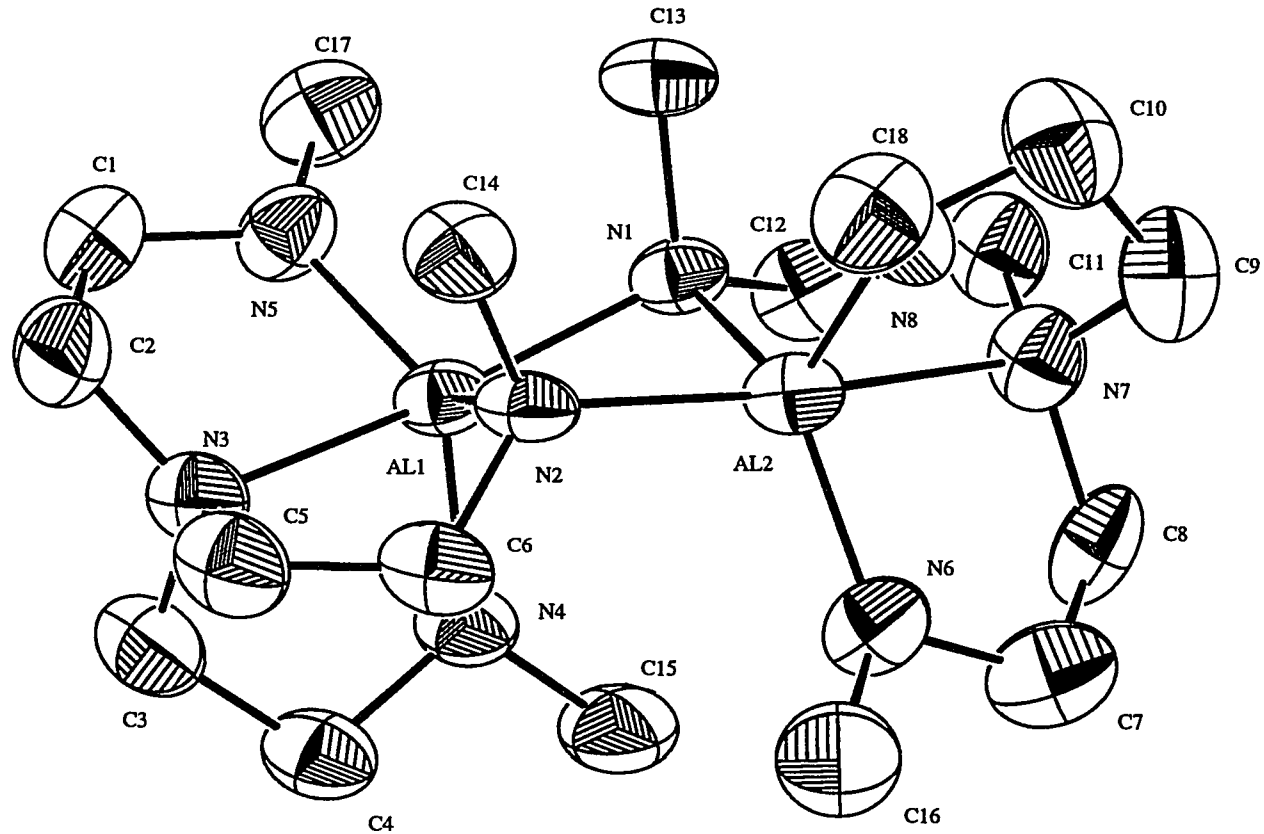

Figure 1. The molecular structure of $[Al(MeNCH_2CH_2)_3N]_2$,**12** ,with the atomic labelling scheme.

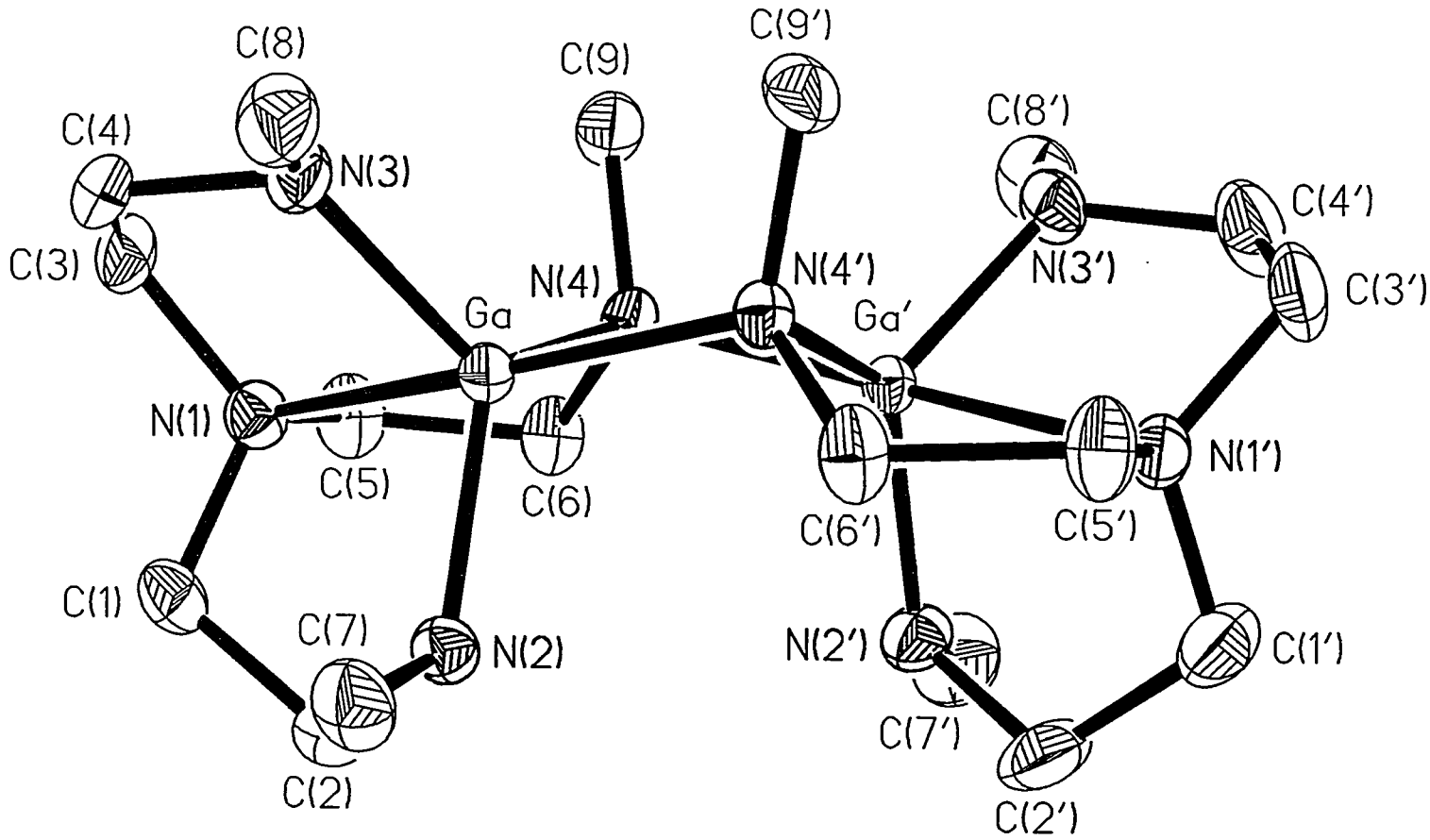

Figure 2. The molecular structure of $[Ga(MeNCH_2CH_2)_3N]_2$,**14** ,with the atom labelling scheme.

Compounds **12**, **13** and **14** are to our knowledge the only structurally proven examples of five-coordinate group 13 atoms surrounded solely by nitrogen ligands. The covalent radii of aluminum and gallium are very similar owing to the poor screening effect of the filled d-electron shell of gallium. The actual values of the covalent radii vary with the method used for their calculation,[38] and this prevents a firm decision regarding their relative sizes. Moreover, the tabulated values usually do not reflect the influence of different coordination numbers.

The corresponding bond distances and angles within the central $(Al\text{-}N)_2$ array of **12** (Table II) are not similar. The Al-N bond lengths range from 1.968(5) Å to 2.059(5) Å, which are comparable to the values found in **13**. Also similar to those in **13** are the internal angles of **12** (80.1(2)° and 81.0(2)° at aluminums and 92.7(2)° and 94.9(2)° at nitrogens). In contrast to **13**, the distances between aluminum and nonbridging equatorial nitrogens in **12** are not all the same and they are spread from 1.821(6) Å to 1.844(6) Å. These distances are comparable to the value of 1.857(2) Å found in **13**.[9] Two transannular $Al\text{-}N_{ax}$ bonds are also dissimilar in **12**, being 2.124(6) and 2.160(6) Å, and they are consonant with the bond distances between a TBP aluminum and an axial nitrogen which fall in the range of 2.054(5) Å to 2.18(1) Å.[9]

A comparison of the Ga-N bond lengths in **14** (Table III) with their Al-N counterparts in **12** reveals that for the same coordination environment, the Ga-N bonds are somewhat longer than the Al-N bonds. A similar observation was reported by Power and coworkers for the monomeric tricoordinate pairs of derivatives $R_2M\text{-}NR'R''$ (M = Al, Ga; R, R', R'' = 2,4,6-*iso*-$Pr_3C_6H_2$, H, 2,4,6-*iso*-

$Pr_3C_6H_2$; *tert*-Bu, $SiPh_3$, adamantyl) wherein the lengthening was about 0.06-0.07 Å.[39] In **14**, we found that the Ga-N bonds within the central ring are on average only 0.03 Å longer than the corresponding Al-N bonds in **12**. However, the equatorial nonbridging Ga-N distances are on average 0.07 Å longer and the transannular bonds are as much as 0.3 Å longer in **14** relative to **12**, which is consistent with a substantial flexibility of the transannular bond.

Table II. Selected Bond Distances (Å) and Angles (deg) for **12**

Al(1)-N(3)	2.124(6)	Al(2)-N(7)	2.160(6)
Al(1)-N(4)	1.843(6)	Al(2)-N(6)	1.829(6)
Al(1)-N(5)	1.821(6)	Al(2)-N(8)	1.844(6)
Al(1)-N(1)	1.968(5)	Al(2)-N(1)	2.032(5)
Al(1)-N(2)	2.049(5)	Al(2)-N(2)	2.022(5)
N(1)-Al(1)-N(2)	81.0(2)	N(1)-Al(2)-N(2)	80.1(2)
Al(1)-N(1)-Al(2)	94.9(2)	Al(1)-N(2)-Al(2)	92.7(2)
N(1)-Al(1)-N(3)	161.9(2)	N(2)-Al(2)-N(7)	160.6(2)
N(3)-Al(1)-N(2)	82.6(2)	N(7)-Al(2)-N(1)	80.9(2)
N(3)-Al(1)-N(4)	84.5(2)	N(7)-Al(2)-N(6)	83.4(3)
N(3)-Al(1)-N(5)	82.1(3)	N(7)-Al(2)-N(8)	84.8(3)
N(2)-Al(1)-N(5)	126.3(2)	N(1)-Al(2)-N(6)	126.0(2)
N(2)-Al(1)-N(4)	108.4(2)	N(6)-Al(2)-N(8)	117.2(3)
N(4)-Al(1)-N(5)	120.8(3)	N(1)-Al(2)-N(8)	112.3(3)

Table III. Selected Bond Distances (Å) and Angles (deg) for **14**

Ga-N(1)	2.284(3)	Ga'-N(1')	2.297(3)
Ga-N(2)	1.908(3)	Ga'-N(2')	1.891(3)
Ga-N(3)	1.900(3)	Ga'-N(3')	1.904(4)
Ga-N(4)	2.037(3)	Ga'-N(4')	2.043(3)
Ga-N(4')	2.048(3)	Ga'-N(4)	2.060(3)
N(4)-Ga-N(4')	82.6(1)	N(4)-Ga'-N(4')	82.2(1)
Ga-N(4)-Ga'	92.4(1)	Ga-N(4')-Ga'	92.6(1)
N(1)-Ga-N(4')	162.7(1)	N(1')-Ga'-N(4)	161.8(1)
N(1)-Ga-N(2)	84.2(1)	N(1')-Ga'-N(2')	83.7(1)
N(1)-Ga-N(3)	82.9(1)	N(1')-Ga'-N(3')	83.0(1)
N(1)-Ga-N(4)	80.1(1)	N(1')-Ga'-N(4')	79.7(1)
N(2)-Ga-N(3)	118.9(1)	N(2')-Ga'-N(3')	120.0(2)
N(3)-Ga-N(4)	120.2(1)	N(3')-Ga'-N(4')	115.7(1)
N(2)-Ga-N(4)	115.7(1)	N(2')-Ga'-N(4')	118.8(1)

The Ga-N bond lengths in **14** can be compared with the values found in other compounds possessing TBP coordinated gallium atoms such as **38**,[36] dimeric dimethylethanolamine and 8-quinolinol derivatives **40**,[40,41,42] monomeric 2-methyl-8-quinolinol compounds **41**,[43,44] the 1,10-phenanthroline complex **42**,[45] arylgallium compounds **43**[46] and **44**[47], pyridine derivative adducts **45**,[48] and **46**[49], the polycyclic cage compound $(GaH)_6(GaH_2)_2(\mu_3\text{-}O)_2(\mu_3\text{-}NCH_2CH_2NMe_2)_4(\mu\text{-}NHCH_2CH_2NMe_2)_2$, **47**[50], and the azacrown ether derivative **48**.[51] Table IV shows that the transannular (Ga-N(1), Ga'-N(1')) and axial bridging (Ga-N(4'), Ga-N(4)) bond lengths in **14** fall within the range established for the axial TBP distances, the axial bridging bond lengths being at the lower limit of this region. The equatorial bridging (Ga-N(4), Ga'-N(4')) distances are also in accord with previously reported values, though there are much less data to compare. The nonbridging equatorial (Ga-N(2), Ga-N(3),

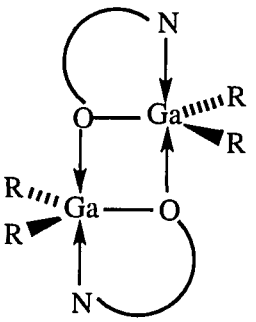

	R	O N
40a	H	$OCH_2CH_2NMe_2$
40b	Me	$OCH_2CH_2NMe_2$
40c	Me	8-quinolinol
40d	$(CH_2)_4CH$	8-quinolinol
45	Me	$OCH_2(C_5H_4N)$

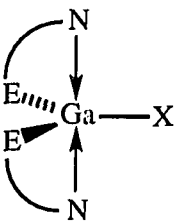

	X	E N
41a	Cl	2-Me-8-quinolinol
41b	$NCCH_2CO_2$	2-Me-8-quinolinol
41c	CH_3CO_2	2-Me-8-quinolinol
41d	$1/2(CH_2CO_2)_2$	2-Me-8-quinolinol
46	Cl	$C(SiMe_3)_2(C_5H_4N)$
43a	Cl	$C_6H_4CH_2NMe_2$
43b	$C_6H_4CH_2NMe_2$	$C_6H_4CH_2NMe_2$

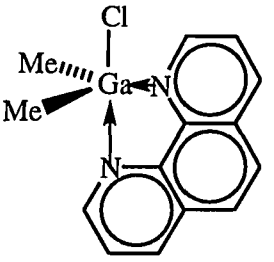

42

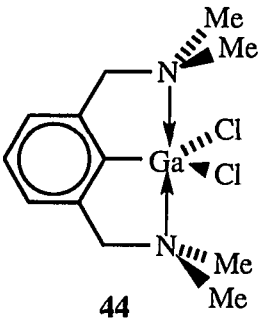

44

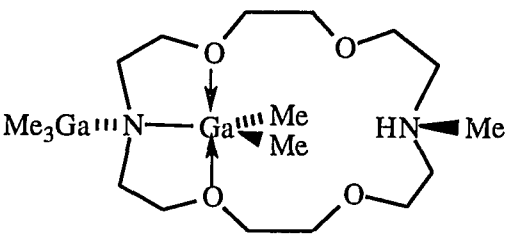

48

Ga'-N(2'), and Ga'-N(3')) distances are shorter than the quoted range. This shortening can be attributed to the lower coordination number of those nitrogens in **14** relative to **47** and **48**.

The major structural difference between azatranes **12** and **14** is in the degree of pyramidality of the equatorial nonbridging nitrogens. In **12**, N(4), N(5), N(6), and N(8) are in a nearly planar environment. The sum of angles around these atoms range from 354.7(7)° to 358.3(6)° which is in the range of values found in **13** implying near sp^2 hybridization. It would appear that while in **13** Si-N π-bonding can be largely responsible for the flattening of these nitrogen geometries, in **12** where no Si is present, we have to invoke the π-interactions between nitrogens and the central aluminum atoms which would be facilitated by the nitrogen planarity. A short Al-N(2) distance and the planarity of N(2) in **49** was explained by the π-donation of the nitrogen N(2) lone

Table IV. Comparison of Ga-N Distances (Å) in Compounds with TBP Gallium Coordination

	equatorial	axial	ref
14	1.891(3)-1.908(3)[a]	2.284(3), 2.297(3)[b]	this work
	2.040(3)[c]	2.048(3), 2.060(3)[c]	
38	–	2.192(5)	36
40a	–	2.279(3)	40
40b	–	2.471(4)	40
40c	–	2.211(3)	41
40d	–	2.207(9)	42
41a	–	2.110(9)	43
41b	–	2.071(2)-2.102(2)	44
41c	–	2.077(3)-2.098(3)	44
41d	–	2.088(3), 2.111(3)	44
42	2.119(6)	2.433(6)	45
43a	–	2.304(6), 2.385(6)	46
43b	–	2.551(2), 2.399(2)	46
44	–	2.355(4)	47
47	1.949(3), 1.999(3)	2.779(3)	50
45	–	2.276(3)	48
46	–	2.186(3), 2.214(4),	49
		2.268(4)[d]	
48	2.164(5)	–	51

[a]Nonbridging. [b]Transannular. [c]Bridging. [d]Three independent molecules.

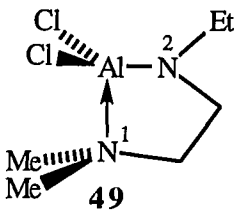

49

pair to the aluminum 3d empty orbitals.[52] In contrast to **12** and **13**, azagallatrane **14** possesses strongly pyramidal nonbridging equatorial nitrogens N(2), N(3), N(2'), and N(3') with a range of the sum of angles around them of 336.4(3)° to 344.9(4)°. This is similar to the angle sum around the axial four-coordinate sp^3 nitrogens N(1) and N(1') which is 342.4(4)°. The difference in the hybridization of the nonbridging equatorial nitrogens in **12** and **14**, both of which possess nearly identical environments, demonstrates the dissimilar tendency of Al and Ga to accept lone pair electron density from N.

Mass Spectroscopy. Because all the group 13 azatranes known so far are volatile solids, they may prove to be interesting precursors for the preparation of nitrides by CVD techniques. We examined the decomposition of **6** by high resolution mass spectroscopy and the results are listed in Table V. All the fragments feature a characteristic isotopic pattern (^{10}B, 19.6%, ^{11}B, 80.4%). Two major fragmentation pathways are shown in Scheme III. The base peak ion **6a** is formed by the loss of $MeNCH_2$ and a proton. The second most important process is the ejection of one complete arm and the formation of **6b** ions which can be protonated (*m/z* 140) or deprotonated (*m/z* 138).

Although the intensity of the parent peak of **14** in its EI mass spectrum is low the characteristic isotopic pattern (^{69}Ga, 60.4%, ^{71}Ga, 39.6%) was clearly identified. Using mild chemical ionization with NH_3, a high intensity of the parent ion can be obtained.

Scheme III

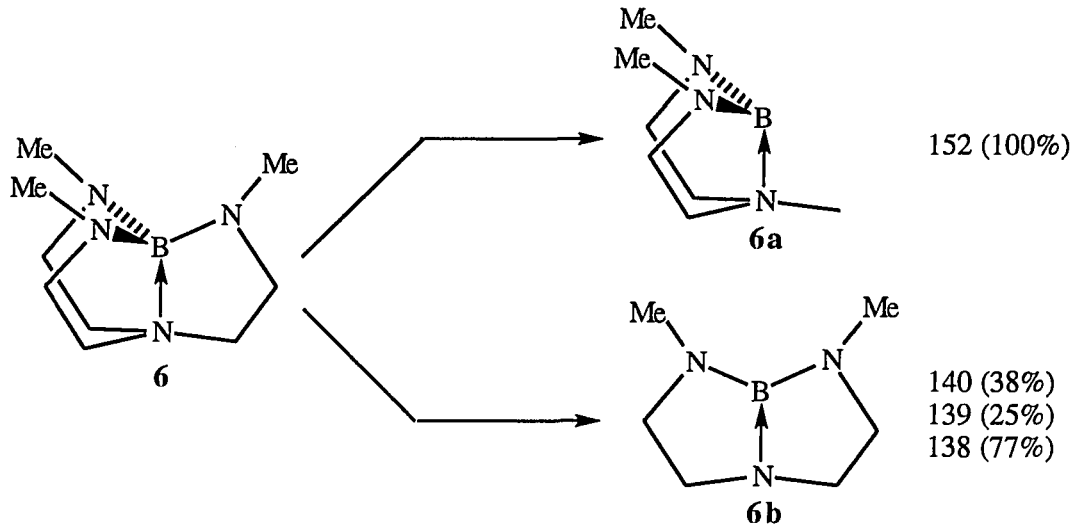

Table V. HRMS Data for Azaboratrane **6**

formula						*m/z*		
^{12}C	^{13}C	^{1}H	^{14}N	^{10}B	^{11}B	found	calcd	%
8	1	21	4	0	1	197.18859	197.18928	6.3
9	0	21	4	0	1	196.18591	196.18593	57.3
9	0	21	4	1	0	195.18834	195.18956	15.7
6	1	15	3	0	1	153.13962	153.13926	10.7
7	0	15	3	0	1	152.13586	152.13590	100.0
7	0	15	3	1	0	151.13925	151.13954	25.1
5	1	15	3	0	1	141.13787	141.13954	2.6
6	0	15	3	0	1	140.13630	140.13590	37.8
6	0	15	3	1	0	139.13963	139.13954	9.4
5	1	14	3	0	1	a	140.13143	a
6	0	14	3	0	1	139.12808	139.12808	25.1

Table V. Continued

6	0	14	3	1	0	138.13151	138.13171	6.0
5	1	13	3	0	1	b	139.12361	b
6	0	13	3	0	1	138.12065	138.12025	76.6
6	0	13	3	1	0	137.12397	137.12384	20.9
6	0	12	3	0	1	137.11273	137.11243	15.1
4	1	12	3	0	1	a	126.11578	a
5	0	12	3	0	1	125.11187	125.11243	7.0
5	0	12	3	1	0	a	124.11606	a
4	1	11	3	0	1	b	125.10796	b
5	0	11	3	0	1	124.10465	124.10460	40.0
5	0	11	3	1	0	123.10824	123.10824	10.0
5	0	10	3	0	1	123.09685	123.09678	13.4

[a]Not observed. [b]Unresolved shoulder.

NMR Spectroscopy. ^{1}H NMR spectra of **6** and **15** measured in both benzene-d_6 and chloroform-d_1 revealed their aromatic solvent-induced shift behavior. For **6**, the change of the solvent from chloroform-d_1 to benzene-d_6 caused a shift of 0.21 ppm to lower field for the NMe signal and upfield shifts of 0.35 and 0.65 ppm for the MeNCH_2 and N$(CH_2)_3$ signals, respectively. Similarly, the CH_3-Si and CH_3-N protons of **15** are shifted downfield by 0.32 and 0.14 ppm, respectively, on going from chloroform-d_1 to benzene-d_6. Conversely, upfield shifts of 0.44 and 0.17 ppm were observed for N$(CH_2)_3$ and MeNCH_2

signals, respectively. This phenomenon can be explained by the formation of collision complexes of **6** and **15** with benzene molecules as shown in Scheme IV.[53] The vector of the dipole moment lies along the N→M (M = B, Si) transannular dative bond and it is oriented from axial nitrogen toward the central atom based on their respective formal positive and negative charges. The electron-rich π-cloud of a benzene molecule is attracted to the positive end of the azatrane cage so that the methylene protons are influenced by the shielding cone of the ring current. Owing to their proximity to the plane of the benzene molecule, the $N(CH_2)_3$ protons display a larger ASIS effect than the more distant $MeNCH_2$ protons. The negative end of the atrane molecule attracts relatively electron deficient hydrogens on the periphery of the benzene molecules, thus exposing the Si-CH_3 and N-CH_3 groups to the deshielding torus of the ring current. A larger downfield shift was observed in **15** for the Si-CH_3 protons relative to the N-CH_3 protons as expected from a closer approach of the former to the benzene molecules.

Scheme IV

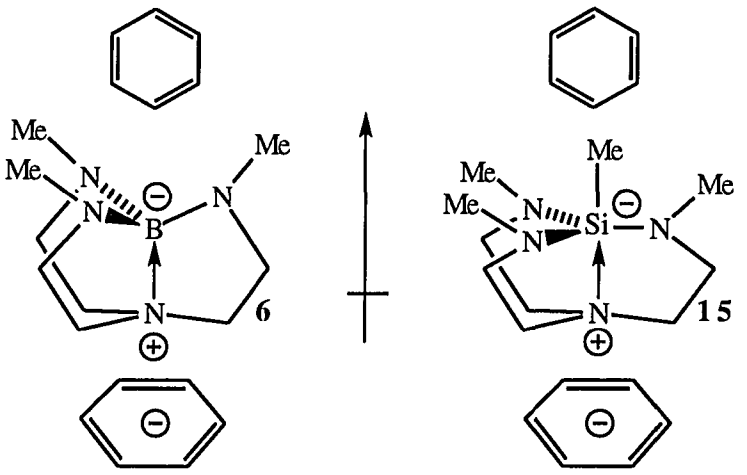

The signals in the ^{1}H and ^{13}C NMR spectra of **19** were unambiguously assigned with the help of a proton-coupled and selectively proton-decoupled ^{13}C NMR spectra. Similar to the situation observed in **6**,[8] the $MeNCH_2$ signal displays a quartet pattern because of long-range coupling with Me-N protons, which clearly distinguishes it from the $N(CH_2)_3$ signal. The upfield position of the $N(CH_2)_3$ signal relative to the $MeNCH_2$ signal in the ^{13}C NMR spectrum of **19** corresponds to assignments for other transition metal azatranes such as **16**, **18**, **25** and **26**.[20,22] Reversed signal positions were found in the main-group azatranes such as **6-11**,[8,9] azasilatranes,[13] and azastannatranes.[54] These observations point to the different electronic properties of the axial and equatorial orbitals of the central atom which are reversed for transition metals relative to main-group elements.[55]

Both the ^{1}H and ^{13}C NMR spectra of **14** reflect its dimeric nature and are depicted together with its ^{1}H, ^{1}H DQF COSY and ^{1}H, ^{13}C heterocorrelated NMR spectra in Figure 3. The presence of a two-fold axis in **14** as the only symmetry element renders inequivalent all the methylene protons as well as the three methyl groups (C(7), C(8), and C(9) in Figure 2) and the three ethylene bridges (C(1), C(2); C(2), C(3); C(4), C(5)). This is manifested by the presence of three methyl singlets and twelve partially overlapped methylene multiplets in the ^{1}H NMR spectrum. Furthermore, the ^{13}C NMR spectrum displays six methylene and three methyl signals. The assignment of the bridging N-Me group C(9,9') was facilitated by the observation of a larger $^{1}J_{CH}$ coupling constant in the ^{13}C proton-coupled NMR spectrum of **14** relative to smaller and identical values for nonbridging N-Me groups C(7,7') and C(8,8').[8] Information obtained from an analysis of ^{1}H, ^{1}H DQF COSY and ^{1}H, ^{13}C heterocorrelated NMR spectra

(Figure 3) allowed us to break the signals into three groups which belong to three inequivalent ethylene bridges. The assignments are summarized in Table VI.

The C_2 molecular symmetry of **14** in the solid state implies the presence of two enantiomers. This prompted us to explore the possibility of distinguishing them by ^1H NMR spectroscopy and to prove directly the presence of the cis diastereomer in solution as well using a chiral lanthanide shift reagent $Eu(hfc)_3$ (hfc = 3-(heptafluoropropylhydroxymethylene)-*d*-camphorate).[56] This chiral shift reagent should produce a different induced shift of the resonances of equivalent nuclei in an enantiomeric pair of **14**. However, using the molar ratio of **14**/Eu > 1, an array of broad resonances was observed in the ^1H NMR spectrum in the region from 25 to -5 ppm together with the unperturbed signals for the excess of **14**. The set of signals for **14** disappeared completely when a molar ratio **14**/Eu ≤ 1 was used. The absence of an expected downfield pseudo-contact shift of the resonances of **14** is presumably caused by the transmetallation reaction of $Eu(hfc)_3$ with **14** similar to the reaction observed for **12** and $Ga(acac)_3$ (Scheme I), but no firm conclusion about the nature of the transmetallated products could be inferred from the complicated and broadened signals.

There are relatively few reports in the literature on ^{71}Ga NMR studies of Ga-N compounds.[57] This is due to the substantially greater linewidths of ^{71}Ga signals which can be broadened beyond the detection limits by quadrupolar relaxation. ^{71}Ga chemical shifts are expected to follow the same trends as the ^{27}Al shifts in corresponding aluminum compounds.[58] The paucity of data makes a comparison of our results difficult, but from Table VII it can be

concluded that similarly to our results obtained for Al-N compounds,[8,9] the shielding of the Ga nucleus increases with increasing coordination number. A very broad signal for **10**, presumably possessing a trigonal monopyramidal Ga center,[9] was observed in the low-field region (~304 ppm). Tetrahedrally coordinated gallium in $[Ga(NMe_2)_3]_2$[14b] was reported at a higher field relative to **10** (276 ppm). Azagallatrane **14** with the coordination number of five displays its chemical shift even further upfield (255 ppm) as expected. For comparison, the shift for **50**[59] is listed, which shows a gallium signal at 2.8 ppm in the expected region for hexacoordinate Ga similar to that of the $Ga(acac)_3$ signal which was recently reported to be unobservable due to severe broadening.[60]

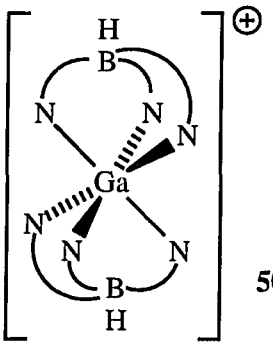

50

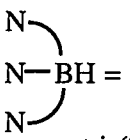

tris(3,5-dimethyl-1-pyrazolyl)hydridoborate

Figure 3. ^{1}H NMR (300 MHz) spectrum of **14** showing twelve methylene multiplets A to L and three methyl singlets (a), the ^{1}H ^{1}H-DQF COSY 2D NMR spectrum (300 MHz) of **14** (b), and the ^{1}H ^{13}C-heterocorrelated 2D NMR spectrum (300 MHz) of **14** showing methyl (c) and methylene (d) regions.

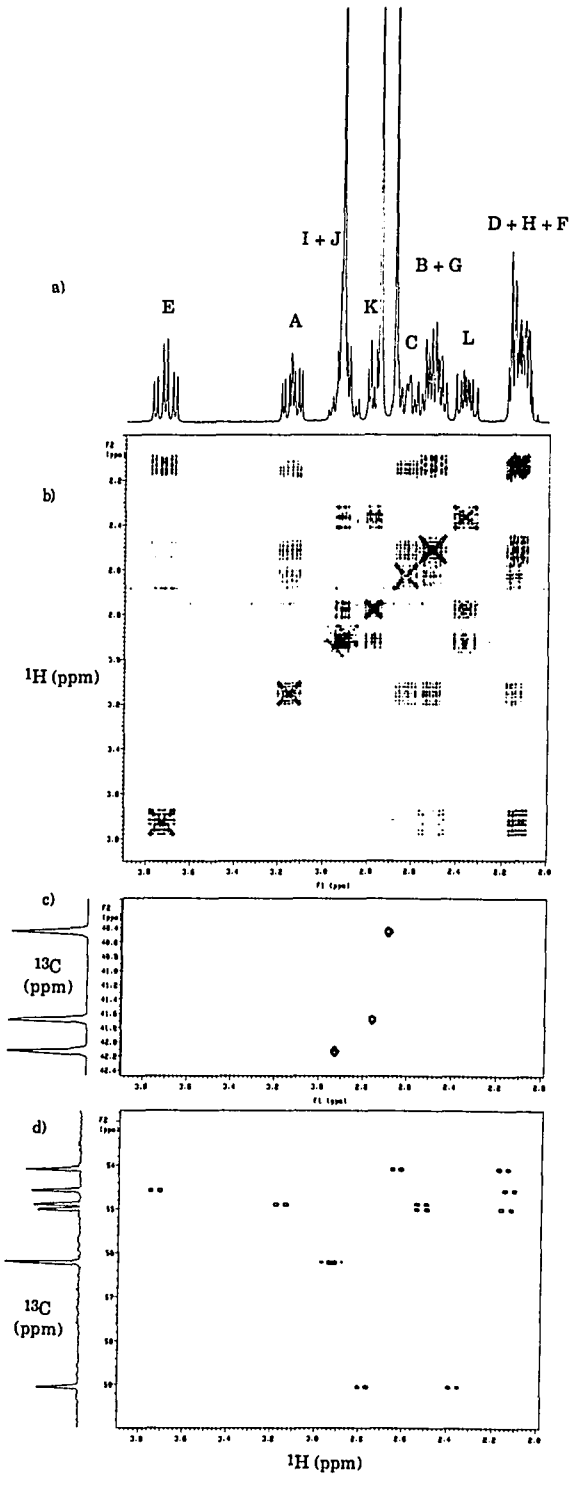
a)
E
A
I + J
K
B + G
C
L
D + H + F
b)
^{1}H (ppm)
c)
^{13}C (ppm)
d)
^{13}C (ppm)
^{1}H (ppm)

Table VI. Results of ^{1}H-^{1}H and ^{1}H-^{13}C NMR Correlation Experiments on **14**

$\delta^{13}C$ (ppm)	$\delta^{1}H$ (ppm), assignment[a]
methyl groups	
40.50	2.68 Me (9, 9')
41.85	2.75 } Me (7, 7') + Me (8, 8')
42.22	2.93 }
methylene groups	
54.03	2.60-2.66, C; 2.10-2.19, D
54.83	3.16, A; 2.47-2.55, B
54.56	3.73, E; 2.10-2.19, F
54.96	2.47-2.55, G; 2.10-2.19 H
56.15	2.87-2.97, I + J
58.86	2.78, K; 2.37, L

[a]For numbering scheme see Figure 2.

Table VII. ^{71}Ga NMR Chemical Shifts for Selected Gallium Compounds

compound	CN[a]	δ^{71}Ga (ppm)	$\Delta\nu_{1/2}$ (kHz)	ref
$Ga(acac)_3$	6	-2[b]	2.8 at 25 °C	this work
50	6	2.8[c]	0.06 at 25 °C	59
14	5	255 ± 5[b]	12 at 70 °C	this work
$[Ga(NMe_2)_3]_2$	4	276[b]	8.4	14b
10	4	304 ± 10[d]	40 at 70 °C	this work

[a]Coordination number. [b]Benzene-d_6 solution. [c]THF-d_8 solution. [d]Toluene-d_8 solution.

CONCLUSIONS

Azaalumatrane **12** and azagallatrane **14** are both dimeric species possessing an unusual cis configuration of the substituents on the central four-membered ring. Both aluminum and gallium are coordinated exclusively by nitrogens in a distorted trigonal bipyramidal geometry. Azaalumatrane **12** was shown to be a versatile reagent in transmetallation reactions by which azatranes of main-group elements and transition metals can be prepared. In order to obtain a preparatively useful system, a methoxide or an ethoxide should be used as a transmetallating agent, so that upon conversion to the corresponding nonvolatile insoluble $[Al(OR)_3]_n$ product it is easily separable from the reaction mixture.

ACKNOWLEDGMENT

The authors are grateful to the National Science Foundation and the Iowa State Center for Advanced Technology Development for grants in support of this work. We thank Dr. Victor Young of Instrument Services at ISU and Tieli Wang and Dr. Robert A. Jacobson for the structural determinations of **14** and **12**, respectively.

REFERENCES

(1) Paine, R. T.; Narula, C. K. *Chem. Rev.* **1990**, *90*, 73.

(2) Wade, T.; Park, J.; Garza, E. G.; Ross, C. B.; Smith, D. M.; Crooks, R. M. *J. Am. Chem. Soc.* **1992**, *114*, 9457.

(3) Jones, C.; Koutsantonis, G. A.; Raston, C. L. *Polyhedron* **12**, 1829.

(4) (a) Almond, M. J.; Jenkins, C. E.; Rice, D. A.; Hagen, K. *J. Organomet. Chem.* **1992**, *439*, 251. (b) Almond, M. J.; Jenkins, C. E.; Rice, D. A. *ibid* **1993**, *443*, 137.

(5) Cowley, A. H.; Jones, R. A. *Angew. Chem., Int. Ed. Engl.* **1989**, *28*, 1208.

(6) Riedel, R.; Schaible, S.; Klingebiel, V.; Noltemeyer, M.; Werner, E. *Zeitschr. Anorg. Allg. Chem.* **1991**, *603*, 119.

(7) (a) Moise, F.; Pennington, W. T.; Robinson, G. H. *J. Coord. Chem.* **1991**, *24*, 93. (b) Atwood, D. A.; Atwood, V. O.; Cowley, A. H.; Atwood, J. L.; Roman, E. *Inorg. Chem.* **1992**, *31*, 3871. (c) Atwood, J. L.; Bott, S. G.; Jones, C.; Raston, C. L. *Inorg. Chem.* **1991**, *30*, 4868.

(8) Pinkas, J.; Gaul, B.; Verkade, J. G. *J. Am. Chem. Soc.* **1993**, *115*, 3925.

(9) Pinkas, J.; Verkade, J. G., submitted.

(10) Pinkas, J.; Verkade, J. G. *Inorg. Chem.* **1993**, *32*, 2711.

(11) Shriver, D. F.; Drezdon, M. A. The Manipulation of Air-Sensitive Compounds; Wiley-Interscience: New York, 1986.

(12) Schmidt, H.; Lensink, C.; Xi, S.-K.; Verkade, J. G. *Zeitschr. Anorg. Allg. Chem.* **1989**, *578*, 78.

(13) Gudat, D.; Verkade, J. G. *Organometallics* **1989**, *8*, 2772.

(14) (a) Ruff, J. K. *J. Am. Chem. Soc.* **1961**, *83*, 2835. (b) Waggoner, K. M.; Olmstead, M. M.; Power, P. P. *Polyhedron* **1990**, *9*, 257. (c) Nöth, H.; Konrad, P. *Z. Naturforsch.* **1975**, *30b*, 681.

(15) Becker, F. *J. Organometal. Chem.* **1973**, *51*, C9.

(16) Chisholm, M. H.; Cotton, F. A.; Murillo, C. A.; Reichert, W. W. *Inorg. Chem.* **1977**, *16*, 1801.

(17) Benn, R.; Rufinska, A.; Janssen, E.; Lehmkuhl, H. *Organometallics* **1986**, *5*, 825.

(18) Akitt, J. W.; Greenwood, N. N.; Storr, A. *J. Chem. Soc.* **1965**, 4410.

(19) Woning, J.; Verkade, J. G. *J. Am. Chem. Soc.* **1991**, *113*, 944.

(20) Plass, W.; Verkade, J. G. *Inorg. Chem.* **1993**, *32*, 3762.

(21) Folting, K.; Streib, W. E.; Caulton, K. G.; Poncelet, O.; Hubert-Pfalzgraf, L. G. *Polyhedron* **1991**, *10*, 1639.

(22) Plass, W.; Verkade, J. G. *J. Am. Chem. Soc.* **1992**, *114*, 2275.

(23) Brown, H. C.; Cha, J. S.; Nazer, B. *Inorg. Chem.* **1984**, *23*, 2929.

(24) (a) Hein, F.; Burkhardt, R. *Zeitschr. Anorg. Allg. Chem.* **1952**, *268*, 159. (b) Fenske, D.; Becher, H. J. *Chem. Ber.* **1972**, *105*, 2085. (c) Lacey, M. J.; Macdonald, C. G. *Aust. J. Chem.* **1976**, *29*, 1119.

(25) Voronkov, M. G.; Dyakov, V. M.; Kirpichenko, S. V. *J. Organomet. Chem.* **1982**, *233*, 1.

(26) TEXSAN-TEXRAY Structure Analysis Package; Molecular Structure Corporation: Woodlands, TX, 1985.

(27) SHELXTL PLUS; Siemens Analytical X-ray Instruments, Inc., Madison, WI, USA.

(28) Cromer, D. T.; Waber, J. T. International Tables for X-ray Crystallography; Kynoch Press: Birmingham, U.K., 1974; Vol. IV.

(29) Ruff, J. K. *J. Org. Chem.* **1962**, *27*, 1020.

(30) George, T. A.; Lappert, M. F. *J. Chem. Soc. A* **1969**, 992.

(31) Müller, R. *Organometal. Chem. Rev.* **1966**, *1*, 359.

(32) Zelchan, G. I.; Voronkov, M. G. *Khim. Geterotsikl. Soed. (Engl. Transl.)* **1967**, *3*, 371.

(33) (a) Cummins, C. C.; Schrock, R. R.; Davis, W. M. *Oragnometallics* **1992**, *11*, 1452. (b) Cummins, C. C.; Lee, J.; Schrock, R. R.; Davis, W. D. *Angew. Chem., Int. Ed. Engl.* **1992**, *31*, 1501. (c) Cummins, C. C.; Schrock, R. R.; Davis, W. M. *Angew. Chem., Int. Ed. Engl.* **1993**, *32*, 756.

(34) Naiini, A. A.; Menge, W. M. P. B.; Verkade, J. G. *Inorg. Chem.* **1991**, *30*, 5009.

(35) Wan, Y.; Verkade, J. G. *Inorg. Chem.* **1993**, *32*, 79.

(36) Rettig, S. J.; Storr, A.; Trotter, J. *Can. J. Chem.* **1974** ,*52*, 2206.

(37) Friedrich, S.; Gade, L. H.; Edwards, A. J.; McPartlin, M. *Chem. Ber.* **1993**, *126*, 1797.

(38) (a) Van Vechten, J. A.; Phillips, J. C. *Phys. Rev. B* **1970**, *2*, 2160. (b) Moeller, T. Inorganic Chemistry; J. Wiley & Sons: New York, 1982. (c) Adams, D. M. Inorganic Solids, J. Wiley & Sons: New York, 1978. (d) Blom, R.; Haaland, A. *J. Molec. Struct.* **1985**, *128*, 21. (e) Sanderson, R. T. Inorganic Chemistry; Reinhold Publ. Co.: New York, 1967. (f) Huheey, J. E. Inorganic Chemistry; Harper & Row: New York, 1983.

(39) Waggoner, K. M.; Ruhlandt-Senge, K.; Wehmschulte, R. J.; He, X.; Olmstead, M. M.; Power, P. P. *Inorg. Chem.* **1993**, *32*, 2557.

(40) Rettig, S. J.; Storr, A.; Trotter, J. *Can. J. Chem.* **1975**, *53*, 58.

(41) Onyiriuka, E. C.; Rettig, S. J.; Storr, A.; Trotter, J. *Can. J. Chem.* **1987**, *65*, 782.

(42) Tao, W.-T.; Han, Y.; Huang, Y.-Z.; Jin, X.-L.; Sun, J. *J. Chem. Soc., Dalton Trans.* **1993**, 807.

(43) (a) Shiro, M.; Fernando, Q. *Anal. Chem.* **1971**, *43*, 1222. (b) Dymock, K.; Palenik, G. J. *J. Chem. Soc., Chem. Commun.* **1973**, 884.

(44) Schmidbaur, H.; Lettenbauer, J.; Kumberger, O.; Lachmann, J.; Müller, G. *Z. Naturforsch.* **1991**, *46b*, 1065.

(45) McPhail, A. T.; Miller, R. W.; Pitt, C. G.; Gupta, G.; Srivastava, S. C. *J. Chem. Soc., Dalton Trans.* **1976**, 1657.

(46) Coggin, D. K.; Fanwick, P. E.; Green, M. A. *J. Chem. Soc., Chem. Commun.* **1993**, 1127.

(47) Cowley, A. H.; Jones, R. A.; Maradones, M. A.; Ruiz, J.; Atwood, J. L.; Bott, S. G. *Angew. Chem., Int. Ed. Engl.* **1990**, *29*, 1150.

(48) Rettig, S. J.; Storr, A.; Trotter, J.; Uhrich, K. *Can. J. Chem.* **1984**, *62*, 2783.

(49) Kynast, U.; Skelton, B. W.; White, A. H.; Henderson, M. J.; Raston, C. L. *J. Organomet. Chem.* **1990**, *384*, C1.

(50) Rettig, S. J.; Storr, A.; Trotter, J. *Can. J. Chem.* **1975**, *53*, 753.

(51) Lee, B.; Pennington, W. T.; Robinson, G. H. *Organometallics* **1990**, *9*, 1709.

(52) Zaworotko, M. J.; Atwood, J. L. *Inorg. Chem.* **1980**, *19*, 268.

(53) (a) Bertrand, R. D.; Compton, R. D.; Verkade, J. G. *J. Am. Chem. Soc.* **1970**, *92*, 2702. (b) Cowley, A. H.; Damasco, M. C.; Mosbo, J. A.; Verkade,

J. G. *J. Am. Chem. Soc.* **1972**, *94*, 6715. (c) Barton, T. J.; Roth, R. W.; Verkade, J. G. *J. Chem. Soc., Chem. Commun.* **1972**, 1101.

(54) Plass, W.; Verkade, J. G. *Inorg. Chem.*, in press.

(55) Gillespie, R. J. *Chem. Soc. Rev.* **1992**, 59.

(56) Kutal, C. in Nuclear Magnetic Resonance Shift Reagents; Sievers, R. E., Ed.; Academic Press: New York, 1973.

(57) Akitt, J. W. in Multinuclear NMR; Mason, J. Ed.; Plenum Press: New York, 1987.

(58) (a) Hinton, J. F.; Briggs, R. W. in NMR and the Periodic Table; Harris, R. K.; Mann, B. E., Eds.; Academic Press: New York, 1978. (b) Bradley, S. M.; Howe, R. F.; Kydd, R. A. *Magn. Res. Chem.* **1993**, *31*, 883.

(59) Cowley, A. H.; Carrano, C. J.; Geerts, R. L.; Jones, R. A.; Nunn, C. M. *Angew. Chem., Int. Ed. Engl.* **1988**, *27*, 277.

(60) Cerny, Z.; Machacek, J.; Fusek, J.; Kriz, O.; Casensky, B. *J. Organomet. Chem.* **1993**, *456*, 25.

SUPPLEMENTARY MATERIAL

Table VIII. Atomic Coordinates and Thermal Parameters ($Å^2$) for **12**

atom	x	y	z	B(eq)
Al(1)	0.16783(5)	0.0242(1)	0.1406(2)	3.2(1)
Al(2)	0.08828(5)	0.0195(1)	0.1529(2)	3.4(1)
N(1)	0.1294(1)	0.0969(3)	0.2398(6)	3.3(2)
N(2)	0.1264(1)	-0.0036(3)	-0.0077(5)	3.5(3)
N(3)	0.1988(2)	-0.0465(4)	-0.0272(6)	4.0(3)
N(4)	0.1761(1)	-0.0806(4)	0.2567(6)	3.9(3)
N(5)	0.2029(1)	0.1117(4)	0.1158(7)	4.2(3)
N(6)	0.0749(2)	-0.0968(4)	0.2162(7)	4.5(3)
N(7)	0.0633(2)	0.0627(4)	0.3640(7)	4.3(3)
N(8)	0.0533(2)	0.0920(4)	0.0618(7)	4.9(3)
C(1)	0.2321(3)	0.0983(6)	0.010(1)	5.8(5)
C(2)	0.2216(2)	0.0230(7)	-0.103(1)	5.4(5)
C(3)	0.2214(2)	-0.1108(6)	0.066(1)	5.1(5)
C(4)	0.1983(2)	-0.1543(5)	0.189(1)	4.6(4)
C(5)	0.1745(2)	-0.0980(6)	-0.133(1)	5.3(5)
C(6)	0.1365(2)	-0.0957(5)	-0.0676(9)	4.2(4)
C(7)	0.0539(3)	-0.1066(6)	0.354(1)	6.0(5)
C(8)	0.0605(2)	-0.0245(7)	0.456(1)	5.5(5)
C(9)	0.0272(2)	0.0974(7)	0.317(1)	6.2(6)
C(10)	0.0315(2)	0.1470(7)	0.163(1)	6.3(5)
C(11)	0.0854(2)	0.1324(6)	0.441(1)	4.7(4)
C(12)	0.1243(2)	0.1104(6)	0.4084(7)	4.1(4)
C(13)	0.1267(3)	0.1919(5)	0.167(1)	4.5(4)
C(14)	0.1247(2)	0.0604(6)	-0.143(1)	4.8(4)
C(15)	0.1588(3)	-0.1193(6)	0.390(1)	5.9(5)
C(16)	0.0683(3)	-0.1789(6)	0.124(1)	6.1(5)
C(17)	0.2117(3)	0.1887(6)	0.217(1)	5.5(5)
C(18)	0.0376(3)	0.0790(7)	-0.088(1)	6.1(5)

$B(eq) = 8\pi^2/3\ \Sigma_i\Sigma_j\ U_{ij}\ a_i^* a_j^*\ (\mathbf{a}_i.\mathbf{a}_j)$

Table IX. Bond Distances (Å) in **12**

AL1	N1	1.968(5)	N8	C10	1.44(1)
AL1	N2	2.049(5)	N8	C18	1.45(1)
AL1	N3	2.124(6)	C1	C2	1.52(1)
AL1	N4	1.843(6)	C1	H1	1.10(7)
AL1	N5	1.821(6)	C1	H2	0.92(6)
AL2	N1	2.032(5)	C2	H3	0.99(6)
AL2	N2	2.022(5)	C2	H4	1.08(7)
AL2	N6	1.829(6)	C3	C4	1.51(1)
AL2	N7	2.160(6)	C3	H5	0.96(7)
AL2	N8	1.844(6)	C3	H6	1.07(6)
N1	C12	1.503(8)	C4	H7	1.02(7)
N1	C13	1.509(8)	C4	H8	1.03(6)
N2	C6	1.470(8)	C5	C6	1.52(1)
N2	C14	1.502(8)	C5	H9	0.94(6)
N3	C2	1.465(9)	C5	H10	1.10(7)
N3	C3	1.491(9)	C6	H11	1.00(6)
N3	C5	1.488(9)	C6	H12	0.97(6)
N4	C4	1.467(8)	C7	C8	1.50(1)
N4	C15	1.448(9)	C7	H13	1.14(9)
N5	C1	1.437(9)	C7	H14	0.94(7)
N5	C17	1.45(1)	C8	H15	1.07(5)
N6	C7	1.44(1)	C8	H16	0.93(6)

Table IX. Continued

C13	H27	1.09(7)	N6	C16	1.45(1)
C14	H28	1.01(6)	N7	C8	1.50(1)
C14	H29	0.98(6)	N7	C9	1.48(1)
C14	H30	0.94(7)	N7	C11	1.458(9)
C15	H31	0.95(8)	C9	C10	1.54(1)
C15	H32	0.95(9)	C9	H17	0.90(8)
C15	H33	1.28(8)	C9	H18	1.09(8)
C16	H34	1.05(8)	C10	H19	1.26(7)
C16	H35	1.00(7)	C10	H20	0.86(7)
C16	H36	0.94(8)	C11	C12	1.50(1)
C17	H37	0.95(7)	C11	H21	0.99(7)
C17	H38	1.01(9)	C11	H22	0.95(6)
C17	H39	0.99(8)	C12	H23	1.03(5)
C18	H40	0.96(7)	C12	H24	0.98(6)
C18	H41	1.23(8)	C13	H25	1.08(6)
C18	H42	0.98(7)	C13	H26	0.90(7)

Table X. Bond Angles (deg) in **12**

N1	AL1	N2	81.0(2)	AL1	N2	AL2	92.7(2)
N1	AL1	N3	161.9(2)	AL1	N2	C6	102.2(4)
N1	AL1	N4	108.0(2)	AL1	N2	C14	114.5(5)
N1	AL1	N5	101.7(2)	AL2	N2	C6	125.0(4)
N2	AL1	N3	82.6(2)	AL2	N2	C14	114.8(4)
N2	AL1	N4	108.4(2)	C6	N2	C14	106.3(5)
N2	AL1	N5	126.3(2)	AL1	N3	C2	107.4(4)
N3	AL1	N4	84.5(2)	AL1	N3	C3	102.5(4)
N3	AL1	N5	82.1(3)	AL1	N3	C5	109.9(5)
N4	AL1	N5	120.8(3)	C2	N3	C3	110.4(6)
N1	AL2	N2	80.1(2)	C2	N3	C5	113.9(6)
N1	AL2	N6	126.0(2)	C3	N3	C5	111.9(6)
N1	AL2	N7	80.9(2)	AL1	N4	C4	117.2(5)
N1	AL2	N8	112.3(3)	AL1	N4	C15	133.5(5)
N2	AL2	N6	104.5(2)	C4	N4	C15	107.4(6)
N2	AL2	N7	160.6(2)	AL1	N5	C1	121.4(5)
N2	AL2	N8	106.3(3)	AL1	N5	C17	127.8(5)
N6	AL2	N7	83.4(3)	C1	N5	C17	109.1(6)
N6	AL2	N8	117.2(3)	AL2	N6	C7	119.4(5)
N7	AL2	N8	84.8(3)	AL2	N6	C16	128.2(6)
AL1	N1	AL2	94.9(2)	C7	N6	C16	107.1(7)
AL1	N1	C12	126.4(4)	AL2	N7	C8	104.7(4)
AL1	N1	C13	109.9(4)	AL2	N7	C9	104.2(5)
AL2	N1	C12	110.2(4)	AL2	N7	C11	110.7(5)
AL2	N1	C13	106.7(4)	C8	N7	C9	111.5(6)
C12	N1	C13	107.0(5)	C8	N7	C11	111.3(6)

Table X. Continued

C9	N7	C11	113.7(6)	C3	C4	H8	118(4)
AL2	N8	C10	115.8(5)	H7	C4	H8	108(5)
AL2	N8	C18	127.0(6)	N3	C5	C6	108.4(6)
C10	N8	C18	114.1(7)	N3	C5	H9	108(4)
N5	C1	C2	108.9(7)	N3	C5	H10	106(3)
N5	C1	H1	118(3)	C6	C5	H9	107(4)
N5	C1	H2	120(4)	C6	C5	H10	109(3)
C2	C1	H1	109(3)	H9	C5	H10	118(6)
C2	C1	H2	106(4)	N2	C6	C5	112.9(6)
H1	C1	H2	94(5)	N2	C6	H11	111(4)
N3	C2	C1	109.8(6)	N2	C6	H12	108(4)
N3	C2	H3	111(4)	C5	C6	H11	111(3)
N3	C2	H4	106(4)	C5	C6	H12	117(4)
C1	C2	H3	114(4)	H11	C6	H12	97(5)
C1	C2	H4	106(4)	N6	C7	C8	109.6(7)
H3	C2	H4	110(5)	N6	C7	H13	118(5)
N3	C3	C4	109.3(7)	N6	C7	H14	110(4)
N3	C3	H5	107(4)	C8	C7	H13	97(4)
N3	C3	H6	108(3)	C8	C7	H14	109(5)
C4	C3	H5	108(4)	H13	C7	H14	112(6)
C4	C3	H6	108(3)	N7	C8	C7	110.0(6)
H5	C3	H6	115(5)	N7	C8	H15	105(3)
N4	C4	C3	107.9(6)	N7	C8	H16	106(4)
N4	C4	H7	114(4)	C7	C8	H15	106(3)
N4	C4	H8	107(4)	C7	C8	H16	114(4)
C3	C4	H7	103(4)	H15	C8	H16	116(5)

Table X. Continued

N7	C9	C10	107.7(7)	N1	C13	H27	115(3)
N7	C9	H17	103(5)	H25	C13	H26	103(6)
N7	C9	H18	111(4)	H25	C13	H27	102(4)
C10	C9	H17	113(6)	H26	C13	H27	111(6)
C10	C9	H18	110(4)	N2	C14	H28	107(4)
H17	C9	H18	111(7)	N2	C14	H29	105(4)
N8	C10	C9	110.4(7)	N2	C14	H30	113(4)
N8	C10	H19	110(3)	H28	C14	H29	120(6)
N8	C10	H20	111(5)	H28	C14	H30	109(6)
C9	C10	H19	105(3)	H29	C14	H30	103(5)
C9	C10	H20	108(5)	N4	C15	H31	117(5)
H19	C10	H20	112(6)	N4	C15	H32	115(5)
N7	C11	C12	107.7(6)	N4	C15	H33	113(3)
N7	C11	H21	107(4)	H31	C15	H32	102(7)
N7	C11	H22	108(4)	H31	C15	H33	119(6)
C12	C11	H21	117(4)	H32	C15	H33	85(5)
C12	C11	H22	115(4)	N6	C16	H34	105(5)
H21	C11	H22	102(5)	N6	C16	H35	115(4)
N1	C12	C11	109.5(6)	N6	C16	H36	115(5)
N1	C12	H23	109(3)	H34	C16	H35	105(6)
N1	C12	H24	110(4)	H34	C16	H36	127(7)
C11	C12	H23	110(3)	H35	C16	H36	88(6)
C11	C12	H24	110(3)	N5	C17	H37	112(5)
H23	C12	H24	108(5)	N5	C17	H38	111(5)
N1	C13	H25	110(3)	N5	C17	H39	106(5)
N1	C13	H26	115(5)	H37	C17	H38	109(6)
H37	C17	H39	109(6)	N8	C18	H42	107(4)
H38	C17	H39	110(7)	H40	C18	H41	110(6)
N8	C18	H40	106(5)	H40	C18	H42	107(6)
N8	C18	H41	103(4)	H41	C18	H42	122(6)

Table XI. Anisotropic Displacement Coefficients ($Å^2$) for **12**

atom	U11	U22	U33	U12	U13	U23
Al(1)	0.057(1)	0.034(1)	0.032(1)	-0.002(1)	-0.003(1)	0.004(1)
Al(2)	0.058(1)	0.037(1)	0.035(1)	-0.003(1)	-0.007(1)	0.000(1)
N(1)	0.056(3)	0.034(3)	0.033(3)	-0.004(3)	-0.005(3)	0.003(3)
N(2)	0.067(4)	0.029(3)	0.037(3)	0.005(3)	-0.004(3)	0.004(2)
N(3)	0.070(4)	0.047(4)	0.037(3)	0.004(4)	0.001(3)	-0.004(3)
N(4)	0.067(4)	0.043(3)	0.038(4)	0.009(3)	-0.002(3)	0.010(3)
N(5)	0.064(4)	0.051(4)	0.047(4)	-0.014(3)	0.006(3)	-0.005(3)
N(6)	0.071(4)	0.054(4)	0.045(4)	-0.014(3)	0.002(3)	-0.004(3)
N(7)	0.060(4)	0.062(4)	0.040(4)	-0.004(3)	0.002(3)	-0.007(4)
N(8)	0.065(4)	0.074(4)	0.049(4)	0.021(4)	-0.015(4)	-0.015(3)
C(1)	0.067(6)	0.065(6)	0.086(7)	-0.010(5)	0.020(6)	0.008(6)
C(2)	0.073(6)	0.075(6)	0.057(5)	0.007(5)	0.018(4)	0.010(5)
C(3)	0.077(6)	0.059(6)	0.060(6)	0.017(5)	0.001(5)	-0.003(5)
C(4)	0.071(6)	0.050(5)	0.055(5)	0.014(5)	-0.010(5)	0.010(4)
C(5)	0.090(7)	0.064(6)	0.046(5)	0.011(5)	0.001(5)	-0.008(5)
C(6)	0.078(6)	0.047(5)	0.033(4)	0.002(4)	-0.011(4)	-0.013(4)
C(7)	0.093(7)	0.067(6)	0.068(7)	-0.011(6)	-0.008(6)	0.010(6)
C(8)	0.069(6)	0.088(7)	0.053(5)	-0.019(6)	0.021(5)	0.010(6)
C(9)	0.064(6)	0.104(8)	0.066(6)	0.000(6)	0.010(5)	-0.010(6)
C(10)	0.065(6)	0.101(8)	0.074(7)	0.024(6)	-0.014(6)	0.006(6)
C(11)	0.070(6)	0.070(6)	0.040(5)	-0.005(5)	0.004(5)	-0.014(4)
C(12)	0.072(6)	0.053(5)	0.032(4)	-0.010(5)	-0.007(4)	-0.014(3)
C(13)	0.075(6)	0.030(4)	0.064(6)	-0.004(5)	-0.007(5)	-0.002(4)
C(14)	0.075(6)	0.066(5)	0.043(5)	0.013(5)	-0.005(5)	0.013(4)
C(15)	0.107(8)	0.053(5)	0.063(7)	0.017(6)	0.016(5)	0.021(5)
C(16)	0.084(7)	0.065(6)	0.085(7)	-0.013(5)	-0.003(6)	-0.016(6)
C(17)	0.077(6)	0.062(5)	0.069(7)	-0.014(5)	-0.005(5)	0.001(5)
C(18)	0.070(6)	0.091(8)	0.071(7)	-0.005(6)	-0.011(5)	0.017(5)

Table XII. Atomic Coordinates ($x10^4$) and Equivalent Isotropic Displacement Coefficients ($Å^2x10^3$) for **14**

Atom	x	y	z	U_{eq}
Ga	1586(1)	6712(1)	7952(1)	27(1)
N(1)	2539(3)	4925(3)	8112(3)	38(1)
C(1)	2961(5)	5300(4)	9489(4)	45(2)
C(2)	3499(5)	6692(4)	10027(4)	48(2)
N(2)	2498(3)	7487(3)	9658(3)	35(1)
C(3)	1346(5)	3975(3)	7616(4)	49(2)
C(4)	11(4)	4599(4)	7946(4)	45(2)
N(3)	-111(3)	5739(3)	7649(3)	38(1)
C(5)	3684(5)	4649(4)	7368(4)	51(2)
C(6)	4073(4)	5783(3)	7005(4)	42(2)
N(4)	2836(3)	6343(3)	6578(3)	32(1)
C(7)	1529(5)	7919(4)	10581(4)	53(2)
C(8)	-1355(4)	6353(4)	8060(5)	53(2)
C(9)	2122(5)	5461(4)	5348(3)	51(2)
Ga'	2947(1)	8201(1)	6704(1)	28(1)
N(1')	2465(3)	10282(3)	7157(3)	38(1)

Table XII. Continued

C(1')	3791(5)	10928(4)	7855(5)	64(2)
C(2')	4505(6)	10229(4)	8605(6)	77(2)
N(2')	4588(3)	8880(3)	7865(3)	45(1)
C(3')	2141(6)	10375(4)	5890(4)	60(2)
C(4')	2841(7)	9438(4)	4928(5)	68(2)
N(3')	2797(4)	8197(3)	5011(3)	44(1)
C(5')	1309(5)	10537(4)	7883(4)	51(2)
C(6')	1052(5)	9466(3)	8382(4)	43(2)
N(4')	1110(3)	8217(3)	7396(3)	29(1)
C(7')	5872(5)	8600(6)	7364(6)	79(3)
C(8')	3681(6)	7411(5)	4167(4)	65(2)
C(9')	-87(4)	7974(4)	6381(4)	49(2)

Equivalent isotropic U defined as one third of the trace of the orthogonalized U_{ij} tensor.

Table XIII. Bond Distances (Å) in **14**

Ga-N(1)	2.284 (3)	Ga-N(2)	1.908 (3)
Ga-N(3)	1.900 (3)	Ga-N(4)	2.037 (3)
Ga-Ga'	2.957 (1)	Ga-N(4')	2.048 (3)
N(1)-C(1)	1.466 (5)	N(1)-C(3)	1.484 (5)
N(1)-C(5)	1.458 (6)	C(1)-C(2)	1.538 (5)
C(2)-N(2)	1.446 (6)	N(2)-C(7)	1.463 (6)
C(3)-C(4)	1.510 (6)	C(4)-N(3)	1.445 (6)
N(3)-C(8)	1.449 (5)	C(5)-C(6)	1.538 (7)
C(6)-N(4)	1.465 (5)	N(4)-C(9)	1.477 (4)
N(4)-Ga'	2.060 (3)	Ga'-N(1')	2.297 (3)
Ga'-N(2')	1.891 (3)	Ga'-N(3')	1.904 (4)
Ga'-N(4')	2.043 (3)	N(1')-C(1')	1.459 (5)
N(1')-C(3')	1.470 (6)	N(1')-C(5')	1.454 (6)
C(1')-C(2')	1.465 (9)	C(2')-N(2')	1.474 (5)
N(2')-C(7')	1.433 (6)	C(3')-C(4')	1.478 (7)
C(4')-N(3')	1.442 (7)	N(3')-C(8')	1.444 (6)
C(5')-C(6')	1.538 (7)	C(6')-N(4')	1.474 (4)
N(4')-C(9')	1.471 (5)		

Table XIV. Bond Angles (deg) in **14**

N(1)-Ga-N(2)	84.2(1)	N(1)-Ga-N(3)	82.9(1)
N(2)-Ga-N(3)	118.9(1)	N(1)-Ga-N(4)	80.1(1)
N(2)-Ga-N(4)	115.7(1)	N(3)-Ga-N(4)	120.2(1)
N(1)-Ga-Ga'	120.2(1)	N(2)-Ga-Ga'	100.1(1)
N(3)-Ga-Ga'	137.2(1)	N(4)-Ga-Ga'	44.1(1)
N(1)-Ga-N(4')	162.7(1)	N(2)-Ga-N(4')	103.3(1)
N(3)-Ga-N(4')	106.2(1)	N(4)-Ga-N(4')	82.6(1)
Ga'-Ga-N(4')	43.7(1)	Ga-N(1)-C(1)	101.5(2)
Ga-N(1)-C(3)	103.0(2)	C(1)-N(1)-C(3)	113.3(4)
Ga-N(1)-C(5)	108.0(3)	C(1)-N(1)-C(5)	114.7(3)
C(3)-N(1)-C(5)	114.6(3)	N(1)-C(1)-C(2)	109.2(4)
C(1)-C(2)-N(2)	111.4(3)	Ga-N(2)-C(2)	112.4(2)
Ga-N(2)-C(7)	113.1(2)	C(2)-N(2)-C(7)	110.9(3)
N(1)-C(3)-C(4)	110.0(3)	C(3)-C(4)-N(3)	111.8(4)
Ga-N(3)-C(4)	114.9(2)	Ga-N(3)-C(8)	120.0(2)
C(4)-N(3)-C(8)	110.0(4)	N(1)-C(5)-C(6)	110.9(3)
C(5)-C(6)-N(4)	111.7(3)	Ga-N(4)-C(6)	107.1(3)

Table XIV. Continued

Ga-N(4)-C(9)	111.3(3)	C(6)-N(4)-C(9)	109.8(3)
Ga-N(4)-Ga'	92.4(1)	C(6)-N(4)-Ga'	119.9(2)
C(9)-N(4)-Ga'	114.5(3)	Ga-Ga'-N(4)	43.5(1)
Ga-Ga'-N(1')	119.0(1)	N(4)-Ga'-N(1')	161.8(1)
Ga-Ga'-N(2')	102.4(1)	N(4)-Ga'-N(2')	103.4(1)
N(1')-Ga'-N(2')	83.7(1)	Ga-Ga'-N(3')	134.7(1)
N(4)-Ga'-N(3')	106.9(1)	N(1')-Ga'-N(3')	83.0(1)
N(2')-Ga'-N(3')	120.0(2)	Ga-Ga'-N(4')	43.8(1)
N(4)-Ga'-N(4')	82.2(1)	N(1')-Ga'-N(4')	79.7(1)
N(2')-Ga'-N(4')	118.8(1)	N(3')-Ga'-N(4')	115.7(1)
Ga'-N(1')-C(1')	101.9(3)	Ga'-N(1')-C(3')	102.9(2)
C(1')-N(1')-C(3')	113.1(4)	Ga'-N(1')-C(5')	108.4(3)
C(1')-N(1')-C(5')	114.9(3)	C(3')-N(1')-C(5')	114.0(4)
N(1')-C(1')-C(2')	111.1(4)	C(1')-C(2')-N(2')	113.1(4)
Ga'-N(2')-C(2')	112.0(3)	Ga'-N(2')-C(7')	116.1(3)
C(2')-N(2')-C(7')	113.1(4)	N(1')-C(3')-C(4')	112.6(4)
C(3')-C(4')-N(3')	113.6(5)	Ga'-N(3')-C(4')	114.0(2)

Table XIV. Continued

Ga'-N(3')-C(8')	118.9(3)	C(4')-N(3')-C(8')	108.9(4)
N(1')-C(5')-C(6')	110.8(3)	C(5')-C(6')-N(4')	111.5(4)
Ga-N(4')-Ga'	92.6(1)	Ga-N(4')-C(6')	118.7(3)
Ga'-N(4')-C(6')	107.5(2)	Ga-N(4')-C(9')	114.6(2)
Ga'-N(4')-C(9')	111.3(3)	C(6')-N(4')-C(9')	110.4(3)

Table XV. Anisotropic Displacement Coefficients ($Å^2x10^3$) for **14**

Atom	U_{11}	U_{22}	U_{33}	U_{12}	U_{13}	U_{23}
Ga	29(1)	25(1)	27(1)	2(1)	6(1)	10(1)
N(1)	43(2)	32(2)	41(2)	6(1)	6(1)	13(1)
C(1)	51(2)	47(2)	44(2)	11(2)	3(2)	25(2)
C(2)	53(3)	48(2)	41(2)	-4(2)	-6(2)	17(2)
N(2)	42(2)	33(2)	32(2)	3(1)	6(1)	11(1)
C(3)	72(3)	23(2)	53(3)	-4(2)	8(2)	15(2)
C(4)	44(2)	42(2)	53(2)	-15(2)	0(2)	24(2)
N(3)	30(2)	41(2)	47(2)	-1(1)	6(1)	20(1)
C(5)	56(3)	38(2)	64(3)	22(2)	24(2)	20(2)
C(6)	41(2)	34(2)	57(2)	16(2)	21(2)	18(2)
N(4)	36(2)	27(1)	35(2)	2(1)	13(1)	9(1)
C(7)	71(3)	51(3)	37(2)	9(2)	21(2)	13(2)
C(8)	39(2)	62(3)	68(3)	0(2)	9(2)	33(2)
C(9)	79(3)	38(2)	32(2)	-7(2)	13(2)	4(2)
Ga'	28(1)	29(1)	30(1)	1(1)	6(1)	12(1)
N(1')	39(2)	33(2)	47(2)	0(1)	5(1)	20(1)

Table XV. Continued

C(1')	56(3)	41(3)	84(4)	-5(2)	-12(3)	17(2)
C(2')	72(4)	46(3)	91(4)	-16(2)	-39(3)	15(3)
N(2')	34(2)	42(2)	57(2)	0(1)	-5(2)	18(2)
C(3')	86(4)	48(3)	60(3)	8(2)	13(3)	38(2)
C(4')	103(4)	63(3)	50(3)	13(3)	17(3)	33(2)
N(3')	56(2)	51(2)	33(2)	1(2)	14(2)	20(1)
C(5')	60(3)	35(2)	69(3)	15(2)	25(2)	25(2)
C(6')	55(2)	33(2)	50(2)	18(2)	28(2)	17(2)
N(4')	27(1)	30(1)	35(2)	5(1)	8(1)	14(1)
C(7')	38(3)	95(4)	114(5)	-3(3)	9(3)	49(4)
C(8')	83(4)	71(3)	46(3)	5(3)	31(3)	19(2)
C(9')	34(2)	68(3)	57(3)	1(2)	0(2)	39(2)

The anisotropic displacement factor exponent takes the form:
$-2\pi^2(h^2a^{*2}U_{11} + k^2b^{*2}U_{22} + l^2c^{*2}U_{33} + 2hka^*b^*U_{12} + 2hla^*c^*U_{13} + 2klb^*c^*U_{23})$

PAPER IV. ALUMATRANE $Al(OCH_2CH_2)_3N$: A REINVESTIGATION OF ITS OLIGOMERIC BEHAVIOR

Reprinted with permission from *Inorg. Chem.* **1993**, *32*, 2711-2716.

ABSTRACT

In various literature reports the behavior of the title compound **1** has been described as dimeric in the gas phase; monomeric, hexameric and octameric in solution; and tetrameric (by X-ray crystallography) in the solid state. Herein we present mass spectral evidence for the presence of both $\mathbf{1}_2$ and $\mathbf{1}_4$ in the gas phase. ^{27}Al NMR evidence is put forth for the tetramer $\mathbf{1}_4$ as the only detectable oligomer in solution, wherein $\mathbf{1}_4$ contains one hexacoordinate and three pentacoordinate aluminums. ^{1}H, ^{1}H DQF COSY experiments confirm the presence of $\mathbf{1}_4$ in solution and VT ^{13}C NMR spectral studies reveal the occurrence of an interesting dynamic behavior of $\mathbf{1}_4$ in which the three pentacoordinate alumatranes rotate around their pseudo three-fold axes while remaining fluxionally oxygen-bridged to the central cage containing the hexacoordinated aluminum. Solid-state ^{27}Al and ^{13}C NMR, and Al_{2p}, N_{1s} and O_{1s} XPS evidence has also been gathered that is consistent with the tetrameric structure of solid alumatrane.

INTRODUCTION

Alumatrane, depicted as a monomer **1**,[1] has been the subject of several studies,[2-5] and its oligomeric properties have been discussed in three reviews.[6-8]

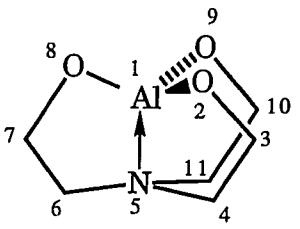

1

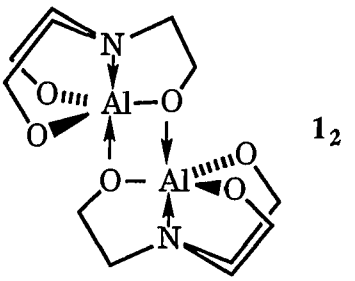

1_2

In benzene solution, a cryoscopic determination of the molecular weight[2] indicated the degree of association to be octameric, while an ebullioscopic measurement[3] suggested hexameric behavior for **1**. A mass spectroscopic (EI 70 eV) study[4] clearly revealed the stability of the dimer **1_2** and ruled out the presence of higher oligomers in the gas phase. The crystal and molecular structure of **1_4**·3*iso*-PrOH·0.5 C_6H_6[5] established the tetrameric nature of **1** in the solid state.

Alumatrane has been prepared by several methods. Transesterification of aluminum alkoxide with triethanolamine can be carried out with or without a solvent[2-4] according to equation 1. Triethylaluminum also reacts with

Reaction 1:

$$nAl(OR)_3 + n(HOCH_2CH_2)_3N \longrightarrow \left[Al(OCH_2CH_2)_3N \right]_n + 3nROH$$

R = *iso*-Pr, *tert*-Bu

Reaction 2:

$$nAl(C_2H_5)_3 + n(HOCH_2CH_2)_3N \longrightarrow \left[Al(OCH_2CH_2)_3N \right]_n + 3nC_2H_6$$

triethanolamine according to equation 2 to afford alumatrane.[7,8]

In our reinvestigation of this compound, we employed the alcoholysis of tris(dimethylamino)aluminum with triethanolamine, and also the transligation of **2**[9] and **3**[9] by triethanolamine (Scheme 1); a reaction we recently reported for azagermatranes.[10] Using mild chemical ionization by NH_3 gas, we have been able to observe both $\mathbf{1_2}$ and $\mathbf{1_4}$ in the gas phase by mass spectroscopy. A paucity of reliable NMR data in the literature led us to perform a multinuclear NMR study on alumatrane which revealed the presence of the tetramer $\mathbf{1_4}$ in solution. An interesting dynamic behavior of $\mathbf{1_4}$

Scheme I

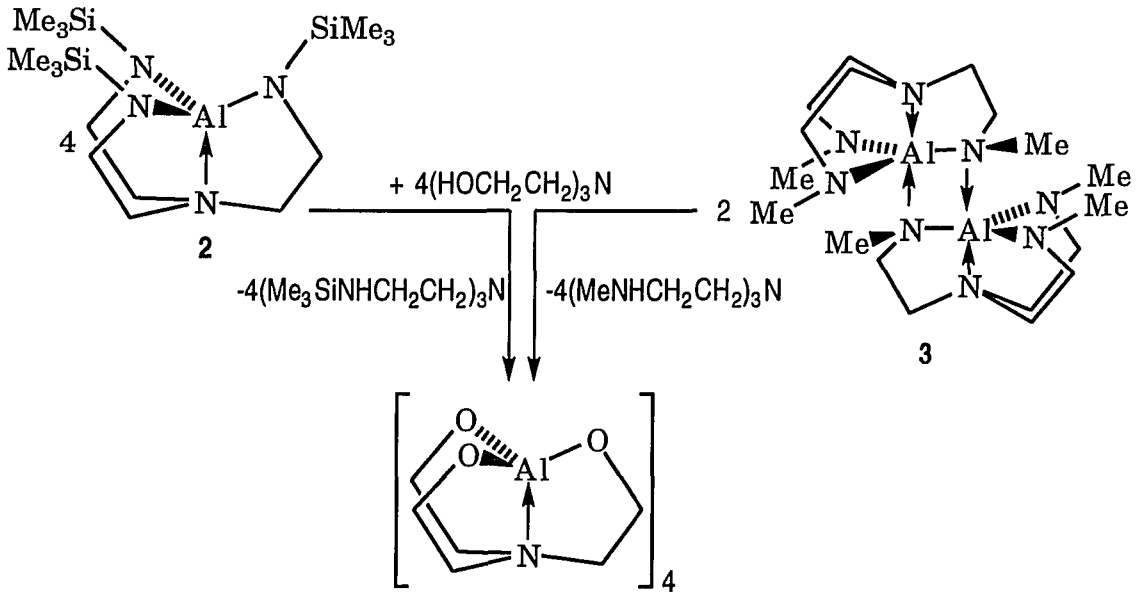

was observed at elevated temperatures in a ^{13}C VT NMR study. Solid-state NMR and XPS data consistent with the tetrameric solid-state structure[5] and with the tetrameric structure found in solution by our NMR studies are also presented.

EXPERIMENTAL SECTION

General Procedures. All reactions were carried out under argon with the strict exclusion of moisture using Schlenk or dry box technique.[11] Solvents were dried over and distilled from Na/benzophenone under nitrogen. Deuterated solvents were dried over and distilled from CaH_2 under an argon atmosphere. The starting material $[Al(NMe_2)_3]_2$ was prepared using the published procedure[12] and it was characterized by ^1H, ^{13}C and ^{27}Al NMR spectroscopy.[12b] Triethanolamine (Fisher) was vacuum distilled at 174-175 °C at 0.03 Torr prior to use. Alumaazatranes **2** and **3** were prepared according to our procedure published elsewhere.[9]

Solution NMR spectra were recorded in sealed 5 mm NMR tubes on a Varian VXR 300 spectrometer with deuterated solvents as an internal lock. ^1H (299.949 MHz) and ^{13}C (75.429 MHz) spectra were referenced to the corresponding TMS signals. A ^1H, ^1H DQF COSY NMR spectrum was acquired with 1024 x 512 data points and was zero-filled to 1024 x 1024 data points before weighting by a sinebell function and Fourier transformation. A digital resolution of 1.1 Hz/point was obtained. ^{27}Al (78.157 MHz) spectra were referenced to the external standard 0.2 M $Al(ClO_4)_3$/0.1 M $HClO_4$ in D_2O. The chemical shifts were corrected for the difference in chemical shift between D_2O and the lock solvent used. The background signal,[13] which was found as a broad peak at ~61 ppm ($\Delta\nu_{1/2}$ = 4100 Hz at 30 °C), did not interfere with our spectra owing to its low intensity.

Solid-state NMR spectra were recorded on a Bruker MSL 300 instrument. ^{27}Al (78.205 MHz) MAS spectra were referenced to the signal from a 1M

aqueous solution of $Al(NO_3)_3$. A 90° pulse length of 4 μs and a relaxation delay of 1s were used. A spinning rate of 3.5 kHz was employed. ^{13}C (75.470 MHz) CP MAS spectra were referenced to the methyl signal of glycine at 43.0 ppm. A standard single contact spin-lock cross polarization sequence with a proton 90° pulse length of 5.5 μs, a contact time of 3 ms, an acquisition time of 96 ms, and a relaxation delay of 6 s were used. The sample was spun at 3.7 and at 3.9 kHz. Samples were packed in a nitrogen-filled glove box into Teflon air-tight rotor inserts which were placed in zirconia rotors with Kel-F or ceramic (in case of measurement at 100 °C) rotor caps.

X-ray photoelectron spectra (XPS) were measured on a Perkin-Elmer 5500 Multitechnique System equipped with a non-monochromated Mg source (E = 1253.6 eV) operated at 300 W. The pressure in the vacuum chamber was less than 5 x 10^{-9} Torr. The energy resolution was 0.86 eV for Ag $3d_{5/2}$ emission, with a pass energy at 11.75 eV. The electron binding energies were calibrated, and charging was referenced to the C_{1s} signal of the methylene groups of alumatrane with the value set to 286.0 eV. The powdery sample of alumatrane was loaded on the probe in a nitrogen-filled glove box.

Mass spectra were recorded on a Finnigan 4000 low-resolution (70 eV EI, NH_3 CI) and a Kratos MS-50 high resolution instrument. The masses are reported for the most abundant isotope present. IR spectra were taken on an IBM IR-98 FTIR spectrometer (4000-400 cm^{-1}) using Nujol mulls between KBr discs or as KBr pellets. Elemental analyses were carried out by Desert Analytics.

Preparation of Alumatrane. *Method A.* Solutions of $[Al(NMe_2)_3]_2$ (0.87 g, 5.5 mmol) in 40 mL of toluene and $(HOCH_2CH_2)_3N$ (0.84 g, 5.6 mmol) in 40 mL

of toluene were added simultaneously within 20 minutes to 150 mL of toluene with vigorous stirring. The reaction solution was stirred at room temperature for 2 h and then heated to reflux for 20 h. After cooling to room temperature, the solvent was removed in vacuum until ~50 mL remained and a white solid began to precipitate. The precipitation was completed by addition of 75 mL of ether. The resulting solid was filtered off, washed with 50 mL of ether and dried in vacuum at 50 °C for 18 hours giving a 77% yield (0.73 g) of product. The product was sublimed at 280-290 °C at 5 x 10^{-3} Torr.

Method B. Triethanolamine (0.95 mL, 0.71 mmol) was added dropwise to a solution of **2** (2.75 g, 0.710 mmol) in 120 mL of toluene. After 79 h of stirring at room temperature, the solvent was removed under vacuum and 120 mL of ether was added. The slurry was stirred for 2 h and then filtered. The resulting white solid was washed with 15 mL of ether and dried under vacuum (2 x 10^{-3} Torr) at 95 °C for 10 h to give 0.77 g (64% yield) of product. ^{1}H NMR (toluene-d_8, -10 °C): δ 2.00-2.46 (m, 6 H), 2.73 (dd, J = 1.5, 13.8 Hz, 1 H), 3.12 (ddd, J = 4.2, 13.5, 13.5 Hz, 1 H), 3.24 (m, 1 H), 3.63-3.87 (m, 5 H), 4.07 (ddd, J = 4.5, 10.2, 10.2 Hz, 1 H), 4.50 (ddd, J = 2.3, 12.2, 12.2 Hz, 1 H). In the ^{1}H NMR spectrum just described, couplings of 1.5-4.5 Hz represent $^{3}J_{HH(gauche)}$ values and those from 10.2-13.8 Hz denote $^{2}J_{HH(geminal)}$ and $^{3}J_{HH(trans)}$ values. ^{13}C NMR (toluene-d_8, -20 °C): δ 60.4, 58.4, 57.8, 56.4 (CH_2O groups), 54.3, 53.9, 53.2, 51.8 (CH_2N groups). ^{27}Al NMR (see discussion and Table I). LRMS (see discussion and Figure 1). IR (KBr pellet, 4000-400 cm^{-1}) ν 2960 s, 2913 s, 2868 s, 2817 s, 2718 w, 2689 w, 1478 vw, 1450 m, 1390 vw, 1374 w, 1364 sh, 1345 vw, 1323 w, 1266 m, 1243 vw, 1203 vw, 1161 vw, 1115 vs, 1094 vs, 1080 vs, 1045 m, 1014 vs, 920 s, 903 s, 874 s, 833 vw, 751 vw, 712 vs, 671 vs, 640 m, 617 s, 603 vs, 548 vs, 503

w, 491 vw, 449 v, 409 m. Anal. Calcd for $C_6H_{12}O_3NAl$: C, 41.62; H, 6.99; N, 8.09. Found: C, 41.99; H, 7.30; N, 8.12.

Reaction of 3 with Triethanolamine. Triethanolamine (0.01 mL, 0.08 mmol) was added to a solution of **3** (0.04 g, 0.09 mmol) in 0.5 mL of benzene-d_6. The gel-like precipitate which initially formed dissolved to give a clear solution within 40 minutes. ^1H and ^{13}C NMR spectra showed the presence of tetrameric $\mathbf{1}_4$ (see above), unreacted excess **3**[9], and $(MeNHCH_2CH_2)_3N$[14] as the only species in the reaction solution.

RESULTS AND DISCUSSION

Syntheses. Alumatrane was prepared in good yield (77%) by the alcoholysis of $Al(NMe_2)_3$ with triethanolamine according to equation 3 in refluxing toluene.

Reaction 3:

$$Al(NMe_2)_3 + (HOCH_2CH_2)_3N \xrightarrow[20\ h.]{toluene} \left[\overline{Al(OCH_2CH_2)_3N}\right]_n + 3\ Me_2NH$$

The alcoholysis of amides has proven to be a useful route to various metallic and metalloidal atranes.[7,15-17] Alumatrane apparently binds solvents very tightly, and long periods of drying under vacuum at elevated temperature were necessary to expel the last traces of solvent. The sample for elemental analysis was sublimed at 280-290 °C at 5 x 10^{-3} Torr, but no differences between sublimed and merely vacuum-dried material could be noted in the MS or ^1H NMR spectra.

An alternative method for the preparation of alumatrane is the transligation of azatranes **2**[9] and **3**[9] with triethanolamine in benzene or toluene according to Scheme 1. This reaction is analogous to the transformation of azagermatranes to germatranes in the presence of triethanolamine which was reported recently from our laboratories.[10] Although transligation is not the method of choice for the preparation of alumatrane, it is interesting to note the facility, with which the central aluminum atom exchanges a tetradentate nitrogen ligand for an oxygen-containing one. This can undoubtedly be attributed to a higher Al-O bond

energy compared with Al-N. Following the reaction of **3** with triethanolamine in benzene-d_6 by ^1H and ^{13}C NMR spectroscopy showed quantitative formation of alumatrane.

Mass Spectra. The electron-impact mass spectrum (70 eV) of alumatrane was identical with the published one,[4] except for the presence of the peak at *m/z* 562. This peak brought to our attention the possible existence of a stable tetrameric ion in the gas phase. Using mild chemical ionization by ammonia gas, both dimeric $(\mathbf{1}_2\text{-H})^-$ and tetrameric $(\mathbf{1}_4\text{-H})^-$ ions were found in the negative ion detection spectrum (Figure 1), together with cluster ions $(\mathbf{1}_2 + NH_3)^-$ and $(\mathbf{1}_4 + NH_3)^-$. The importance of NH_3 as an ionizing agent in this instance was demonstrated by the failure of our attempt to chemically ionize alumatrane by Ar gas.

Solution NMR Spectra. Two reports on the ^{27}Al NMR spectroscopy of alumatranes **1**, **4** and **5** have appeared,[18,19] claiming monomeric behavior

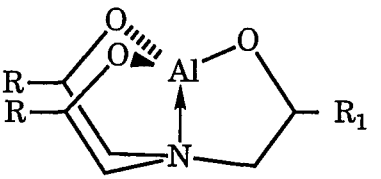

	R	R_1
4	Me	H
5	Me	Me

for these compounds in chloroform solutions and a tetrahedral environment around the central aluminum atom. These conclusions are based on measured values of ^{27}Al chemical shifts of 122, 117, and 124 ppm for **1**, **4**, and **5**, respectively. Our results, which are in sharp contrast to those given in the previous studies,[18,19] are listed in Table I. As an example of our observations, the ^{27}Al NMR spectra of alumatrane at 30 °C and 100 °C in toluene-d_8 are

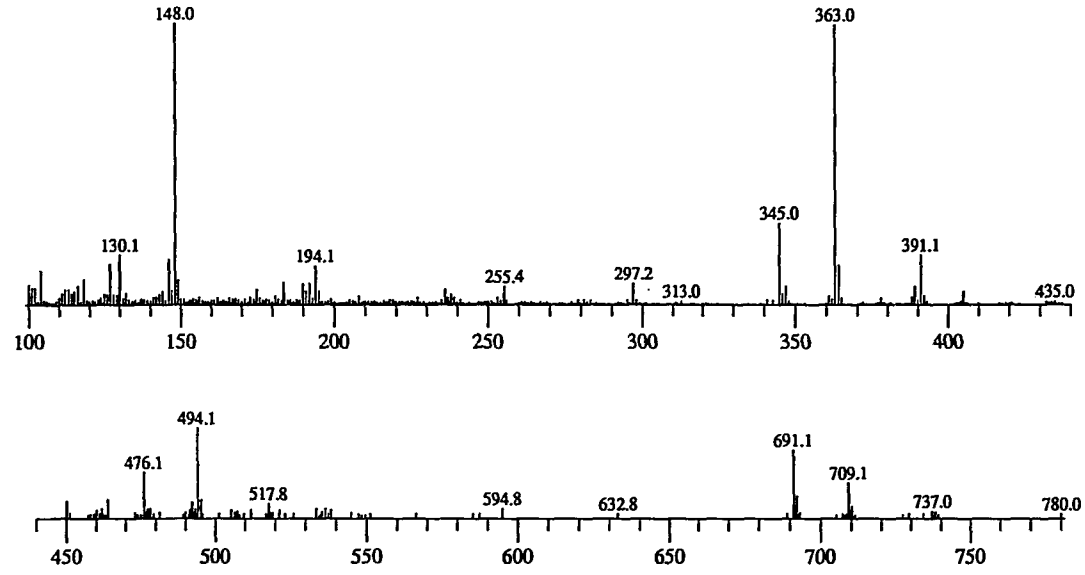

Figure 1. Negative-ion NH_3-CI mass spectrum of alumatrane. The enhancement factor of the lower trace is 5 times that of the upper trace.

Table I. Solution and Solid-State ^{27}Al NMR Data for Alumatrane

medium	$\delta^{27}Al$ (ppm)	$\Delta\nu_{1/2}$ (Hz)[a]	T(°C)	I[b]
toluene-d_8	5.2 ± 0.1	75	30	1.0
		60	50	1.0
		45	100	1.0
	67 ± 1	2300	30	2.5
		2100	50	2.8
		1100	100	3.0
chloroform-d_1	4.9 ± 0.1	110	25	1.0
		70	50	1.0
	66 ± 1	2300	25	2.3
		1600	50	2.5
acetonitrile-d_3	5.2 ± 0.1	90	50	1.0
	66 ± 1	1100	50	2.7
solid state	3.3 ± 0.2[c]	680[d]	20	-
		610[d]	50	-
		560[d]	100	-

[a]A line broadening factor of 10 Hz was applied. [b]Integral intensity. [c]The single-maximum peak is accompanied by a spinning side-band pattern of low intensity. [d]A line broadening factor of 20 Hz was applied.

shown in Figure 2. The main features of these spectra in all three solvents (toluene-d_8, chloroform-d_1, and acetonitrile-d_3) are a broad peak at approximately 66 ppm, a sharp signal at 5 ppm, and a small broad resonance at 30 ppm. Although elevated temperatures reduce the quadrupolar relaxation rate of aluminum nuclei[20] (I = 5/2) thus causing narrowing of the signals, the chemical shifts are temperature-independent within experimental error. The integrated intensities at 100 °C for the signals at 67 and 5.2 ppm in toluene-d_8 are 3 and 1, respectively. These observations are consistent with the presence of tetramer $\mathbf{1}_4$[5] (Figure 3) in solution as a major species. The relatively sharp signal at 5.2 ppm belongs to a single hexacoordinated aluminum atom, whereas the broad signal at 67 ppm can be assigned to three equivalent pentacoordinated aluminum atoms. For comparison, the chemical shifts of hexacoordinated aluminum atoms in the series of tetrameric $[Al(OR)_3]_4$ (R = Et, *iso*-Pr, *iso*-Bu, *n*-Pent, *iso*-Pent, *n*-Hex, *c*-Hex, benzyl)[20,21] range from 3 to 7.5 ppm and their line widths at the half-height range from 50 to 170 Hz at 70 °C. The assignment of the signal at 67 ppm is based on a comparison of ^{27}Al chemical shifts of the few compounds known to possess a pentacoordinated aluminum. Their shifts span a range from 112 ppm ($\Delta\nu_{1/2}$ = 7200 Hz at 27 °C) for compound **6**,[22,23] through 83 ppm ($\Delta\nu_{1/2}$ = 557 Hz at 70 °C) for compound **3**[9] and 41-44 ppm ($\Delta\nu_{1/2}$ = 280-5000 Hz) for five-coordinated aluminum atoms in the series of derivatives **7**,[23,24] to 33.1 ± 0.3 ppm ($\Delta\nu_{1/2}$ = 1100 Hz at 70 °C) for pentacoordinated aluminum in trimeric aluminum *iso*-propoxide.[20]

The small signal at 30 ppm can be tentatively assigned to a pentacoordinate aluminum atom in dimeric $\mathbf{1}_2$. The large linewidth of this signal even at 100 °C, precluded reliable integration. Therefore no conclusions

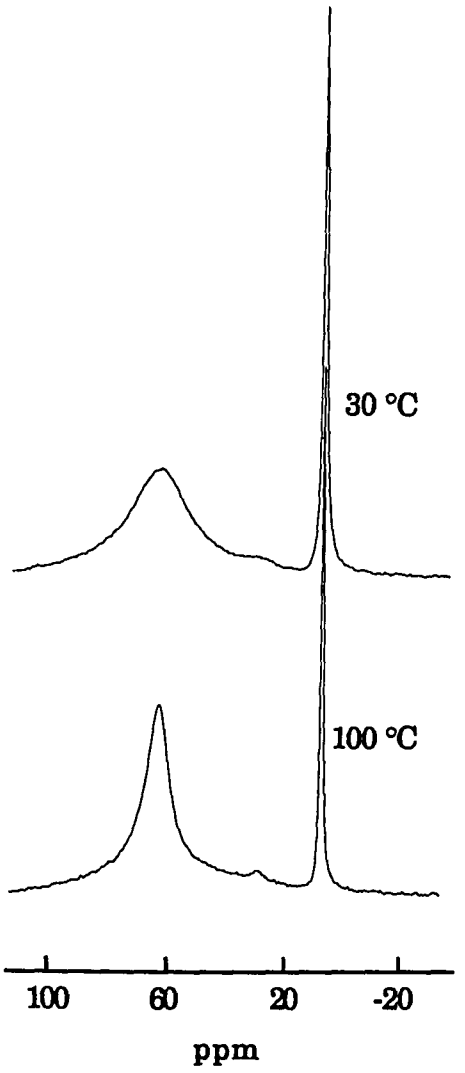

Figure 2. ^{27}Al NMR spectra of alumatrane in toluene-d_8 at 30 and 100°C.

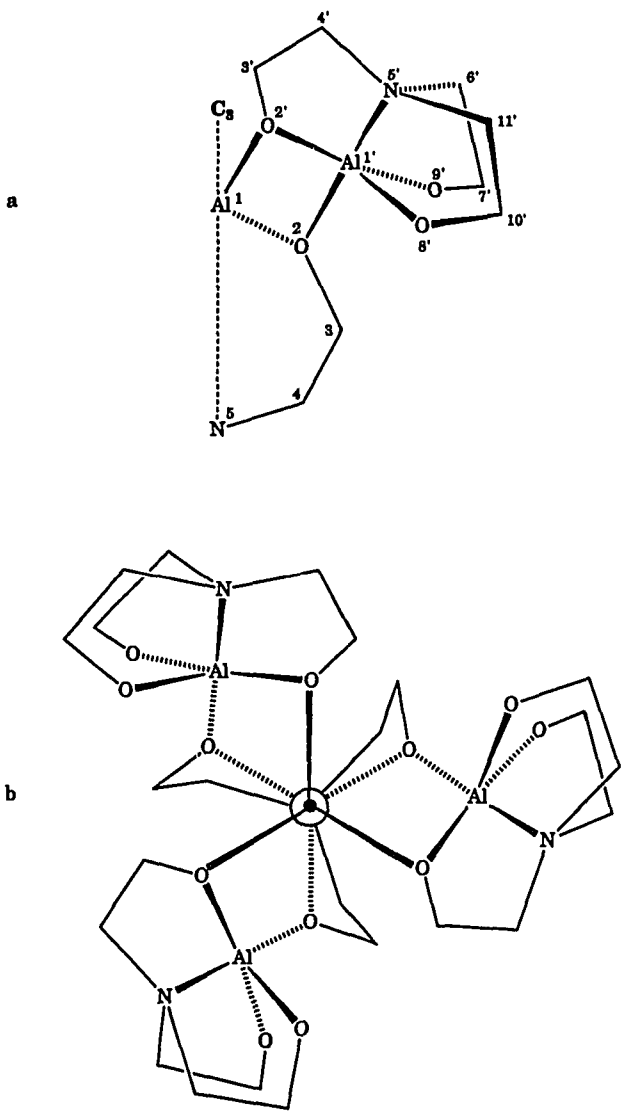

Figure 3. Side view of an equivalent one-third of tetrameric alumatrane **1**$_4$ with the numbering scheme (a) and a view down the C_3 axis of tetramer**1**$_4$ (b).

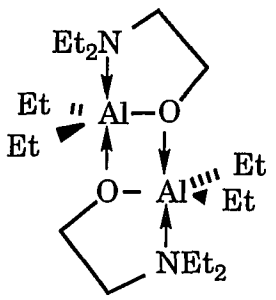

6

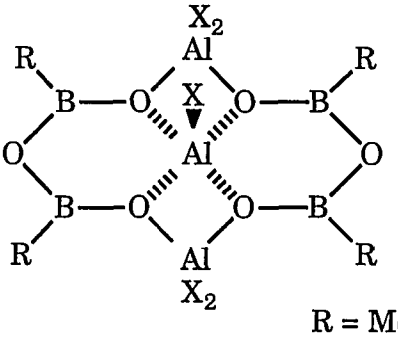

7

R = Me, Et, *n*-Bu, Ph
X = Cl, Br

can be drawn on a possible dynamic equilibrium between tetrameric $\mathbf{1}_4$ and dimeric $\mathbf{1}_2$ in solution. The difference in the ^{27}Al chemical shift between the pentacoordinate aluminum atoms in $\mathbf{1}_4$ and in $\mathbf{1}_2$ can be rationalized by postulating the presence of different degrees of transannulation in the two structures. A wide range of transannular bond distances has recently been reported in a series of phosphorus analogues **8** where Z varies in electron withdrawing power.[25]

Interestingly, compound **9** was found[26] to exhibit a ^{27}Al chemical shift of 68 ppm ($\Delta\nu_{1/2}$ = 3000 Hz) and to react with benzylamine affording a 1:1 adduct allegedly possessing pentacoordinated aluminum. However, two signals in the ^{27}Al NMR spectrum of that adduct were reported, namely, 66 ppm ($\Delta\nu_{1/2}$ = 800 Hz) and 3.9 ($\Delta\nu_{1/2}$ = 30 Hz), without explanation. These results can be rationalized by the presence of a tetramer $\mathbf{9}_4$ (66 and 3.9 ppm) analogous to $\mathbf{1}_4$ in solution.

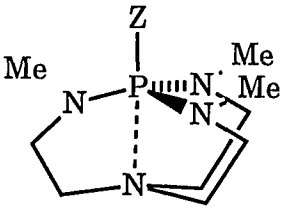

8

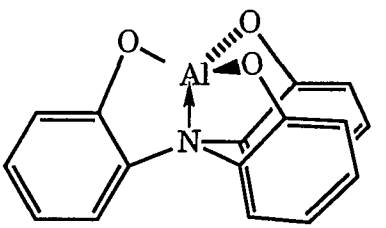

9

Tetramer $\mathbf{1}_4$ was shown by X-ray means to possess C_3 symmetry in the solid state[5], implying the presence of two enantiomers in the solid state and perhaps also in solution at low temperature. With a three-fold axis as the only symmetry element, the tetrameric molecule of alumatrane features eight non-equivalent carbon atoms (Figure 3) which can be observed as separate peaks of approximately equal intensity in the ^{13}C NMR spectrum of $\mathbf{1}_4$ at -50 °C (Figure 4). Upon raising the temperature, a complex dynamic process begins to take place. At lower temperatures (up to 50 °C), the prevailing process is assumed to be racemization via synchronous conformational flipping of the five-membered rings containing Al(1) and N(5), and the four-membered Al(1)-O(2)-Al(1')-O(2') rings, which averages the four signals from carbons 7', 10' and 6', 11' into two broad signals. A further temperature increase presumably accelerates the rotation of peripheral alumatrane units around the Al(1')-N(5') axes, ultimately averaging carbon signals 7', 10', 3', and 6', 11', 4' into two broad singlets at 100 °C. Signals arising from two carbons of the central alumatrane unit (i.e., 3, 4) remain as sharp singlets within the temperature range measured. This, together with the unchanged appearance of ^{27}Al NMR spectrum from 25 to 100 °C, demonstrates that any dissociation of the tetramer into smaller units or any exchange of peripheral and central alumatrane units is undetectable in this novel fluxional process. The rotation of peripheral units can be accomplished by a temporary breakage of the Al(1)-O(2') bond and it is completed by a 120° flip around the Al(1')-N(5') axis allowing O(8') or O(9') to bind to Al(1). We assume that all three peripheral units flip quickly and randomly one at a time, thus preserving, on the average, the C_3 symmetry of

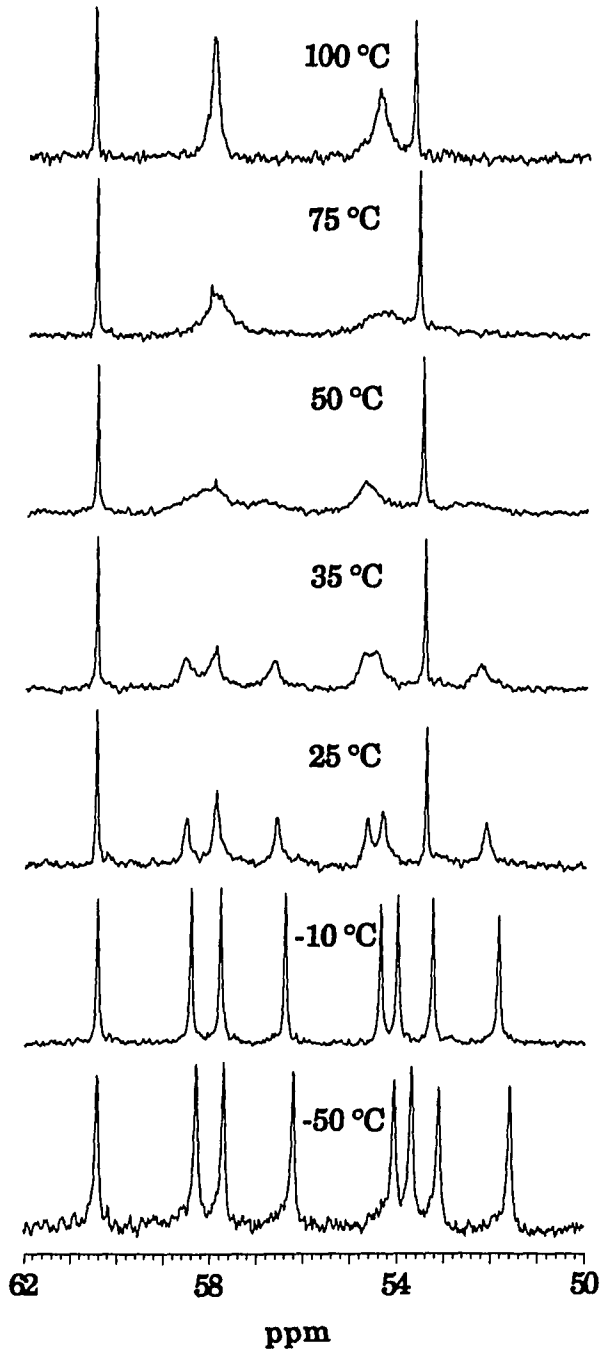

Figure 4. Variable-temperature ^{13}C NMR spectra of alumatrane in toluene-d_8.

the tetramer. Simultaneous flipping of all three peripheral units would be expected to be inhibited on energy grounds.

The ^1H NMR resonances of alumatrane are broadened by the aforementioned dynamic process at higher temperatures, and they are complicated by the diastereotopicity of the methylene protons at lower temperatures (Figure 3). The ^1H NMR spectrum of a chloroform-d_1 solution of alumatrane at -30 °C exhibits four complicated multiplets centered at 2.86, 3.54, 3.79, and 4.05 ppm. Better separation of these signals was obtained by using toluene-d_8 as a solvent, and the spectrum is shown in Figure 5 together with the result of a ^1H, ^1H DQF COSY experiment. By the analysis of integrals of individual multiplets and the cross-peak pattern, sixteen proton signals can be identified and broken down into four groups: A, B, C, D / E, F, G, H / I, J, K, L / M, N, O, P, which belong to four inequivalent OCH_2CH_2N arms, as expected for the rigid tetramer $\mathbf{1_4}$. Further separation was not attained even at -50 °C, and only substantial broadening and overlapping of some of the signals occurred. An attempt to simplify the appearance of the ^1H NMR spectrum by recording it at 100 °C in toluene-d_8 was only partially successful. Signals A, C, and D (Figure 5) remained virtually unchanged, while the other signals broadened and overlapped into four broad signals at 2.41, 2.47, 3.67, and 3.86 ppm, thus precluding a complete assignment.

Solid-State NMR Spectra. To relate our results from the solution NMR measurements to the known crystal and molecular structure of alumatrane,[5] we have recorded the ^{27}Al and ^{13}C solid-state NMR spectra of alumatrane at 20, 50, and 100 °C. The ^{27}Al spectrum (Table I) features a relatively sharp peak at 3.3 ± 0.2 ppm with one maximum.[27] Its linewidth decreases as the

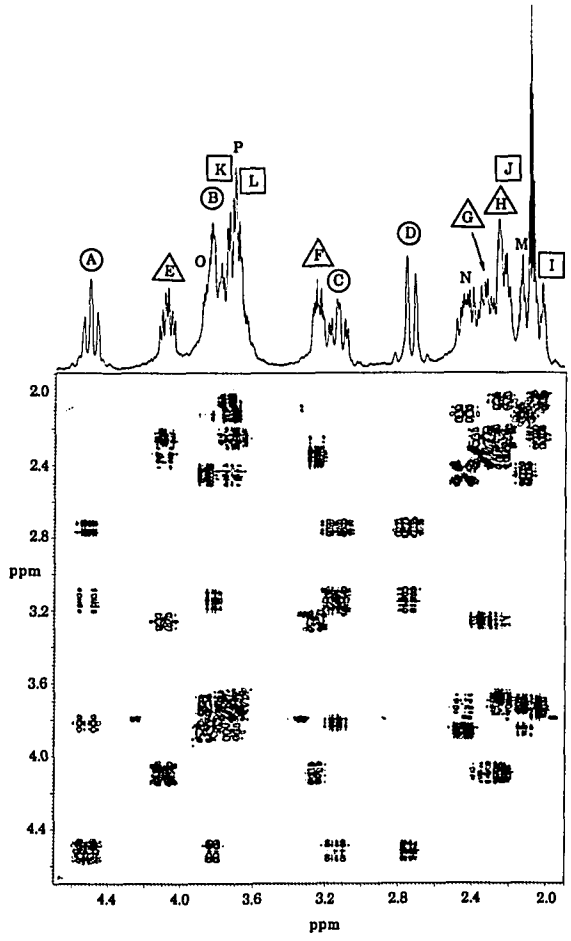

Figure 5. ^{1}H , ^{1}H DQF COSY NMR spectrum of alumatrane with a conventional ^{1}H NMR spectrum as the upper trace. The spectra were acquired at -10°C in toluene-d_8. The quintet at 2.07 ppm arises from a methyl group of the solvent.

temperature is raised, while the value of the chemical shift remains constant. Based on these observations, this peak can be reliably assigned to the hexacoordinated aluminum atom in an axially symmetrical environment in the central alumatrane unit (Figure 3). The lack of a signal for the pentacoordinate aluminum can be ascribed to a large asymmetry of the charge distribution around the five-coordinate aluminum nucleus, causing the quadrupole interaction to broaden the signal beyond the limit of detection. A ^{13}C CP MAS spectrum at 25, 50, and 100 °C shows in each case, two broad overlapping signals at 58 and 55 ppm ($\Delta\nu_{1/2}$ = 300 and 490 Hz), which can be assigned to the CH_2N and CH_2O groups, respectively.

X-ray Photoelectron Spectra. The XPS data in Table II are consistent with the tetrameric structure of alumatrane in the solid state. The results of the non-linear least-squares curve-fitting procedure for Al_{2p}, N_{1s}, and O_{1s} peaks are shown in Figure 6. The authors of the previously reported XPS study on alumatrane, as well as its analogues **10** and **11**, found one type of aluminum, oxygen and nitrogen and concluded that these compounds were monomeric with

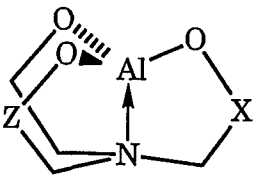

	X	Z
10	CH_2	C=O
11	C=O	C=O

tetracoordinate aluminum atoms.[28] As the atomic composition of the alumatrane sample surface shows (Table II), the ratio of the elements is close to expected value 1Al:3O:1N:6C. (It is reasonable to assume here that the surface can be considered to represent the bulk of the sample.) If contamination of the sample surface by moisture followed by subsequent

Table II. XPS Data for Alumatrane.

element[a]	binding energy (eV)[b]	peak area[c]	whm (eV)[d]
Al_{2p}	73.8	2.6	1.6
	74.6	1.0	1.7
C_{1s}	286.0	e	1.8
N_{1s}	400.1	3.3	1.7
	398.8	1.0	1.6
O_{1s}	531.0	1.0	1.6
	532.1	1.1	1.7

[a]The atomic composition of the sample surface was Al, 1.00; O, 3.37; N, 0.92; C, 5.75. [b]The C_{1s} peak was used as a reference. [c]Peaks were curve-fitted by a non-linear least-squares optimization procedure and integrated by parabolic interpolation using the PHI software package. [d]Width at half maximum. [e]The peak cannot be resolved into two components.

hydrolysis of alumatrane had occurred during sample preparation, a dramatic increase of the oxygen content would have been expected. In our experiment, two kinds of nitrogen were identified in the ratio 1:3. Their N_{1s} binding energies of 398.8 and 400.1 eV correspond nicely to values for amine and ammonium types of nitrogen, respectively.[29] The O_{1s} peak was separated into two components of equal intensity. The high and low binding energy bands at 532.1 and 531.0 eV represent six tricoordinate and six dicoordinate

oxygens in alumatrane **1**$_4$, respectively. Because the separation between the two maxima for the Al_{2p} peaks is close to the resolution of the measurement we tentatively assign the larger peak with the binding energy of 73.8 eV to the three pentacoordinate aluminum atoms, and the smaller peak at 74.6 eV to the unique hexacoordinate aluminum. Values of binding energies of octahedrally coordinated aluminum species vary from 72.9 eV for $Al(acac)_3$ through 74.0 eV for γ-Al_2O_3, to 74.7 eV for corundum and spinel.[29] AlN with the wurtzite structure displays the value of 74.4 eV for tetrahedrally coordinated aluminum,[29] indicating little dependence of the Al_{2p} binding energy on coordination number.

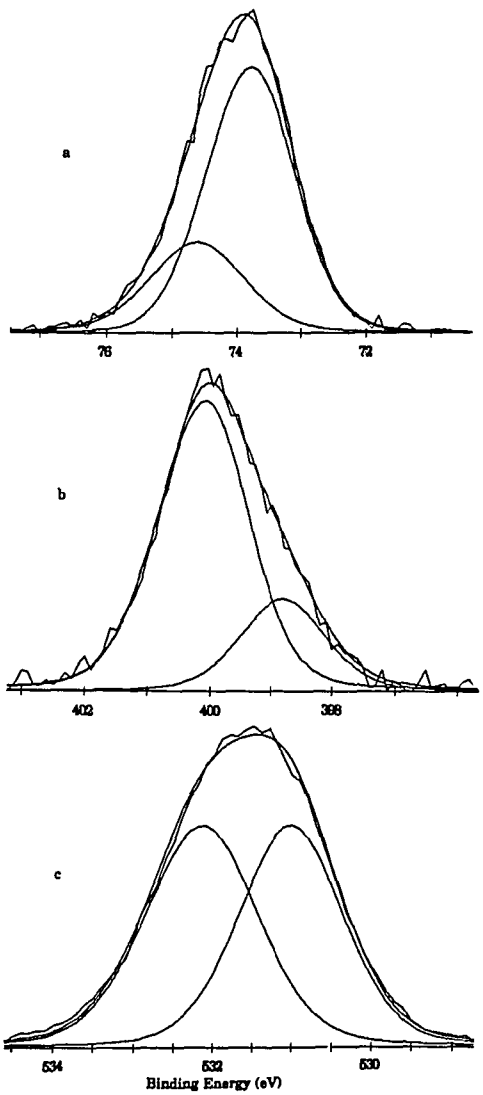

Figure 6. XPS spectra of alumatrane for Al_{2p} (a), N_{1s} (b), and O_{1s} (c) electrons.

CONCLUSIONS

According to our ^{27}Al, ^{1}H and ^{13}C NMR results, alumatrane is tetrameric in solution. This contrasts earlier molecular weight measurements based on colligative properties of solutions, indicating hexameric[3] and octameric behavior,[2] and a monomeric structure based on a single broad peak observed in a ^{27}Al NMR spectrum.[18,19] The solution NMR data we obtain for $\mathbf{1}_4$ are consistent with the tetrameric structure found in the solid state,[5] with the added feature that three peripheral alumatrane units of the tetramer rotate around their three-fold axes while remaining fluxionally oxygen-bridged to the central unit. Our CI mass spectra clearly reveal the presence of $\mathbf{1}_4$ in the gas phase, while an earlier EI study[4] ruled out gas phase oligomers above $\mathbf{1}_2$.

ACKNOWLEDGMENT

The authors are grateful to the National Science Foundation and the Iowa State Center for Advanced Technology Development for grants in support of this work. We thank Dr. J. W. Anderegg for recording XPS spectra.

REFERENCES

(1) 2,8,9-trioxa-5-aza-1-alumatricyclo[3.3.3.$0^{1,5}$]undecane

(2) Hein, F.; Albert, P. W. *Z. Anorg. Allgem. Chem.* **1952**, *269*, 67.

(3) Mehrotra, R. C.; Mehrotra, R. K. *J. Indian Chem. Soc.* **1962**, *39*, 677.

(4) Lacey, M. J.; McDonald, C. G. *Aust. J. Chem.* **1976**, *29*, 1119.

(5) Shklover, V. E.; Struchkov, Yu. T.; Voronkov, M. G.; Ovchinnikova, Z. A.; Baryshok, V. P. *Doklady Akademii Nauk SSSR* **1984**, *277*, 723 (Engl. Transl.).

(6) Bradley, D. C.; Mehrotra, R. C.; Gaur, D. P. Metal Alkoxides; Academic Press: New York, 1978, p. 226.

(7) Voronkov, M. G.; Baryshok, V. P. *J. Organometall. Chem.* **1982**, *239*, 199.

(8) Mehrotra, R. C.; Rai, A. K. *Polyhedron* **1991**, *10*, 1967.

(9) Pinkas, J.; Gaul, B.; Verkade, J. G. *J. Am. Chem. Soc.*, accepted.

(10) Wan, Y.; Verkade, J. G. *Inorg. Chem.*, **1993**, *32*, 79.

(11) Shriver, D. F.; Drezdon, M. A. The Manipulation of Air-Sensitive Compounds; Wiley-Interscience: New York, 1986.

(12) (a) Ruff, J. K. *J. Am. Chem. Soc.* **1961**, *83*, 2835. (b) Waggoner, K. M.; Olmstead, M. M.; Power, P. P. *Polyhedron* **1990**, *9*, 257.

(13) Benn, R.; Rufinska, A.; Janssen, E.; Lehmkuhl, H. *Organometallics* **1986**, *5*, 825.

(14) Schmidt, H.; Lensink, C.; Xi, S. K.; Verkade, J. G. *Z. Anorg. Allg. Chem.* **1989**, *578*, 75.

(15) Menge, W. M. P. B.; Verkade, J. G. *Inorg. Chem.* **1991**, *30*, 4628.

(16) Lukevic, E. J.; Solomennikova, I. I.; Zelchan, G. I.; Yankovska, I. C.; Mazheika, I. V.; Liepinsh, E. E. *Latv. PSR Zinat. Akad. Vestis, Kim. Ser.* **1975**, *4*, 483.

(17) Verkade, J. G. *Acc. Chem. Res.*, submitted.

(18) Li, E.; Xu, G.; Wang, T.; Lu, K.; Wu, G.; Tao, J.; Feng, Y. *Huaxue Tongbao* **1985**, *6*, 22; *Chem. Abstr.* **1986**, *104*, 121849h.

(19) Wang, T.; Lu, K.; Wu, G. *Huaxue Tongbao* **1986**, *5*, 33; *Chem. Abstr.* **1987**, *105*, 202098k.

(20) Kriz, O.; Casensky; B.; Lycka, A.; Fusek, J.; Hermanek, S. *J. Magn. Res.* **1984**, *60*, 375.

(21) Monsef-Mirzai, P.; Watts, P. M.; McWhinnie, W. R.; Gibbs, H. W. *Inorg. Chim. Acta* **1991**, *188*, 205.

(22) Benn, R.; Rufinska, A.; Lehmkuhl, H.; Janssen, E.; Krüger, C. *Angew. Chem. Int. Ed. Engl.* **1983**, *23*, 779.

(23) Benn, R.; Rufinska, A. *Angew. Chem. Int. Ed. Engl.* **1986**, *25*, 861.

(24) Köster, R.; Angermund, K.; Serwatowski, J.; Sporzynski, A. *Chem. Ber.* **1986**, *119*, 1301.

(25) Tang, J.; Laramay, M. A. H. and Verkade, J. G. *J. Am. Chem. Soc.*, **1992**, *114*, 3129.

(26) Paz-Sandoval, M. A.; Frenandez-Vincent, C.; Uribe, G.; Contreras, R. *Polyhedron* **1988**, *7*, 679.

(27) Engelhardt, G.; Koller, H. *Magn. Res. Chem.* **1991**, *29*, 941.

(28) Wang, D.; Dai, Y.; Wang, T.; Lu, K.; Wu, G. *Kexue Tongbao* **1986**, *31*, 820.

(29) Handbook of X-Ray Photoelectron Spectroscopy; Chastain, J., Ed.; Perkin-Elmer, Physical Division: Eden Prairie, MN, Oct 1992.

GENERAL SUMMARY

In this research we have demonstrated two methods for synthesizing group 13 azatranes: $[M(RNCH_2CH_2)_3N]_n$ (M = B, Al, Ga; R = H, Me, $SiMe_3$, $SiMe_2$-*tert*-Bu; n = 1,2). The first method is a transamination reaction of a dimethylamide of M with a tripodal tetramine ligand. The new bulky tripodal ligand (*tert*-$BuMe_2SiNHCH_2CH_2)_3N$ was prepared by two general methods which can be extended to syntheses of other silylated polyamines. The second preparative route to azatranes is a transmetallation reaction of either dimeric or monomeric azaalumatranes initially studied with $B(OMe)_3$ and $Ga(acac)_3$. The scope of this complex metathetical reaction was extended to include main-group and transition metal alkoxides as reactants thus affording main-group and transition metal azatranes as products.

A series of group 13 azatranes was characterized by multinuclear and two-dimensional NMR, FT-IR, and high-resolution MS techniques. These azatranes were shown to be monomeric or dimeric in the solution and solid states depending on the nature of the central atom and the size of the substituents on the equatorial nitrogens. Bulky groups such as $SiMe_3$ and $SiMe_2$-*tert*-Bu on the tripodal amine ligand stabilize monomeric triptych structures of azaalumatranes and azagallatranes by sterically shielding the central atoms and preventing additional coordination. Conversely, the smaller Me groups on the tripodal amine ligand allow formation of dimers as was shown by spectroscopic methods. The crystal and molecular structures of three dimeric azatranes were examined by X-ray crystallographic methods and these molecules were demonstrated to possess an unusual cis

configuration of the substituents on the central four-membered ring. This configuration is remarkably stable and is retained in solution even after heating

The results of single-crystal X-ray diffraction experiments on monomeric $Al(Me_3SiNCH_2CH_2)_3N$ showed a rare trigonal monopyramidal (TMP) coordination geometry around the aluminum atom imposed by the tripodal ligand. The dynamic behavior of monomeric azabora- and azaalumatranes in solution was examined by variable temperature ^1H NMR spectroscopy. While azaalumatranes and trimethylazaboratrane were found to be conformationally fluxional on the NMR time scale down to -95°C, $B(Me_3SiNCH_2CH_2)_3N$ is rigid at room temperature owing to a steric strain imposed by the bulky $SiMe_3$ groups on the molecule. The fluxional process at elevated temperatures was explained in terms of a racemization of two enantiomers, Δ and Λ, and the negative value of the activation entropy suggested a concerted interconversion mechanism with C_{3v} symmetry of the transition state.

^{27}Al NMR studies of a series of monomeric aluminum amides and monomeric and dimeric azaalumatranes as a function of aluminum coordination numbers spanning a range from three to five demonstrated a trend in the ^{27}Al NMR shifts toward a higher field with increasing coordination number.

We have also demonstrated a facile conversion of group 13 azatranes to the corresponding atranes in their reaction with triethanolamine, emphasizing a remarkable stability of the atrane structure. The oligomeric behavior of alumatrane was examined in the solution, solid, and gas phases. Multinuclear, two-dimensional, and variable temperature NMR spectra

revealed the presence of a tetramer $[Al(OCH_2CH_2)_3N]_4$ in solution with a complex mode of fluxionality. The solid-state NMR and XPS spectra are also in accord with the tetrameric formulation, while MS experiments with mild ionization by ammonia gas revealed the presence of both dimeric and tetrameric ions in the gas phase.

ACKNOWLEDGMENTS

I would like to thank following people for their support and help in my effort :

Dr. John G. Verkade for his kind guidance, patient support, and friendly and stimulating environment for my graduate work.

Dr. Winfried Plass for helpful discussions, suggestions and know-how.

Dr. Victor Young for the crystallographic results reported in this dissertation and for instructions on X-ray crystallography.

Tieli Wang and Dr. Robert A. Jacobson for the crystallographic results reported in this dissertation.

Dr. Gordie Miller and Dr. John D. Corbett for the use of their glove boxes.

Dr. Dave Scott and Dr. Karen Ann Smith for their assistance in NMR spectroscopy.

Jan Beane and Dr. Kamel Harrata for mass spectral measurements.

Dr. Robert J. Angelici for the use of the A-team Mac.

I would like to thank the following past and present members of the Verkade group: Dr. Martina Schmidt, Dr. Mark Mason, Dr. T. Mohan, Dr. Andrzej Wroblewski, Dr. Krzysztof Erdmann, Dr. Fazlur Rahman, Dr. Wiro Menge, Dr. Mao Chun Ye, Dr. Ahmad Naiini, Dr. Mary Laramy, Yanjian Wan, Llorente Ting Bonaga, S. Geetha, Jiansheng Tang, Yong Han, and Jong-Hwan Lee.

My thanks go to my mother for her 1000^{+} days of waiting and my sister for her support.

Finally, I would like to thank my wife Jana for sunshining my life and giving a new sense to my journey.